Einar Reistad
Sondre Kofstad
Torgeir Brandsar

Desktop-sized fatigue testing machine

Design and prototype

Bachelor's thesis

NTNU
Norwegian University of Science and Technology
Faculty of Engineering
Department of Mechanical and Industrial Engineering

NTNU

Norwegian University of
Science and Technology

Einar Reistad
Sondre Kofstad
Torgeir Brandsar

Desktop-sized fatigue testing machine

Design and prototype

Bachelor's thesis in Maskiningeniør
Supervisor: Per Harald Ninive
May 2023

Norwegian University of Science and Technology
Faculty of Engineering
Department of Mechanical and Industrial Engineering

NTNU
Norwegian University of
Science and Technology

NTNU
Institutt for vareproduksjon
og byggteknikk

Oppgavens tittel:	Dato: 22.05.2023			
Desktop-sized fatigue testing machine: *Designing and building a working prototype*	Antall sider: 145			
	Masteroppgave:		Bacheloroppgave	X

Navn:
Einar Reistad, Sondre Kofstad og Torgeir Brandsar

Veileder:
Per Harald Ninive

Eventuelle eksterne faglige kontakter/ veiledere:

Sammendrag:

I denne bacheloroppgaven utvikles det et design for en utmattelsesmaskin i skrivebordstørrelse. Hensikten med designet er at det skal være en maskin som er enkel og rimelig å bygge. Designet har blitt utviklet ved å bruke ingeniørmetoder slik som dataassistert design (CAD), mekanikk og koblingsskjemaer for elektronikken. I tillegg har det blitt laget programkode for å sette opp tester og kode som kjøres på maskinen slik at den utfører testene og lagrer resultatene. Designet ble testet ved at det ble laget prototyper. Prototypene ble brukt til å evaluere designet. Evalueringen avslørte visse mangler knyttet til egnetheten av enkelte av motorene og sensorene brukt. Det ble også oppdaget at noen av dimensjonene måtte endres. Avslutningsvis diskuteres disse manglene, hvordan de kan forbedres og hvordan designet kan videreutvikles.

Stikkord:

Fatigue testing machine
Prototyping
Mechatronics

(sign.)

Einar Reistad	Torgeir Brandsar	Sondre Kofstad

Preface

We want to thank Per Harald Ninive for guiding us through this bachelor thesis.

Abstract

Fused Deposition Modelling and other rapid prototyping methods make it easy and inexpensive to produce parts with complex geometries. It should be of interest to test the mechanical properties of these produced parts in a similarly easy and inexpensive way as they were produced. The goal of this bachelor thesis is to develop and present a design for a desktop-sized fatigue testing machine that can be used for testing the fatigue limits of these parts.

The presented design includes production drawings, diagrams for electronics and program code for the machine. The design and program code have been made open source by making all code, drawings, and computer-aided design (CAD) files available on a shared Google Drive folder. In this thesis, methods such as CAD, diagramming of electronics, mechanics calculations and finite element analysis were applied in the development of the design.

Another important method utilized was prototyping. Building the prototype resulted in that various flaws with the design, program code and electronics were revealed. Most of these flaws were related to the quality of the electronics components, choice of electrical motors and some of the dimensions in the design. At the end of the thesis, the design for the fatigue machine is evaluated based on the prototype and further work and improvements are suggested.

Content

Figure list

Table list

1 Introduction

1.1 Background and motivation

This bachelor thesis is inspired by an article published in the International Journal of Mechanical Engineering and Robotics Research Vol.11, No. 4, April 2022. In this article, a simple desktop-sized testing rig was made for fatigue testing of 3D-printed[1], small-scale wind turbine blades (Zawadzki, et al., 2022). The testing was done with an ad-hoc set-up where the force applied was determined by using beforehand measurements of force applied and resulting displacement (Zawadzki, et al., 2022). The rig was then set up so that the test subject was displaced to a given value. The test subjects were replaced manually after each test subject broke.

This bachelor thesis presents a new design for a desktop-sized fatigue testing machine and evaluates a prototype built on this design. The design is made to be easily accessible with open-source code, drawings, and CAD files; and should be fairly easy to build.

1.2 Research question and overall goal

The overall goal of this bachelor thesis is to create a design for a desktop-sized fatigue testing machine. The design should be open-source and easy to build. This overall goal can be broken down into the following subgoals:

1. The machine should measure the force applied on the test subject from the power used (in DC, the voltage drops over the motor).

2. The machine should count the number of cycles and measure the force applied at a user-defined sampling rate.

---

[1] «3D-printing» is used in this thesis as a colloquial reference to the Fused Deposition Modelling (FDM).

3. The machine should have a functional design and be user-friendly. It should be easy to export data from the tests.

4. The design of the machine should be based on mechanical engineering principles, with dimensions and material choices informed by mechanical calculations and finite element analysis.

5. The machine should be quite simple to build, and the bachelor thesis should outline how to build the machine in a manner that is easy to follow. Any code, electronic wiring, CAD files, and such should be made available or transparent.

6. The machine should be able to change test subjects automatically so that several tests can be run without needing manual replacement.

7. Make a prototype of the design and evaluate weaknesses with the design.

The thesis ends with an evaluation of the prototype and outlines how the design may be improved. Since this is an open-source project, all designs and diagrams are attached to the thesis report, and all CAD files and program code are distributed on a [google drive shared folder,](#) which can be accessed with the link in appendix 8.3.

1.3 Main terminologies used for different parts

Figure 1 shows the final design and some of the terminology used to refer to the different parts of the machine in this report.
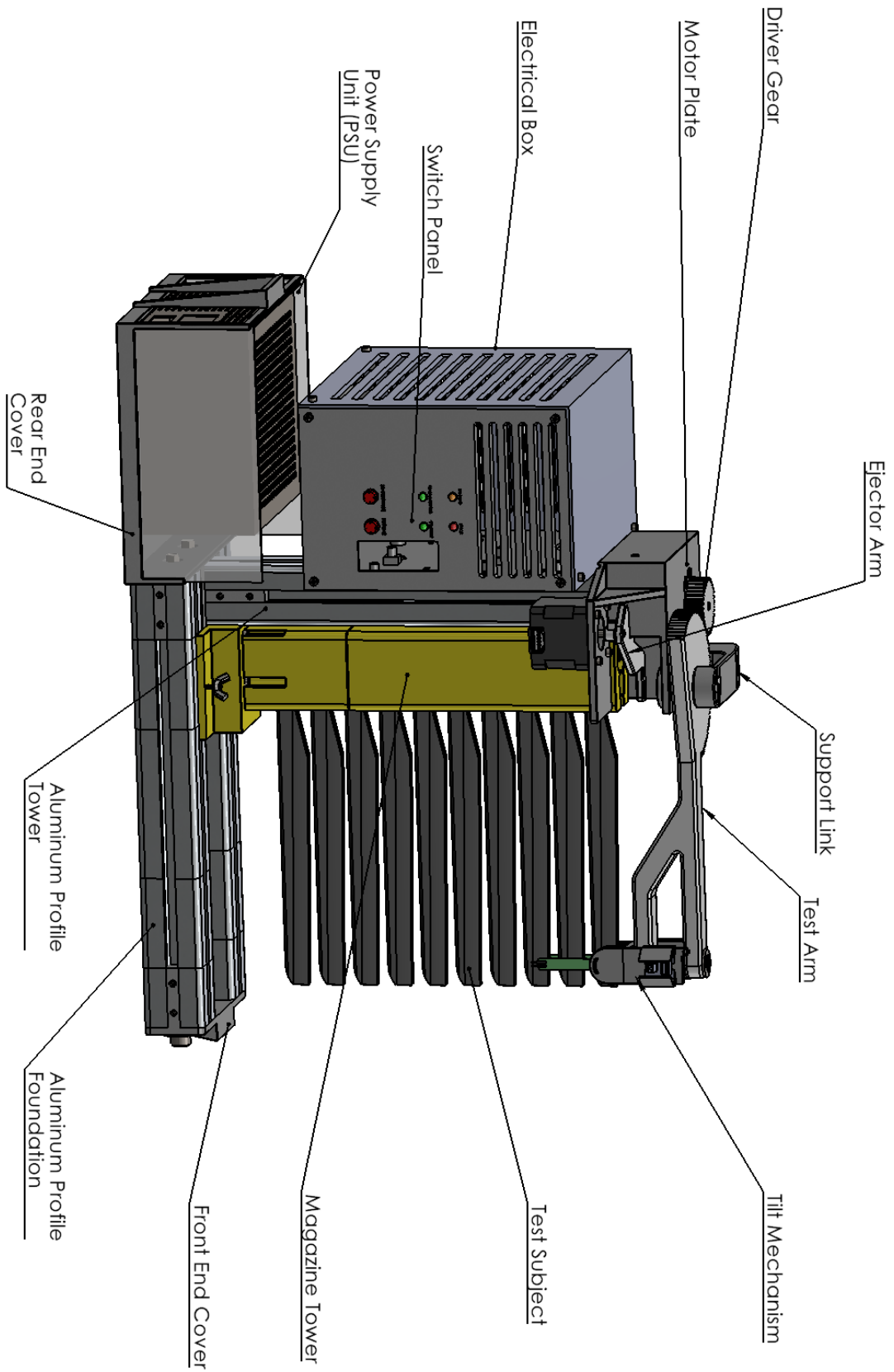
Figure 1 Terms for the main parts of the fatigue test machine.

2 Relevant Theory and project implications

2.1 About fatigue testing

Fatigue is a failure that occurs after cyclic stress is applied to a part. It has been estimated that about 90% of the failures in parts and constructions made of metals and polymers are caused by fatigue (Callister & Rethwisch, 2010). Therefore, it is important to fatigue test parts to establish the number of cycles at a given stress level it can take before failure. This is done by applying sequential loads of a given magnitude to the test subject (Falck-Ytter, 2014). The fatigue test can take several different forms of loading by cyclic bending, torsion, or compression and strain (Falck-Ytter, 2014, p. 74). The design of the fatigue testing machine in this thesis will only perform cyclic bending on the test subject.

Fatigue is a failure that occurs after cyclic stress is applied to a part. It has been estimated that about 90% of the failures in parts and constructions made of metals and polymers are caused by fatigue (Callister & Rethwisch, 2010). Therefore, it is important to fatigue test parts to establish the number of cycles at a given stress level it can take before failure. This is done by applying sequential loads of a given magnitude to the test subject (Falck-Ytter, 2014). The fatigue test can take several different forms of loading by cyclic bending, torsion, or compression and strain (Falck-Ytter, 2014, p. 74). The design of the fatigue testing machine in this thesis will only perform cyclic bending on the test subject.Besides changing the form of loading, one can also change the magnitude of the load (Falck-Ytter, 2014), as illustrated in Figure 2. These three test configurations can be distinguished from each other with the parameters the mean stress and the stress amplitude. The mean stress and stress amplitude is defined with the following equations (Callister & Rethwisch, 2010, p. 255):

$$Mean\ stress: \sigma_m = \frac{\sigma_{max} + \sigma_{min}}{2}$$

(1)

$$\text{Stress amplitude: } \sigma_a = \frac{\sigma_{max} - \sigma_{min}}{2} \qquad (2)$$

$\sigma_{max} \dots \max stress\ applied.$

$\sigma_{min} \dots \min stress\ applied.$

In Figure 2 the difference between the tests is that test 2 has a higher mean stress than test 1 and 3, because it is never fully unloaded. Test 3 has a lower stress amplitude than test 1 and 2. For the testing machine developed in this bachelor thesis, the stress amplitude and mean stress applied in each test are specified in the test setup. The test setup is defined in a custom-made software described in section 3.10.1.
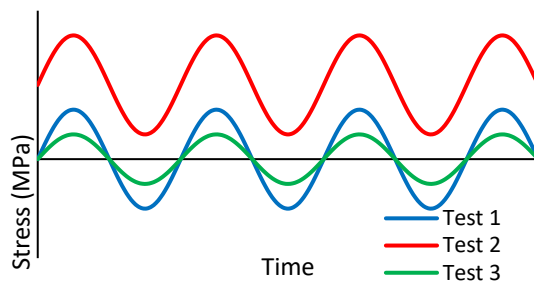
Figure 2 Fatigue tests with different amplitudes or mean stress.

2.2 Fastening

The most common way to join components is to use bolted connections. This can consist of bolts, nuts, washers and lock washers. When torque is applied to a bolt, it creates a preload due to the stretching of the bolt. The preload should not overcome the yield strength of the material, which is marked as point B in Figure 3. Material is elastic up to its yield strength. If the stress exceeds the yield strength, the material enters the plastic zone, resulting in permanent deformation.
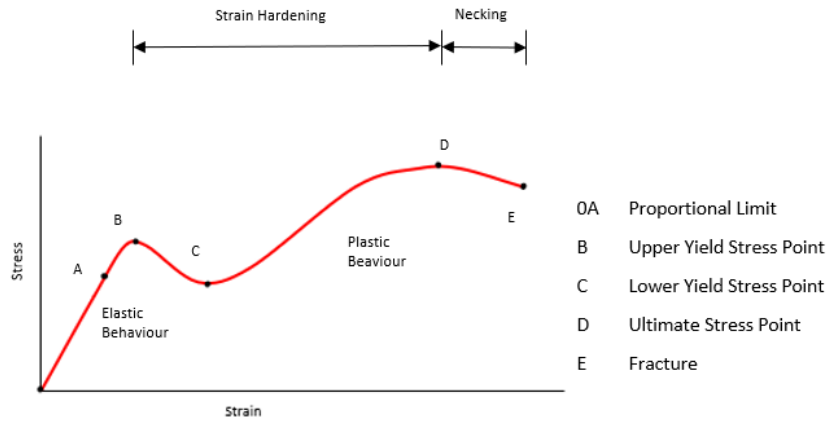
Figure 3 Example of the stress-strain curve.

The grade of preload has to be verified from documentation (Teknikbog, u.d., p. 33), but normally 70% of yield strength is used (MiSUMi, 2014). In the interface between the components, there will be a resultant force occurring that is called "clamp force" (Ignatowitz, 2021, p. 121), as illustrated in figure 4.
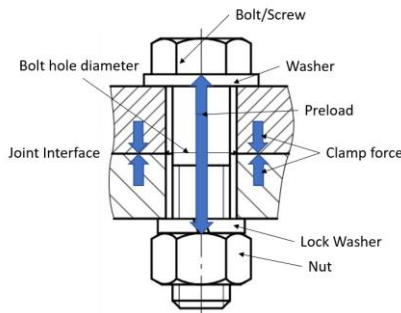
Figure 4 Schematic example of bolted joint with nut (Андрей, 2022). Distributed under CC0 1.0 license.
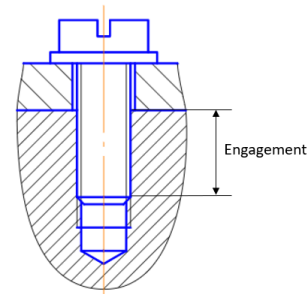
Figure 5 Schematic example of a bolted joint without a nut (Андрей, 2022). Distributed under CC0 1.0 license.

2.2.1 Bolts

The bolt/screw has threads pointing outwards from the center and they can have a variety of different head-types. The most common one is hexagon, but also Torx socket head cap, slotted cheese or countersunk head is quite common. The threads come in numerous different types such as metric, unified (UN) threads, pipe threads, parallel/tapered, trapezoidal, knuckle, buttress, cycle, Edison, partly or fully threaded, square threads and also left/right-handed threads. They are available in several dimensions. Here is an example of a bolt with

metric thread: DIN 961-M10x1.25x40-8.8-ZN. This stands for: DIN 961, which is a standard hexagon head screw fully threaded with fine threads. M10 means that the nominal diameter is 10mm. The 1.25 designates the lead pitch's linear travel per revolution in mm. 40 refers to a 40mm shaft length. The number 8.8 is a combination of the bolt's ultimate tensile strength and the yield strength. The ultimate tensile strength is derived by multiplying the first number with a hundred $8 * \frac{100N}{mm^2} = 800 \frac{N}{mm^2} = 800\ MPa$. The yield strength is derived by multiplying the second number divided by ten with the ultimate tensile strength $\frac{8}{10} *$ $800\ MPa = 640\ MPa$ (Dahlvig, 1991). ZN means that there is a zinc-plated layer at the outer face, done with electricity (Gomeringer, et al., 2017, pp. 207-220).

2.2.2 Nuts

The nuts have threads pointing in opposite directions compared to the bolts. The most common type of nut has hexagon heads, but they are also available with different head styles such as square, castle, flanged, lock, cap and wing heads. They come with the same type of threads as the bolts and with the same material properties (Ignatowitz, 2021, p. 123).

If a nut is not used on the bolt, then it is important to have enough engagement for the threads in the hole, as illustrated in Figure 4 and 5 and values in Table 1.

Table 1:

Actual values of minimum engagement depth in blind hole (Gomeringer, et al., 2017, p. 216).

Material of engagement	3.6-4.6 (bolt/screw property)	4.8-6.8 (bolt/screw property)
Aluminum alloy	1.2xDiameter	1.6xDiameter
Plastics	2.5xDiameter	

2.2.3 Washer

Washers are mostly used to distribute the load from the preload of bolted connections against the face of the component but are also used with different designs for securing the bolt/nut from loosening or as a spacer. The material is hardened or stainless steel with different coatings to prevent corrosion. Round washers are the most common, but they also come in square variants (Dahlvig, 1991, p. 79).

2.2.4 Set screws

Set screws are used to secure an object in a hole in the body, like an axle. The most common is a screw which is fully threaded all the way and does not have an external head but instead has an internal slot. This can for example be an internal hexagon-style head. Set screws are not used with nuts but it is possible use two set screws in the same threaded hole for securing (Leyton Fasteners, u.d.).

2.3 Bearings

A bearing is a construction that transfers forces between parts that are moving relative to one another. In most cases, it is used to obtain movement of rotation between two parts, for instance one axle and one fixed support. There are two main types of bearings defined by principles of construction. One type has rollers of different forms to obtain rotation (SKF, u.d.), as illustrated in Figure 6. The other type is sliding bearings which is made for a linear movement, made of a suitable bearing material, and a clearance containing a film of lubrication that reduces the friction and separate the parts (NTN, u.d.).
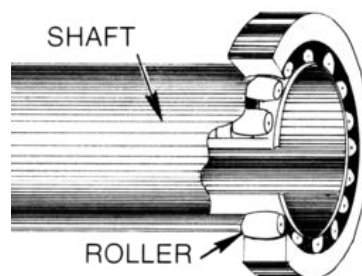
Figure 6 Example of roller bearing (Anon., 2020).
Distributed under CC0 1.0 license.

2.4 Gears

The main purpose of gears are to transfer torque, change the speed or change the direction of rotation movement between two parallel axles. The most common type of gear is the spur gear, as illustrated with CAD models in Figure 7 made in SolidWorks.
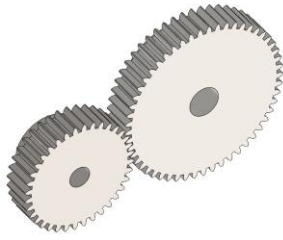
Figure 7 Example of spur gear.
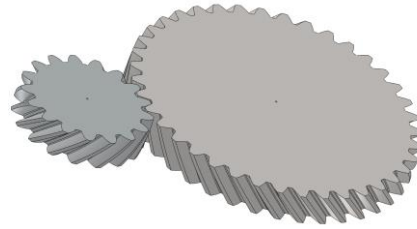
Figure 8 Example of helical gear.

The spur gears are easy to produce, has a low cost and can be manufactured at high tolerance. A downside of the spur gear is that at high speed they are especially noisy. Some other gear types are the single helical gear, as illustrated in Figure 8, which has teeth with an angle against the axis of the gear. This type of gear has a higher load capacity and is less noisy than spurs gears, but since the teeth have an angle, the gear needs support for forces along the gear axis (Mobley, 2001, pp. 631-633). To function properly, it must be a set of at least two gears with the same size of teeth that are "integrated" into each other. The gear ratio is changed by changing the number of teeth on one gear compared to another, and thus one can attain the desired number of revolutions on the driven gear per revolution on the driving gear, and increase or decrease the torque of the driven/driving gear (Ignatowitz, 2021, p. 105) as illustrated in Figure 9.
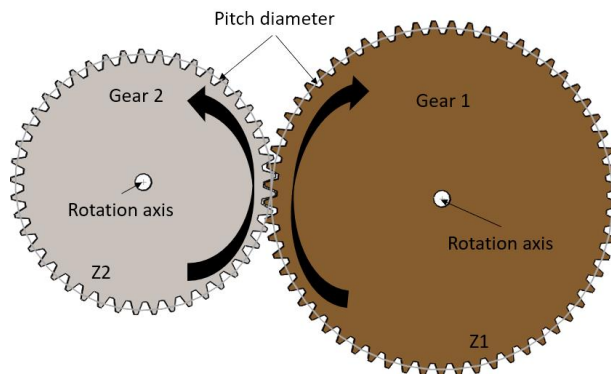
Figure 9 Illustration of a transmission with gears.

The gear ratio is useful for calculating torque and the rotation speed of the gears (Dahlvig, 1991). Below is the formula for calculating the gear ratio (Gomeringer, et al., 2017, pp. 260-261):

20

$$i = \frac{Z_2}{Z_1}$$

$i \,...\, ratio$

$Z_1 \,...\, Number\ of\ teeath\ at\ the\ driving\ gear$

$Z_2 \,...\, Number\ of\ teeth\ at\ the\ driven\ gear$

The gears are manufactured with different designs and also with different numbers of teeth and different diameters. These can be combined in many different standards, often referred to as modules, which simplifies how to refer to the dimensions of a gear as they can be calculated from a module. E.g the number of teeth can be calculated from the following formula ratio if the module is given (Gomeringer, et al., 2017, pp. 260-261):

$$N = \frac{d}{m} = \frac{d_0 - 2*m}{m} \qquad (4)$$

$m \,...\, module$

$d \,...\, pitch\ diameter/circle$

$N \,...\, Number\ of\ teeth$

$d_0 \,...\, Addendum\ circle\ /\ Outside\ diameter$

2.5 Electrical motors

In this project, at least three electrical motors are needed: one to control the test arm that bends the test subject, one to change test subjects after failure and a third for ejecting the failed test subjects. This section reviews some theories about electrical motors and mechatronics with the purpose of determining the most suitable electrical motor to use for the prototype.

2.5.1 AC and DC electrical motor

Direct current (DC) electrical motors are most used in modern control systems (Bolton, 2019, p. 232). As the name suggests, it uses a direct current power source. This means that it can easily be powered by batteries or directly from the microcontroller (if the power consumption is in the range of specification). Another advantage of DC motors over alternating current (AC) motors is that it is easier to have control over the torque (Aksdal, 2003, p. 20; Bolton,

2019, p. 243). The ease of control over torque weighs heavily in the choice, and thus a DC electrical motor seems more appropriate to use in this project.

2.5.2 Stepper motor and servo motors

Most motors are made for the purpose of going around at a certain RPM. In this project, the needed functionality of the motors is to bend the test subject to a certain position and hold it, and then bend it back. Stepper motors and servo motors are especially suited for this application (Bolton, 2019, pp. 243-51).

Stepper motors are designed with many different poles and shifting the polarity of these poles allows the motor to rotate with a "step", where each step equals the same degrees of rotation (Bolton, 2019, p. 243; Allegro MicroSystems LLC, 2014). Some common applications are CNC machines, 3D-printers and printers, applications in which they are especially useful since stepper motors can be directly controlled by PLCs/computers (Hughes & Drury, 2019, p. 376). Various CNC equipment does have some similarities in functionality to that of a fatigue testing machine regarding the need for accurate movement and also by applying force onto a work piece.

Stepper motors have a holding torque, which is the maximum torque that can be applied without the motor spinning away from its position (Bolton, 2019, p. 245). This is a very desirable feature as this gives good control over the force the fatigue testing machine applies to the test subject. Another feature is that stepper motors can be controlled without positional feedback, and it works as an open-loop control system (Hughes & Drury, 2019; Hughes & Drury, 2019; Bolton, 2019). However, calculating the load torque from the voltage and current is a very involved affair and not easily (Hughes & Drury, 2019; Hughes & Drury, 2019; Bolton, 2019). Since this project is attempting to estimate the force applied to the test subject indirectly through the electric system, choosing the stepper motor may not be ideal for operating the test arm. It is nevertheless a viable choice for driving the mechanism that changes test subjects after failure.

Servomotors may be a better choice for driving the test arm as they also can move a certain angle, but unlike the stepper motor, this is achieved using an encoder that tracks the position of the rotor shaft (Bolton, 2019, p. 250). However, servomotors do not have a holding torque per se, they can still generate something similar (Bolton, 2019, pp. 25-1), but this requires

appropriate sizing of the motor to avoid oscillations which must be avoided in this type of machine (Lackey, 2023).

2.5.3 Estimating load torque from angular velocity, voltage and current

The torque produced by an electrical motor can according to theory be calculated from its current consumption, voltage and a set of parameters specific to the motor (Bolton, 2019; Hughes & Drury, 2019). The relationship between torque and voltage can be expressed with the following equation (Bolton, 2019, p. 234):

$$T = \frac{K_t}{R}(V - K_v\omega) \Leftrightarrow V = \frac{R}{K_t}T + K_v\omega \tag{5}$$

V… Voltage (V)
ω … angle speed of rotation (1 / s)
T… torque
R… the resistance of the armature coil
K_t… motors torque constant
K_v… back e.m.f constant of the motor

According to this equation one needs to alter the motor's speed. At very low speed ω becomes approximately zero and the speed can be ignored, then the torque becomes proportional with the voltage.

Torque can also be simplified as a function of current (Bolton, 2019, p. 233):

$$T = K_t i \tag{6}$$

i… current carried by armature conductor.

The mechanical load/torque is therefore proportional to the current drawn by the electrical motor (Hughes & Drury, 2019, p. 35). It should therefore be possible to calculate the load on the motor by just measuring the current and not altering the motor's speed.

However, a simpler approach is to use the equation for the power drawn by the motor, load/torque and the rotational speed of the motor shaft. It is common knowledge that the

power (P) in a circuit equals current (I) multiplied by the voltage (V) (Gomeringer, et al., 2017, p. 56):

$$P = IV \qquad (7)$$

By definition, torque can be written as a formula in terms of force (F) and lever length (r) (Gomeringer, et al., 2017, p. 35):

$$T = Fr \qquad (8)$$

The power applied in the circular motion of a wheel can be written as a function of the torque and the angular velocity (Gomeringer, et al., 2017, p. 37):

$$P = T\omega \qquad (9)$$

Combining equation (7) and (9) gives an expression that expresses torque in terms of current and voltage (or power):

$$P_t = IV = T_t\omega \iff T_t = \frac{IV}{\omega} \qquad (10)$$

This means that if the current or voltage is higher, then the theoretical torque (T_t) is higher, but if the angular velocity is higher then, ceteris paribus, the theoretical torque is lower. In theory, this should be a good way to measure the torque the electrical motor provides. However, the electrical motor is not perfectly efficient and some of the power input to the motor is lost to heat or copper loss, iron loss/hysteresis loss and mechanical loss such as friction (Aksdal, 2003, pp. 18-9). This loss can be expressed as an efficiency factor $\eta = \frac{P_{out}}{P_{in}}$ (Aksdal, 2003, p. 19). Using this, the theoretical torque from the equation above can be translated into the actual torque (T) outputted by the motor:

24

$$P = \eta IV = T\omega \Leftrightarrow T = Fr = \frac{\eta IV}{\omega} \Leftrightarrow$$

$$F = \frac{\eta IV}{\omega r} \qquad (11)$$

If assuming that all these values are constant, it should be possible to calculate the load applied to the electrical motor from the current and the voltage.

2.6 Electrical motor selection

Three factors to be considered when choosing an electrical motor are inertia matching, torque requirements and power requirements (Bolton, 2019, p. 251). The necessary theory and equations for finding inertia matching, torque requirements and power requirements will be reviewed in this section. In addition to these factors, it is also necessary to consider the availability and the cost of the electrical motor.

2.6.1 Inertia matching

Inertia matching is about having control over the load on the motor shaft, minimizing the torque needed to achieve a certain acceleration (Bolton, 2019, pp. 251-2) and avoiding overshooting and oscillations when positioning (Lewotsky, 2015). In this project, a high gear ratio will probably be used, meaning that the motor's shaft will rotate much faster than the actual load (loaded test arm) will move. This reduces the effective torque and is favorable regarding inertia matching (Hughes & Drury, 2019, p. 421). Maximum power transfer and control is achieved when the following equivalence is achieved (Knight, 2023, p. 4):

$$I_m = \frac{I_L}{n^2} \qquad (12)$$

I_m… Second moment of area of the motor

I_L… Second moment of area of the load

n… Gearing ratio.

However, inertia matching is not the only concern. Thus, matching perfectly is not necessarily desirable as there are other aspects to consider in regard to gear ratios (power transmission,

torque, speed and control). The rule of thumb says that the load inertia to motor inertia should not exceed 10:1 (Lewotsky, 2015; Collins, 2014), but in practice, it is very system dependent (Lewotsky, 2015). There are a lot of trade-offs to consider in regard to speed, torque production and so on. However, in this project the load should be modest, the test arm is not rotating completely, the load is actually working in opposite directions of the test arm (except when centering back the test arm) and there is no need for extreme precision (like in industrial robots). Thus, inertia matching is not expected to be the biggest challenge in this project.

2.6.2 Torque requirement

Torque requirement is the maximum torque required by the motor to avoid stalling and overheating (Bolton, 2019, pp. 252-3). It is necessary to determine the required torque at the start and with full load given a speed.

Torque requirement is the maximum torque required by the motor to avoid stalling and overheating (Bolton, 2019, pp. 252-3). It is necessary to determine the required torque at the start and with full load given a speed. If the motor starts unloaded, then the required torque only needs to be greater than the load torque, i.e. the torque at maximum load (Aksdal, 2003, p. 39). This can easily be determined by comparing the calculated maximum torque in the datasheet with the calculated maximum torque that will be applied to the test arm. A motor with maximum torque close to but above this should be selected (Aksdal, 2003, p. 41).

If the motor starts with a load and the load is constant, then it is important that the motor's maximum torque for different RPM does not have a saddle point below the load torque (Aksdal, 2003, p. 40). If the load increases linearly from zero, then it is sufficient to make sure that the maximum moment of the motor is higher than the load moment at a given RPM (Aksdal, 2003, p. 40).

In this project, the load on the motor is expected to mostly increase linearly with the RPM as the test arm's angle from the center becomes larger. This is because the test subject will press more and more back against the test arm as the test subject's displacement is increased. The fatigue testing machine will only elastically deform the test subjects. In elastic deformation, the force applied increases linearly with the displacement/strain (Falck-Ytter, 2014). Therefore, the force the test subject will press back with on the test arm will increase linearly.

26

In this project, the load on the motor is expected to mostly increase linearly with the RPM as the test arm's angle from the center becomes larger. This is because the test subject will press more and more back against the test arm as the test subject's displacement is increased. The fatigue testing machine will only elastically deform the test subjects. In elastic deformation, the force applied increases linearly with the displacement/strain (Falck-Ytter, 2014). Therefore, the force the test subject will press back with on the test arm will increase linearly. The power requirement can also be expressed mathematically in terms of the required torque from the motor (T_m), the load torque (T_L) and gearing ration (n) (Bolton, 2019, p. 254):

$$T_m > \frac{T_L}{n} + I_m \alpha_m \tag{13}$$

$I_m \alpha_m$ is the torque required for a motor with a moment inertia of I_m to accelerate with an angular acceleration of α_m (Bolton, 2019, p. 254). If the required acceleration is very low, then this part of the equation can probably be omitted, which is most likely the case for making the fatigue testing machine, as acceleration is not important for it to function. Therefore, a simplified version of this equation is:

$$T_m > \frac{T_L}{n} \tag{14}$$

2.6.3 Power requirement

The power requirement (P) is the energy per time unit needed to accelerate the load and compensate for the friction, which can be calculated from the frictional torque (T_f), the load's second moment of area (I_L), angular acceleration (α) and angular speed (ω) (Bolton, 2019, p. 254):

$$P = T_f \omega + I_L \alpha \omega \tag{15}$$

However, in many cases $I_L \alpha \omega$ is dropped from the equation, due to acceleration being slow or not important. Below is a simpler formulation of the required power (Aksdal, 2003, p. 41):

$$P = \omega T_L = 2 * \pi * RPM * T_L \tag{16}$$

Using equation 8 and then inserting the result into equation 7 and solving for α will yield the acceleration of the test arm.

2.7 Material choices

When choosing materials for a project, it is important to consider different material types against the requirements that the task calls for. There is an ever-growing number of different materials to choose from. Choosing the right material can help the project to become a success and increase the lifetime of the device (Corrosionpedia, 2019). On the other hand, the task of identifying the best materials might become complex. However, all materials can be categorized into one of the general types of materials like ferrous materials, nonferrous materials, polymers, ceramics and composite materials (Kalpakjian & Schmid, 2014, p. 13).

An example of how to approach a material selection is to divide the problem into three by analyzing the aspects of the properties of materials, availability and service life. The properties of the materials are maybe what first comes to mind when choosing materials and include all physical, mechanical, chemical and manufacturing properties as well as appearance. The interplay between physical and mechanical properties is often considered in order to produce an ideal product. This can for example be the strength-to-weight ratio which is important to take into account when high mass significantly reduces performance (Kalpakjian & Schmid, 2014, pp. 13-14). The second aspect to consider is the availability of the materials. This factor is just as important as technical properties, as one has to get hold of the actual material in order to make use of it. It is also vital to consider economic aspects as this will have a significant impact on the profitability of the product. Included in the economic aspect is the additional cost of processing the material if it is not delivered in the desired state (Kalpakjian & Schmid, 2014, p. 14).

The third aspect to consider is the service life. This factor should not only consider what the material will be used for, but also for how long the material/product will be used or for how many cycles. It should also be considered what kind of and how much maintenance that will be required to keep the material serviceable. This should be compared to other alternatives of adequate materials. Maybe a material that is more expensive to buy will be cheaper over the lifespan of the product because it requires less costly maintenance (Kalpakjian & Schmid, 2014, p. 14).

If the viewpoint is expanded from focusing solely on the project alone, there are other factors that also can be included in the selection of materials. It can be argued that environmental aspects can and should be considered by any modern engineer. The United Nations sustainability goals can be used for guidance (United Nations, u.d.). Especially relevant is goal 12 that involves a sustainable consumptions and production, of which recycling is important (United Nations, 2023). Materials that are located far away need to be transported over long distances in order to be utilized and will therefore lead to greater levels of emission than locally available materials. Another aspect to consider is whether the material has been transported back and forth during the production and assembly process in order to exploit cheap and specialized manpower in different areas of the world (Quest International, u.d.). Shortage of certain materials such as zinc and gallium are a growing concern in the world (Solomon, 2022). If other materials can be used with the same effect this should be selected instead in order to minimize the pressure on limited resources.

2.8   Production methods

In the construction of the prototype, various production methods have been utilized. This section reviews some relevant theories for these production methods. The theories reviewed in this section are limited to the production methods utilized in the project. E.g. aluminum was cut to length by the team, but the aluminum profiles themselves were procured; therefore, only the cutting of the profiles will be discussed and not how they were produced.

2.8.1 Fused-deposition modeling (3D-printing)

Making prototypes with most traditional manufacturing production is very time consuming and costly, thus rapid prototyping speeds up the production of high-quality prototypes (Kalpakjian & Schmid, 2014, pp. 535-7).

In this thesis, additive rapid prototyping (commonly referred to as 3D-printing) is utilized to produce many of the more complex parts in the project that are not easily constructed with more traditional production methods. The 3D-printer brand used is Prusa i3 mk3 and the parts are printed in a thermoplastic called polylactide (PLA). This particular form of additive rapid prototyping is called fused-deposition modeling (FDM) and involves extruding thermoplastic

through an extrusion-die which then is laid layer-on-layer on top of each other (Kalpakjian & Schmid, 2014, p. 540). The thermoplastic is laid out in long fibers/threads that bond together (Kalpakjian & Schmid, 2014, p. 540), which is possible as polymer molecules can bond together through weaker secondary forces such as van der Waals, dipole and hydrogen bonds (McCrum, et al., 1997, p. 49). These fibers tend to be very strong along the fibers as they have covalent bonds and much weaker perpendicular to the fibers (McCrum, et al., 1997). Therefore, the parts made with the additive rapid prototyping is expected to have very anisotropic properties, depending on how they are printed (orientation of the print).

The best possible tolerances expected to be achieved with FDM is determined by the extrusion-die diameter (Kalpakjian & Schmid, 2014, p. 541). In the case of the Prusa i3 mk3 the extrusion-die is 0.4 mm (Prusa Reserach, 2023), but in addition to this, several other factors affect the actual possible tolerance achieved such as quality of the assembly, wear and tear and more. It is thus expected that the best achievable tolerance is ±0.4 mm, but realistically it will be larger than this.

2.8.2   Circular saw: miter saw

Miter saw has been used to cut the aluminum profiles. Miter saw is a kind of circular saw used a lot by craftsmen and carpenters and is mounted on a portable platform. Circular saws give good dimensional control and result in relatively smooth cut surfaces (Kalpakjian & Schmid, 2014, p. 689). Many miter saws come with a laser that is useful for getting precise cuts to achieve desired dimensions. The operation of the miter saw is done by firstly letting it get up to speed and then gently but firmly pushing it through the material. It can be angled by rotating it along the longitudinal-axis and the lateral-axis. Most saw blades can be used for wood, aluminum and steel (not stainless/inox). Safety handling requires first securing the material that is to be cut. Make the cut with a firm and controlled movement through the material and back again while keeping your hands away from the work plate. Maintain a steady footing, avoiding having loose fitting cloths, jewelry, or hair in the way. The use of safety goggles and sound protection is also necessary.

A circular saw should be able to achieve fairly decent tolerances if calibrated correctly. However, it is a manual process, so wrong aligning, wrong measurement and wrong drawing of the cut line are the most likely sources for inaccuracies. When measuring with a meter stock, the best achievable tolerance is at best ±1 mm (EUR-Lex, 2014, p. 87).

2.8.3 Drill

Holes are used to enter threads, bolts, studs, axles, wiring, tie straps and numerous other components into or through. One can use a handheld drilling machine or, when needed for more accuracy, a drill press with a lockable table and the possibility to fasten the object in a vice. The most commonly used drill bits are made of high-speed steel and have an outer layer of titanium nitride or titanium carbonitride in order to make them stronger. These drill bits can be capable of drilling thousands of holes before wearing out. It is essential to drill according to specifications, illustrated in Table 2. Before starting to drill, it is important that the location of the hole is well measured and marked according to drawings. This is done by using a punch mark. If the hole is small, it can be drilled directly with the correct dimension. If the hole is bigger, it is best to first drill a starting hole with a small drill bit or a center drill. It is important when drilling to use a suitable cutting oil for lubricating and cooling (Gomeringer, et al., 2017).

Table 2:
Some values for holes and threads with coated high speed steel drill bits (Gomeringer, et al., 2017, pp. 210,216,338-341).

Type of metric threads	Drill bit size/Rotational speed in wrought Aluminum/Thermoplastics (MM/RPM/RPM)	Clearance holes middle type for screws / Rotational speed in Aluminum/Thermoplastics (MM/RPM/RPM)	Revolutions for thread machine (RPM)
M3	2.5/11077/3819	3.4/8144/2808	1697
M4	3.3/8391/2893	4.5/6153/2122	1273
M5	4.2/6593/2273	5.5/5035/1736	1018
M6	5.0/5538/1909	6.6/4195/1446	848
M8	6.8/4072/1404	9/3076/1061	636

2.8.4 Angle grinder

An angle grinder is a power tool that uses electricity or compressed air to drive a gear. It is mostly used to cut, grind and polish metal and can normally use discs from 2-16 inches in diameter (Hufford, 2015). The tool comes in various sizes, ranging from small one-handed to larger two-handed models. The type of disc used depends on the desired outcome. Discs can be made of metal with a diamond-coated edge or a hard metal alloy. Alternatively, they can be made of resin bonding with abrasive materials such as aluminum oxide, silicon carbide, and ceramic alumina. It is important to follow the manufacturer's specifications for the disc (Smith, 2009).

2.8.5 Adhesives

Adhesives are used to connect two surfaces together by creating adhesive bonding. To get a better bonding, one can sand the surfaces first with sandpaper before cleaning with a proper degreaser, like a mixture of isopropyl alcohol, to remove dirt and grease. The adhesive should be applied on one of the surfaces before holding the surfaces together until the adhesive cures. In order to speed up the curing process, an activator can be used (Loctite, u.d.).

2.8.6 Soldering

Soldering is a process used to connect electric cables together or to an electric connector of soldering type using a filler metal. The process is started by removing the isolation layer of the electric cable with a cable wire stripper. To keep the cables steady when soldering, it is best practice to use a soldering vise clamp to hold the cables in place while heating up the electric wire with a soldering iron. At the same time, one must apply filler metal which melts when in contact with the heated wires. The soldering wire roll made for soldering is with a tin flux core inside. The soldering tin should then melt thoroughly into the electric wire before removing the soldering iron. The filler metal should solidify and cool down before the part is being used (Kalpakjian & Schmid, 2014, p. 939).

2.8.7 Threading and use of various hand tools

A tap is used for making internal threads and a die is used for external threads. Normally in industry, the threads are done by drilling machine or by lathe. For this project, threading is done by hand with a ratcheting thread tap wrench with T-handle in a drill press. It is important that the threads are created perpendicular to the surface and to apply a suitable cutting oil.

Various hand tools are required when producing the machine. The following list shows examples of used tools, but list is not exhaustive: screwdrivers, combination and hex wrenches, vice, keys, pipe socket set, multimeter, wiring cutter, side cutter, circlip plier, crimping tool, heating gun and rubbing blocks.

2.9 Electronics

2.9.1 Microcontroller: Raspberry Pi 4B

Microcontrollers are necessary for more complex control situations where sets of electronic integrated circuits alone are not sufficient to control the machine or system (Bolton, 2019, p. 259). Microcontrollers are able to receive and send information through Input/Output (I/O) pins as well as process and store information (Bolton, 2019). There is a myriad of different microcontrollers on the market (Bolton, 2019). Two of the more popular choices currently on the consumer market are the models Arduino and Raspberry Pi. This thesis has chosen to use the Raspberry Pi 4B for its prototype, because the project's members are most familiar with the Raspberry Pi and the Python programming language that can easily be run on it.

The Raspberry Pi 4B has 40 general-purpose Input/Output (GPIO) pins. Some of these can be used for input and output signals, while others are just for ground or to provide either 3.3V or 5V (Raspberry Pi Fundation, 2023). Only 28 of these pins can be used for software-controlled input and output (Raspberry Pi Ltd., 2019). These pins will in this project be used to get the microcontroller to send signals to regulate the motors and to receive information from the machine's sensors. Some of these pins are dedicated to special purposes by the manufacturer. In the Raspberry PI 4B datasheet, it is mentioned that GPIO0/ID_SC and GPIO1/ID_SD is reserved for specific integrated circuit and should otherwise be left unconnected (Raspberry Pi Ltd., 2019, p. 9). GPIO 12 and 13 also distinguish themselves form the others since these pins can be used for pulse-width-modulation (PMW) (Raspberry Pi Ltd., 2019, p. 9). In addition to these GPIOs, there are many more pins with various special functions or utilities (Raspberry Pi Ltd., 2019, p. 10). There are too many different and alternative functions for each GPIO to describe all of them in this section. Rather, we will defer to instructions in datasheets and documentation for the different IC and cards on which GPIOs should be used and describe it under each section dedicated to that IC or card.

Unlike some microcontrollers like Arduino which have analog input pins (Bolton, 2019, pp. 286-9), the Raspberry Pi 4B only has digital inputs (Raspberry Pi Ltd., 2019). Since some of the components used in the fatigue testing machine constructed in the project send analog signals, it is necessary to convert these into digital signals. This is done by using an analog-to-digital converter (ADC) which samples an analog signal and converts it into a digital signal.

The cost of this is the adding of one more component (the converter) and a slight time delay as this is required to perform the converting (Bolton, 2019, pp. 104-5).

2.9.2 Encoder for the motor

During testing it is important to have control of the position, speed, direction of movement and force of the motor driving the test arm, so a device will be needed as a reference for this. There are different types of encoders using various technologies based on magnetic, mechanical, resistive and optical principles. The technologies can also be divided into absolute or incremental types. The absolute decoder gives a signal that indicates the position, speed, and angle of the shaft. The incremental encoder gives a signal with information about the motion and speed of the shaft and it can also give information about position if it has a base point of reset that it can count from (Society Of Robots, 2005). The encoder is mounted on the motor and measures the movement. The microcontroller unit receives signals of the movement and calculates position according to set values programmed.

2.9.3 DC motor drive card

In order to supply the DC motor with correct voltage and current, a motor drive card is normally needed between the microcontroller and the motor. This is because most microcontrollers have a low voltage and ampere output (OurPCB, u.d.). Motor drivers also function as a hub for inputs affecting the motor drive. Along with inputs from a power supply the motor drive card will have input stations for control signals. These inputs and signals are processed in the logic of the motor driver and is often just two wires going to the motor.

When operating with a DC motor it should be possible to set the speed of the motor on a scale. If one has an analog output as the control signal, the signal is already in a scale by nature. The Raspberry Pi 4B is not able to create analog signals. With an ordinary digital output which is either HIGH or LOW the signal reads either full speed or no speed. However, there are methods to cope with this. For instance, digital signal types like serial communication and pulse-width modulation (PWM) can be used to control a DC motor (Agnihotri, u.d.).

PWM signals are periodically rectangular, and the repetition frequency can be set by the programmer. The intensity of the signal varies by manipulating the amount of HIGH and

LOW there is in each period. If each period has the same amount of HIGH and LOW, the intensity of the signal would be 50 %. This is called the duty cycle and is the ratio between the HIGH and LOW time. If this signal were used on a motor, it would spin at half speed. Likewise, an LED would be shining at half brightness. A rule of thumb is that the frequency must be high enough to avoid oscillations. For an LED this means that it has to be high enough to avoid visible flickering. For a motor it should be high enough for the motor to respond to the average of the PWM signal; therefore, the frequency for a motor-controlling signal must often be above 1 kHz (Alciatore, 2019, p. 481).

In this project, the AQMH3615NS V2.00 motor driver will be used. This is a driver that uses a PWM signal to control the motor, which is suitable for the selected DC motor in this project. It has two input pins for power which are 9-36V and ground. The board has an additional four input pins, which are COM, IN1, IN2 and PWM. These are all meant to get input from a microcontroller. COM is ground and IN1 and IN2 are motor steering control signal inputs. These signals are used together with the PWM to control the speed and direction of the motor. If IN1 is HIGH and IN2 is LOW, it will signal the motor to go forward with the intensity from the PWM signal. If it is the other way around, the motor will go in reverse at the same speed. If both control signals are LOW the motor will stop (DFRobot, u.d.).

2.9.4   Stepper motor drive card: A4988

In order to control the stepper motors, motor drivers are used, one for each motor. Even though the motors are slightly different, both are controlled by the same type of motor driver in this project. The driver used is the A4988 micro-stepping driver from Allegro. This is a driver that can control bipolar stepper motors. It can control in a range from full-step mode to one over sixteenth-step mode. The driver includes a translator, which simplifies the motor driver command to depend on two inputs called direction (DIR) and steps (STEP). When the STEP pin receives a signal sequence going from LOW to HIGH it will make the motor move by one increment. How large physical movement this creates will depend on which step mode it is in (Allegro MicroSystems, LLC, u.d.).

Figure 10 A4988 Stepper motor driver card.

The rotational direction of the stepper motor is decided by the signal coming in on the DIR pin. A HIGH signal will make the motor spin clockwise when observed from above, and a LOW signal will make the motor spin counterclockwise. The SLEEP pin has the ability to set the driver into sleep mode to minimize power consumption. This mode is activated when the signal is LOW. The RESET pin has the ability to reset the translator to a predefined condition. This is toggled by sending a LOW signal followed by a HIGH signal.

The signal to RESET must be HIGH in order for the driver to register inputs on the STEP pin. The MS1, -2 and -3 are used to select the step mode. All pins at LOW give a full step condition and all pins at HIGH give the one over sixteenth step condition. The other step conditions are achieved by different combinations of HIGH and LOW. The ENABLE input will turn off all field effect transistor (FET) outputs when in HIGH (Allegro MicroSystems, LLC, u.d.).

The driver has two power inputs. VDD and VMOT, both with corresponding ground pins. The VDD and ground must be connected to the logic device, for instance Raspberry Pi. The VMOT and ground are connected to a power supply delivering in the range from 8V to 35V (Allegro MicroSystems, LLC, u.d.). Between the VMOT and ground, it is recommended to install a capacitor to protect the driver from possible voltage spikes from the power supply (Last Minute Engineers, u.d.).

2.9.5 Analog-to-digital IC: MCP3008

Many of the sensors in this project have analog output signals. Since the Raspberry Pi 4 has no analog input pins (Raspberry Pi Ltd., 2019, pp. 10-11), it is necessary to convert these analog signals to digital ones that can be processed by the Raspberry Pi. It is here the MCP3008 integrated circuit (IC) comes into the picture. There are documented examples of

this IC being used to convert analog signals for the Raspberry Pi (see (DiCola, 2016) and (Sklar, 2012)).

There are two different ways the MCP3008 can be connected to the Raspberry Pi, with software SPI or hardware SPI (DiCola, 2016). SPI stands for serial peripheral interface and is a method of synchronous data transferring (Bolton, 2019, p. 364). The practical difference is that the hardware SPI requires that the SPI pins CLK, DOUT, DIN and CS/SHDN connect to their GPIO counterparts on the Raspberry Pi (DiCola, 2016) (Microchip, 2008) , unlike the software SPI where this can be set in the software (DiCola, 2016). These four connections are used to send and receive information from the Raspberry Pi. The digital information sent is received on one or more of the MCP3008's eight analog channels called CH0, CH1, … and CH7 (Microchip, 2008, p. 15).

The maximum voltage for the input at the channels equals the reference voltage V_{ref}, which is a maximum of 5V (Microchip, 2008, p. 3). It is powered by supplying the MCP3008 with a voltage between 2.7V and 5.5V to V_{ref} and V_{dd} (Microchip, 2008, p. 1), but keeping in mind that maximum power into the channels is limited by V_{ref}. It should therefore be made sure that no input to the channels exceeds 3.3V, alternatively, V_{ref} and V_{dd} could be supplied with 5V if it will receive signals with higher voltage.

2.9.6 Force/pressure sensors in the testing arm

Force-sensitive resistors (FSR) are used to measure the force applied to the test subject by the testing arm. These sensors work by having a connective film laying on top of a circuit with high resistance and form the pressure pad (Bolton, 2019, p. 60) (Interlink Electronics, 2017). When pressure is applied to the connective film, the current in the circuit can flow through more of the connective film, lowering the resistance and leading to a drop in the voltage (Bolton, 2019, p. 61) (Interlink Electronics, 2017). Consequently, the output voltage increases and can be used to measure the force applied to the FSR sensor.

In this thesis, two *Interlink Electronics FSR 402*. These sensors have a sensitivity range of 0.2N to 20N (Interlink Electronics, 2017). Therefore, the upper limit is twice the 10 N that has been assumed as the maximum force to be applied to the test subject. However, the 0.2N sets the lower limit for the force (and thus stress) that can be tested by the fatigue testing machine.

The *Interlink Electronics FSR 402* can take an input voltage of +5V and depending on the resistors (or sensor card) used, it outputs from 0V close up to 5V depending on the pressure applied to the pressure pad (Interlink Electronics, 2017). Thus, one can adjust this as needed, but it heavily affects the linearity characteristics of the sensor (Interlink Electronics, 2017). There are three connections for the sensor: 1) 5 voltage in, 2) voltage out to ground, and 3) the analog out signal that signifies the force applied to the pressure sensor (Interlink Electronics, 2017). The 3D model is downloaded from Grabcad (Grabcad, 2019).

2.9.7 Power supply unit (PSU)

The power supply unit (PSU) has the purpose of supplying electricity to the various electrical components and to the motors. There exists a multitude of options. In this project, a commercial PSU designed for personal computers is utilized to power the machine. This project uses the ATX motherboard connectors pinouts. These pinouts give different levels of voltages like GND, 3.3V, 5V, 12V and -12V (Rozenblat, 2022). In addition to these, there are special pinouts like PS ON that must be connected to ground in order for the PSU to supply any voltage in the pinouts (Rozenblat, 2022) and there is a pinout called PWR_OK which shows whether the power output is within specs and is used to signal the motherboard to reboot (Kozierko, 2001).

2.9.8 Potentiometer

The most common type of variable resistors is called potentiometers or just pot. The resistance can be changed through a range by manipulating a knob, slide or mechanical screw (Alciatore, 2019, p. 19).

In this project, a through-hole potentiometer will be used, which is suitable for mounting on the test arm. It is a rotary position sensor and has a minimum resistance of 2,5 kΩ and maximum resistance of 10 kΩ. The resistance of this potentiometer is varied by rotating an inner ring formed as a D (Bourns, u.d.).

2.9.9 Wire diameter and current

Wires have resistance and can cause heat development if the current is high enough. Therefore, which type of wire to use must be considered. Higher cross-section areas (A) mean that the current (I) can easier flow through the wire, thus less current density (J). The current density is defined $J = \frac{I}{A}$ and the graph in Figure 11 shows the allowable current density for wires (Gomeringer, et al., 2017, pp. 53-4).

Allowable current denisty
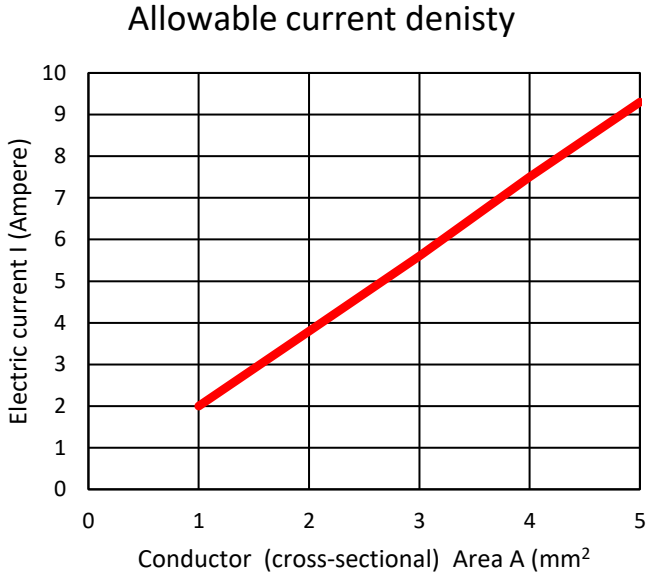
Figure 11 Allowable current density (remade based on Gomeringer, et al., 2017, p. 54).

2.10 Mechanics and von Mises yield criterion

Von Mises yield criterion in mechanics is used to calculate whether a part will fail by yielding, assuming that the material is ductile (Bell, 2014). The criterion states that a yield will happen when the following equivalence is satisfied (Bell, 2014, p. 325):

$$\sigma_j = f_y \tag{17}$$

Here σ_j is the von Mises stress and is defined as the following equation (Bell, 2014, p. 325):

$$\sigma_j = \sqrt{\sigma_1^2 + \sigma_2^2 - \sigma_1^2 \sigma_2^2} \tag{18}$$

This requires the calculations of the principal stresses σ_1^2 and σ_2^2, which are defined as (Bell, 2014, p. 273):

$$\sigma_{1,2} = \frac{\sigma_x + \sigma_z}{2} \pm \sqrt{\left(\frac{\sigma_x - \sigma_z}{2}\right)^2 + \tau^2} \tag{19}$$

σ_x is the normal stress along the x-axis, σ_z is the normal stress along the z-axis and τ is the shear stress (Bell, 2014). The normal and shear stress can be calculated from these formulas based on superposition (Bell, 2014, p. 83):

$$\sigma_x = \frac{M}{I_y} z + \frac{N}{A} \tag{20}$$

$$\tau = \frac{VS}{I_y b} \tag{21}$$

Where:

$\sigma_x \ldots normal\ stress$

$\tau \ldots shear\ stress$

$M \ldots bending\ moment$

$I_y \ldots second\ moment\ of\ area$

$z \ldots position\ on\ the\ cross\ section\ along\ axis$

$N \ldots axial\ force$

$A \ldots area\ of\ cross\ section$

$V \ldots shear\ force$

$S \ldots first\ moment\ of\ area$

When calculating these values, some of the values can be looked up in tables in Bell (2014), such as the second and first movement of area, but it is necessary to make a share and moment diagram to obtain M, N and V (Bell, 2014, pp. 33-4). This requires the drawing of a free body diagram (FBD). The procedure on how to make these two diagrams will not be elaborated on in this thesis but will follow the procedures described in Bell (2014). The share and moment diagram requires to calculate all the forces in the system, which can be done in a static system by using the equilibrium equations (Bell, 2014, pp. 45-47, 70, 111-28):

$$\text{Either} \sum F_x = 0 \ \ \text{and} \ \sum F_z = 0 \ \ \text{and} \sum M_p = 0$$

$$\text{or} \quad \sum F_{x\ or\ z} = 0 \ \ \text{and} \ \sum M_A = 0 \ \ \text{and} \sum M_B = 0 \qquad\qquad (22)$$

$$\text{or} \quad \sum M_A = 0 \ \ \text{and} \ \sum M_B = 0 \ \ \text{and} \sum M_C = 0$$

2.11 Finite Element Method

When designing complex geometric structures, it can be challenging to calculate stress and deformation. To address this issue, engineers and scientists often use the finite element method (FEM). FEM is a numerical method that involves dividing a complex object into smaller, simpler parts or elements that are connected at specific points or nodes. By applying mathematical principles and techniques using computer software, Finite Element Analysis (FEA) determines the behavior of each element and their interactions with each other (Kurowski, 2020, pp. 5-7).

FEM can be used to analyze various physical phenomena, including structural mechanics, soil mechanics, fluid mechanics, acoustic and electromagnetism. It is commonly used in the design and optimization of products and systems in aerospace, automotive, civil and mechanical engineering fields (Brush, 2019). FEM has improved and simplified the design process by enabling engineers and scientists to test prototypes using simulations in software. This allows them to make changes to the design and solutions before starting the physical building process of the prototype (Kurowski, 2020, p. 7).

The FEM process involves several steps, including defining the geometry of the object, selecting material properties, creating a mesh or network of elements, applying boundary conditions and loads, and finally, performing the analysis and interpreting the results. FEM is a powerful tool for predicting the behavior of complex systems, reducing costs and improving efficiency in the design and manufacturing processes (DNV-GL, 2016).

2.11.1 Simulation software

The Software that has been used is SolidWorks 2022-2023 Education edition from Dassault Systems, this is a well-known CAD software, and this has also been used in the Mechanical Engineer study program at NTNU. For FEM analysis, the simulation part integrated into the 3D CAD software has been used.

2.11.2 Mesh

To be able to do the calculation of a geometric model with simulation software, it is necessary to divide the model into small elements and connected them with each other through common points called nodes. This operation is called meshing and is important in the analysis of the designed geometric model. The simulation program automatically generates different types of mesh, such as solid mesh for solid models with tetrahedral solid elements, shell mesh for surface geometry with thin parts such as sheet plates, and beam mesh for structural elements made of beams and pipes. Often in design, it will be a combination of types of mesh since the model can have thin plates in combination with a solid structure (Dassault Systems, 2021).

First-order elements are used when the model has straight lines before and after the load. Second-order elements, such as tetrahedral elements, are used when the model has surfaces and thicker bodies (Ninive, 2018). A smaller size of mesh elements increases the quality of

the mesh and leads to more calculations during simulations. This sets a higher demand for the capacity of the computer, and it will take additional time to do the calculations. Mesh control can be applied to areas with high stress to reduce the number of calculations and computer capacity required. This results in a higher quality mesh for the selected area compared to the rest of the object (Kurowski, 2020, p. 83). Therefore, the result can get more accurate by use of this. Also, during simulations to avoid high stress singularities in areas with sharp edges it can be added fillets or created a radius. To check the quality of a mesh one can use the function named aspect ratio on (Solid Mesh) the element, that is the ratio between the longest edge and the shortest edge (Kurowski, 2020, p. 442), where a perfect mesh will have a ratio close to 1 (100%). A mesh with an acceptable ratio has a ratio of less than 5 in 90% of the elements. For second-order mesh (shell and high-quality solid mesh), Jacobian can be used. For second order elements, the closer it is to 1 the better. If the location of the mid-side node is located right above the middle of a line between the edges, the value is 1.0. The Jacobian gains when the deflection of the edges get bigger. A good quality mesh has a ratio of 1 to 10 in 90% of its elements (Kurowski, 2020, p. 442). Figure 12 is an example of meshing.

No. of DOF: 10524 Curvature mesh: (1.845-5.537) mm Mesh control: NA Max stress: 117,484 MPa	No. of DOF: 64980 Curvature mesh: (1.435-4.3065) mm Mesh control: 1.4355mm Max stress: 119,197 MPa	No. of DOF: 109095 Curvature mesh: (0.9399-2.8198) mm Mesh control: 1.4355mm Max stress: 119,602 MPa	No. of DOF: 266760 Curvature mesh: (2.00) mm Mesh control: 1.048mm Max stress: 119.441 MPa
Jacobian ratio: min: 1.00, max: 1,465	Jacobian ratio: min: 1.00, max: 1,447	Jacobian ratio: min: 1.00, max: 1,493	Jacobian ratio: min: 1.00, max: 1,312
Aspect ratio: min: 1.102, max: 3.432, Percent W/aspect ratio <3: 99.7, Percent W/aspect ratio<10: 0	Aspect ratio: min: 1.038, max: 3.3,784, Percent W/aspect ratio <3: 99.5, Percent W/aspect ratio<10: 0	Aspect ratio: min: 1.054, max: 3.514, Percent W/aspect ratio <3: 99.9, Percent W/aspect ratio<10: 0	Aspect ratio: min: 1.043, max: 3.992, Percent W/aspect ratio <3: 99.9, Percent W/aspect ratio<10: 0

Figure 12 Maximum von Mises on different sized elements.

2.11.3 Convergence of Stress

It is necessary to check that the maximum stress from the simulation converges when the element size in the mesh is decreased to ensure that the mesh applied to the model yields a good analysis and avoids stress singularity in sharp edges (Kurowski, 2020, pp. 68-9). A convergence test that pass is illustrated in Figure 13.
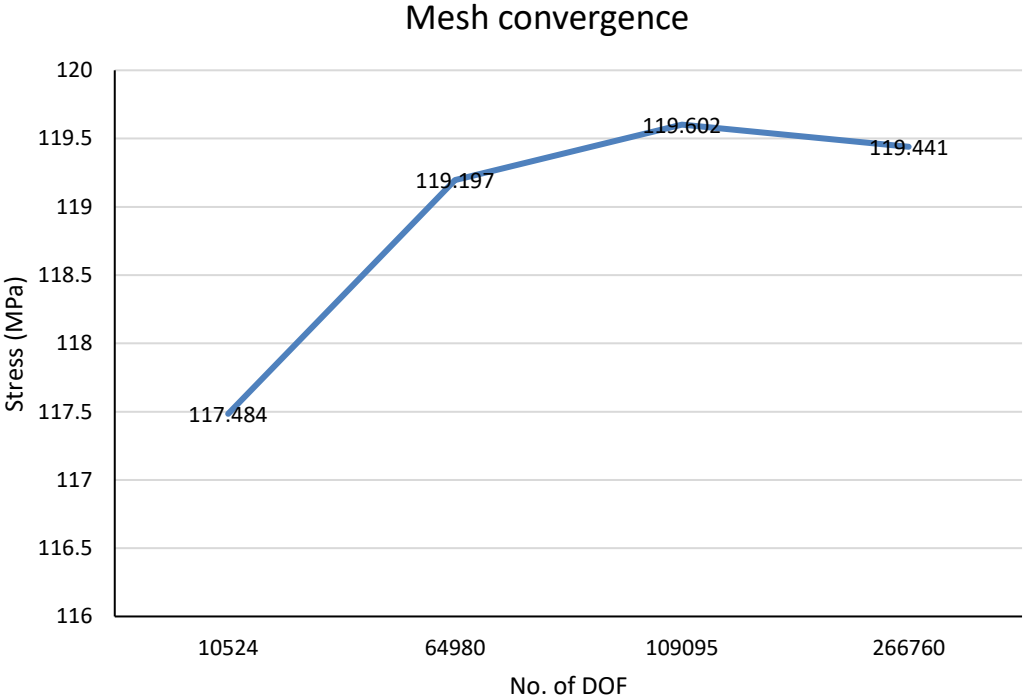
Mesh convergence

Figure 13 Convergence of stress values from Figure 12.

3 Method and analysis

3.1 Early sketches

The process of creating the machine has had several distinct phases. In the elongation of the ide-phase hand drawn sketches were made to visualize the different ideas and discuss the advantages and disadvantages of each proposal. Even though each team member had the same concept in mind of the fatigue machine, the hand sketches and solutions on how the testing would take place were quite different (some of these sketches are shown in Figure 14). This phase was important as verbal explanations of the different ideas became insufficient in detail as the concept developed. When each team member had presented their sketches and then their refined sketches, the next phase was to develop CAD-models.
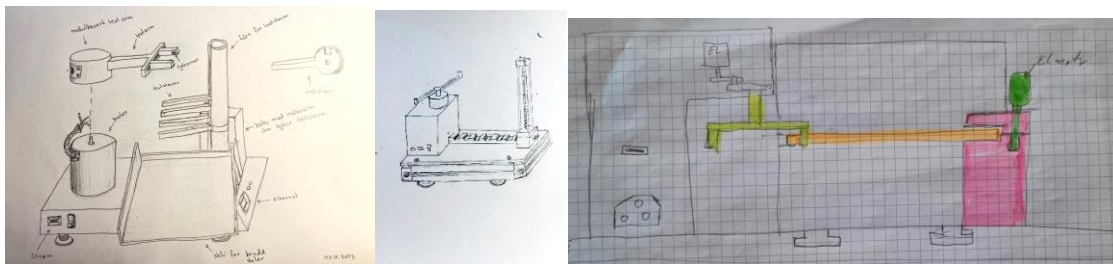
Figure 14 Early sketches.

3.2 CAD-Models: rejected designs

The design of the fatigue testing machine is important for reaching the different goals set in the thesis. The aim of the design has been to model a machine that fulfills all listed capabilities in the introduction (the sub-goals) as well as meeting the overall intention of being inexpensive and easy to build. This task can be somewhat contradictory, as a complex design and over-dimensioning is a natural consequence when focusing on reaching the desired capabilities, but this affects how simple and economic the machine is. The design phase has brought different ideas on how to manage this dilemma.
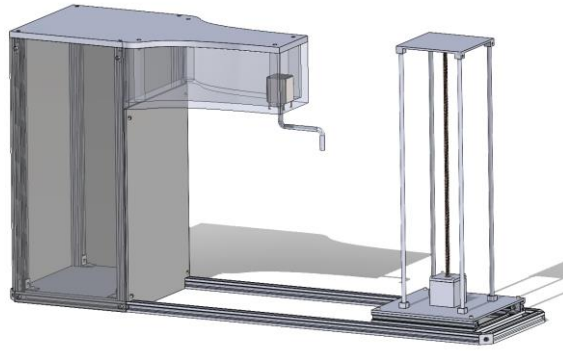
Figure 15 Prototype 1.

Prototype number one used a test arm that was attached directly to the engine shaft. This is not ideal as the connection between the test arm and engine shaft could get a high strain load. Due to the inversion of the engine, the test arm would also have to be connected thoroughly for the fixture in the vertical axis in order for it to not fall down. The casing holding the motor was intended as a cover for the electronics. However, this housing did prove to be much larger than necessary.
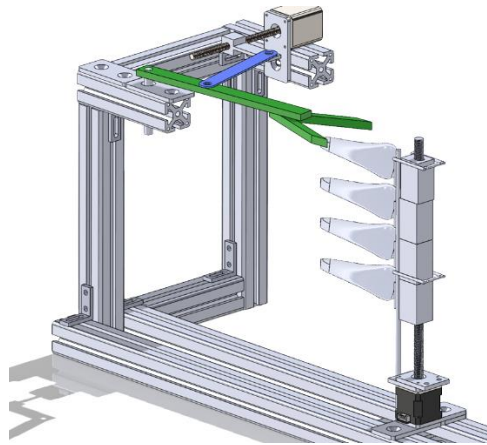
Figure 16 Prototype 2.

Prototype number two continued the use of aluminum profiles in the design. A new test arm was fitted to the design in order to insert a gear ratio between the engine shaft and the test arm. It was also intended to reduce the bending moment across the engine shaft. A flaw of this design is that the screw connection between the mechanism of the test arm and the engine shaft would probably have produced excessive heat due to friction. The test machine should be able to operate for many consecutive hours as it is intended to load and run multiple tests on the magazine. Therefore, parts producing a large amount of heat should be avoided.

46

The prototype contains a magazine mechanism for the test subjects, which uses custom steel bars as the frame. Finite element method simulation revealed that a custom-made plastic part produced with additive manufacturing would be sufficient as it will cope with the applied load. As it is easier to produce the part in plastic, this was redesigned for the final prototype design. Prototypes one and two were drawn with a stepper motor for moving the test arm, as they were produced before the choice of a DC motor engine type was made.

3.3 CAD-Models: chosen design

The chosen design, also called the final prototype, shown in Figure 17 was drawn based on lessons learned from the rejected designs, as well as through brainstorming sessions. The chosen design has itself been further developed through multiple instances of trials and errors, much like the rejected designs, but with less comprehensive changes. The figures underneath display the final version of the chosen design. Compared to the earlier sketches and rejected designs, the test samples are mounted the other way around. This results in an overall reduced frame, minimizing the space between the stepper motor powering the magazine screw and the electrical box. This also makes the design tidier as the cables going to the motor can be kept near the electrical hub while still being able to vary the size of the test subjects. The magazine tower can be moved by loosening the wing screws.
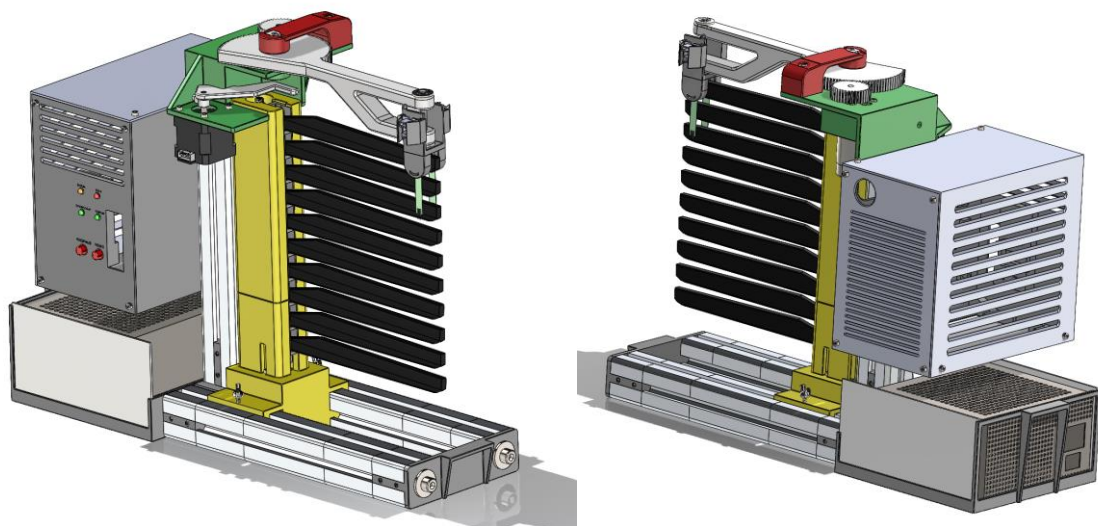
Figure 17 Chosen design front (left) and aft (right).

The aluminum frame is held together by 3D-printed plastic parts. These are connected and fastened to the aluminum profiles by the use of screws. Plastic parts have also been used to make the magazine tower, motor plate, end covers, frame for the power supply unit and the electrical box. The magazine tower is printed in two parts as its long dimension is unsuitable for many common 3D printers. It is assembled by using a strong adhesive. The motor plate is attached to the frame by a screw. The plate has slots and holes for fastenings for the DC motor, gears, test arm and two stepper motors.

A gear drive has been incorporated between the DC motor and the test arm. This makes the test arm move less than a direct connection would, as well as delivers more torque to the test subjects. At the end of the test arm, a tilt mechanism is installed so that the added force sensors will get a perpendicular force application from the test samples. On top of the support link of the test arm, there is a potentiometer reading the angle of the test arm. This will, along with the encoder of the DC motor, give angular data to the microcontroller. An ejector arm is fitted to a second stepper motor. The purpose of the ejector arm is to remove test subject holders and the remainder of the test subjects after a sample is complete. The idea is that the magazine stepper motor should first change the active test subject by rotating the threaded rod in the magazine, before the ejector arm removes the remains making the test machine ready for a new sample without physical interference from the old.

The power supply unit sits opposite the test subjects and is installed in a frame connected to the main frame via the end covers. Above the PSU there is an electrical box. This box houses electrical components such as a microcontroller, motor driver boards, bread boards, voltage and ampere sensors as well as a large part of the wiring. On the side of the electrical box there is a panel with four status lights and two switches used to observe and interfere with the different states of the machine. As the electrical box is positioned between the motor plate and the PSU there is a short distance between the majority of the connected parts. This helps both the general tidiness of the machine as well keeping wire lengths to a minimum.

3.4 Production drawings and instructions for assembly

SCALE 1 : 5

ITEM NO.	PART NUMBER	DESCRIPTION	Weight
1		Frame Assembly	2586.87
2		Magazin Tower	1686.55
3		Motorplate assembely_1	1115.51
4		Rear end cover assembly	177.848
5		Electronic Box	427.808

UNLESS OTHERWISE SPECIFIED:
DIMENSIONS ARE IN MILLIMETERS
UNLESS OTHERWISE SPECIFIED
TOLERANCES: +/-0.5. HOLES H8/h9

FINISH:

DEBURR AND BREAK SHARP EDGES

DO NOT SCALE DRAWING

REVISION

	NAME	SIGNATURE	DATE
DRAWN	Einar Reistad		14.05.2023
CHK'D	Torgeir Brandsar		14.05.2023
APPV'D			
MFG			
Q.A			

TITLE:

Test Machine

MATERIAL:

DWG NO.

Assembly

A3

WEIGHT: 6165.212

SCALE:1:6

SHEET 1 OF 2B
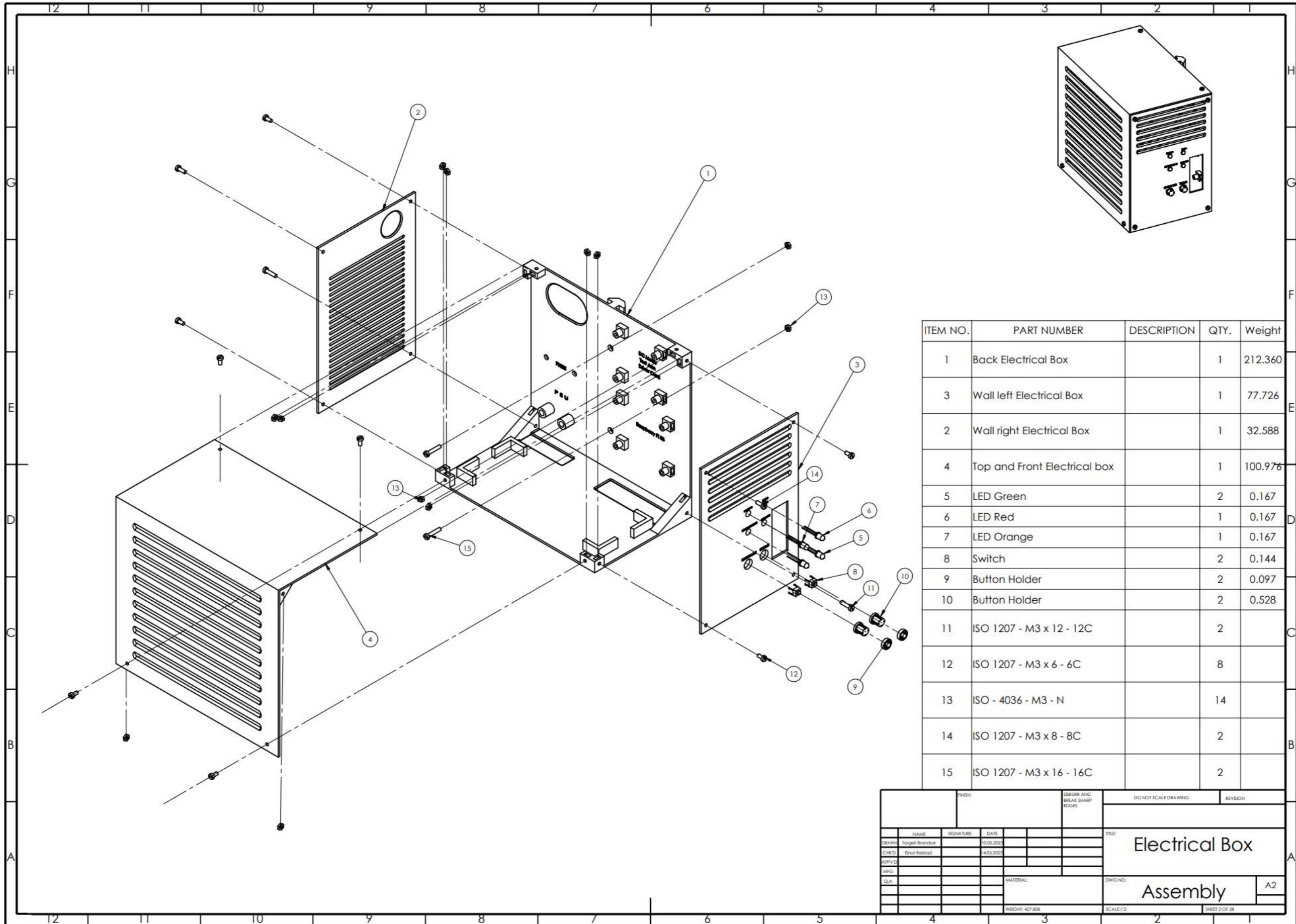
ITEM NO.	PART NUMBER	DESCRIPTION	QTY.	Weight
1	Back Electrical Box		1	212.360
3	Wall left Electrical Box		1	77.726
2	Wall right Electrical Box		1	32.588
4	Top and Front Electrical box		1	100.976
5	LED Green		2	0.167
6	LED Red		1	0.167
7	LED Orange		1	0.167
8	Switch		2	0.144
9	Button Holder		2	0.097
10	Button Holder		2	0.528
11	ISO 1207 - M3 x 12 - 12C		2	
12	ISO 1207 - M3 x 6 - 6C		8	
13	ISO - 4036 - M3 - N		14	
14	ISO 1207 - M3 x 8 - 8C		2	
15	ISO 1207 - M3 x 16 - 16C		2	

	NAME	SIGNATURE	DATE		TITLE:	
DRAWN	Torgeir Brandsar		10.05.2022			
CHK'D	Einar Reistad		14.05.2022		Electrical Box	
APPV'D						
MFG						
Q.A					Assembly	A2

FINISH: DEBURR AND BREAK SHARP EDGES   DO NOT SCALE DRAWING   REVISION

WEIGHT: 427.808   SCALE:1:2   SHEET 2 OF 28

50

Technical drawing: Wall right — Electrical Box

Dimensions (mm): Ø3.0, Ø25.0, 20.0, 30.0, 1.0, 180.0, 6.0, 7.0, 1.7, 92.0, 122.0

ITEM NO.	PART NUMBER	DESCRIPTION	QTY.	Weight
3	Wall right Electrical Box		1	32.588

UNLESS OTHERWISE SPECIFIED:
DIMENSIONS ARE IN MILLIMETERS

UNLESS OTHERWISE SPECIFIED
TOLERANCES: +/- 0.5. Holes H8/h9
SCALE 1:2

FINISH:

DEBURR AND BREAK SHARP EDGES

DO NOT SCALE DRAWING

REVISION

	NAME	SIGNATURE	DATE				TITLE:
DRAWN	Torgeir Brandsar		10.05.2023				Electrical Box
CHK'D	Einar Reistad		14.05.2023				
APPV'D							
MFG							
Q.A							

MATERIAL:
Polymer (PLA)

DWG NO.
Wall right

A4

WEIGHT: 32.588

SCALE:1:2

SHEET 3 OF 29

ITEM NO.	PART NUMBER	DESCRIPTION	QTY.	Weight
2	Wall left Electrical Box		1	77.726

UNLESS OTHERWISE SPECIFIED: DIMENSIONS ARE IN MILLIMETERS

UNLESS OTHERWISE SPECIFIED TOLERANCES: +/- 0.5. Holes H8/h9 SCALE 1:2

FINISH:

DEBURR AND BREAK SHARP EDGES

DO NOT SCALE DRAWING

REVISION

	NAME	SIGNATURE	DATE
DRAWN	Torgeir Brandsar		10.05.2023
CHK'D	Einar Reistad		14.05.2023
APPV'D			
MFG			
Q.A			

TITLE:

Electrical Box

MATERIAL: Polymer (PLA)

DWG NO.

Wall left

A4

WEIGHT: 77.726

SCALE:1:2

SHEET 4 OF 28

SECTION E-E

DC Motor
Test Arm
Driver Card

Raspberry PI 3B

FUSES

PSU

E

ITEM NO.	PART NUMBER	DESCRIPTION	QTY.	Weight
1	Back Electrical Box		1	212.360

UNLESS OTHERWISE SPECIFIED:
DIMENSIONS ARE IN MILLIMETERS

UNLESS OTHERWISE SPECIFIED
TOLERANCES: +/- 0.5. Holes H8/h9
SCALE 1:2

FINISH:

DEBURR AND
BREAK SHARP
EDGES

DO NOT SCALE DRAWING

REVISION

	NAME	SIGNATURE	DATE
DRAWN	Torgeir Brandsar		09.05.2023
CHK'D	Einar Reistad		14.05.2023
APPV'D			
MFG			
Q.A			

TITLE:

Electrical Box

MATERIAL:
Polymer (PLA)

DWG NO.

Back

A3

WEIGHT: 212.360

SCALE:1:2

SHEET 5 OF 28

ITEM NO.	PART NUMBER	DESCRIPTION	QTY.	Weight
4	Top and Front Electrical Box		1	100.976

UNLESS OTHERWISE SPECIFIED:
DIMENSIONS ARE IN MILLIMETERS

UNLESS OTHERWISE SPECIFIED
TOLERANCES: +/- 0.5. Holes H8/h9
SCALE 1:2

FINISH:

DEBURR AND BREAK SHARP EDGES

DO NOT SCALE DRAWING

REVISION

	NAME	SIGNATURE	DATE
DRAWN	Torgeir Brandsar		10.05.2023
CHK'D	Einar Reistad		14.05.2023
APPV'D			
MFG			
Q.A			

TITLE:

Electrical Box

MATERIAL:
Polymer (PLA)

DWG NO.
Top and Front

A3

WEIGHT: 100.976

SCALE:1:2

SHEET 6 OF 28

54

ITEM NO.	PART NUMBER	DESCRIPTION	QTY.	Weight
9	Button Holder		2	0.097
10	Button		2	0.528

UNLESS OTHERWISE SPECIFIED:
DIMENSIONS ARE IN MILLIMETERS

UNLESS OTHERWISE SPECIFIED
TOLERANCES: +/- 0.5. Holes H8/h9
SCALE 4:1

FINISH:

DEBURR AND
BREAK SHARP
EDGES

DO NOT SCALE DRAWING

REVISION

	NAME	SIGNATURE	DATE
DRAWN	Torgeir Brandsar		11.05.2023
CHK'D	Einar Reistad		14.05.2023
APPV'D			
MFG			
Q.A			

MATERIAL:
Polymer (PLA)

TITLE:
Electrix Box

DWG NO.
Button and
Button Holder

A4

WEIGHT:

SCALE:1:2

SHEET 7 OF 28

55

DETAIL A
SCALE 4 : 1

A

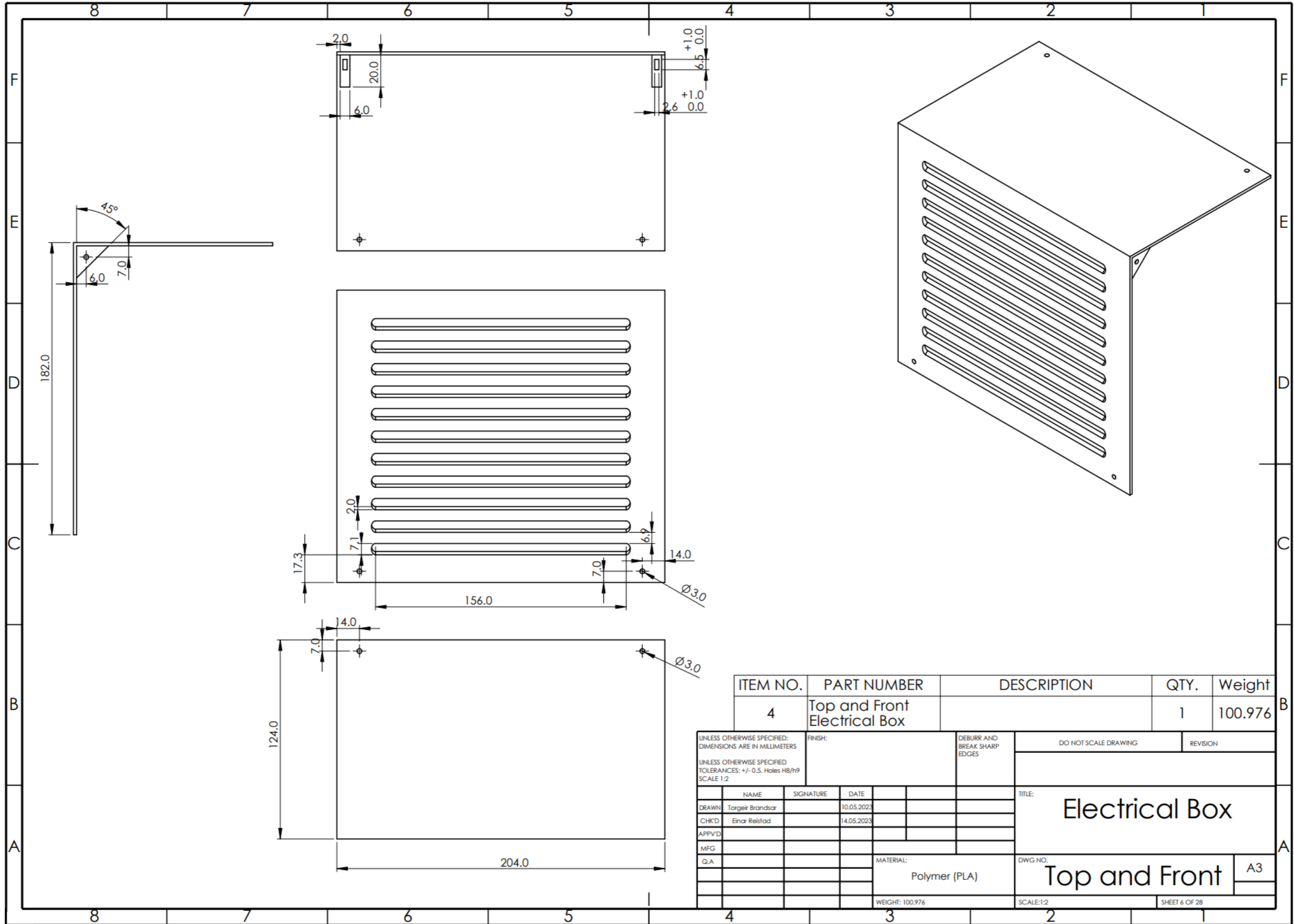| ITEM NO.	PART NUMBER	DESCRIPTION	QTY.	Weight
4	Lower part rear end cover		1	177.848

UNLESS OTHERWISE SPECIFIED:
DIMENSIONS ARE IN MILLIMETERS

UNLESS OTHERWISE SPECIFIED
TOLERANCES: +/- 0.5. Holes H8/h9
SCALE 1:2

FINISH:

DEBURR AND
BREAK SHARP
EDGES

DO NOT SCALE DRAWING

REVISION

	NAME	SIGNATURE	DATE
DRAWN	Torgeir Brandsar		10.05.2023
CHK'D	Einar Reistad		14.05.2023
APPV'D			
MFG			
Q.A			

TITLE:

Test Machine

MATERIAL:
Polymer (PLA)

DWG NO.
Lower part rear End Cover

A3

WEIGHT: 177.85

SCALE:1:3

SHEET 8 OF 28
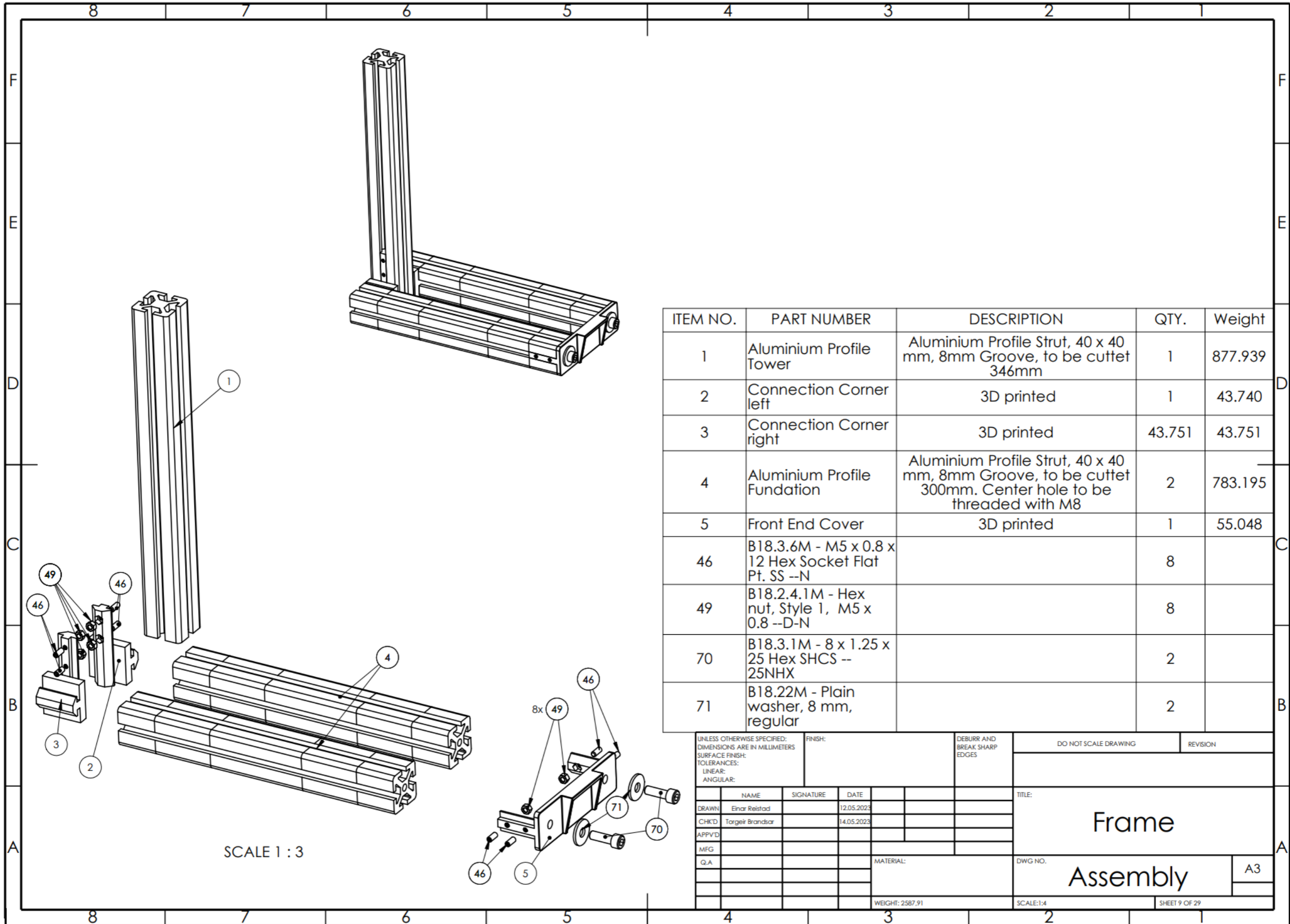
56

ITEM NO.	PART NUMBER	DESCRIPTION	QTY.	Weight
1	Aluminium Profile Tower	Aluminium Profile Strut, 40 x 40 mm, 8mm Groove, to be cuttet 346mm	1	877.939
2	Connection Corner left	3D printed	1	43.740
3	Connection Corner right	3D printed	43.751	43.751
4	Aluminium Profile Fundation	Aluminium Profile Strut, 40 x 40 mm, 8mm Groove, to be cuttet 300mm. Center hole to be threaded with M8	2	783.195
5	Front End Cover	3D printed	1	55.048
46	B18.3.6M - M5 x 0.8 x 12 Hex Socket Flat Pt. SS --N		8	
49	B18.2.4.1M - Hex nut, Style 1, M5 x 0.8 --D-N		8	
70	B18.3.1M - 8 x 1.25 x 25 Hex SHCS --25NHX		2	
71	B18.22M - Plain washer, 8 mm, regular		2	

SCALE 1 : 3

UNLESS OTHERWISE SPECIFIED:
DIMENSIONS ARE IN MILLIMETERS
SURFACE FINISH:
TOLERANCES:
  LINEAR:
  ANGULAR:

FINISH:

DEBURR AND BREAK SHARP EDGES

DO NOT SCALE DRAWING

REVISION

	NAME	SIGNATURE	DATE
DRAWN	Einar Reistad		12.05.2023
CHK'D	Torgeir Brandsar		14.05.2023
APPV'D			
MFG			
Q.A			

TITLE:

Frame

Assembly

A3

MATERIAL:

DWG NO.

WEIGHT: 2587,91

SCALE:1:4

SHEET 9 OF 29

57

SCALE 1.5 : 1

16.9

140.0
115.2
20.2
8.2
7.5
40.0
R4.0
4.7
6.4
12.4

8.1
20.0 10.0
5.0
4x Ø4.2

100.0
2x Ø8.4
5

56.0
3.5
R0.5

Ø4.2mm Holes to be threaded to M5
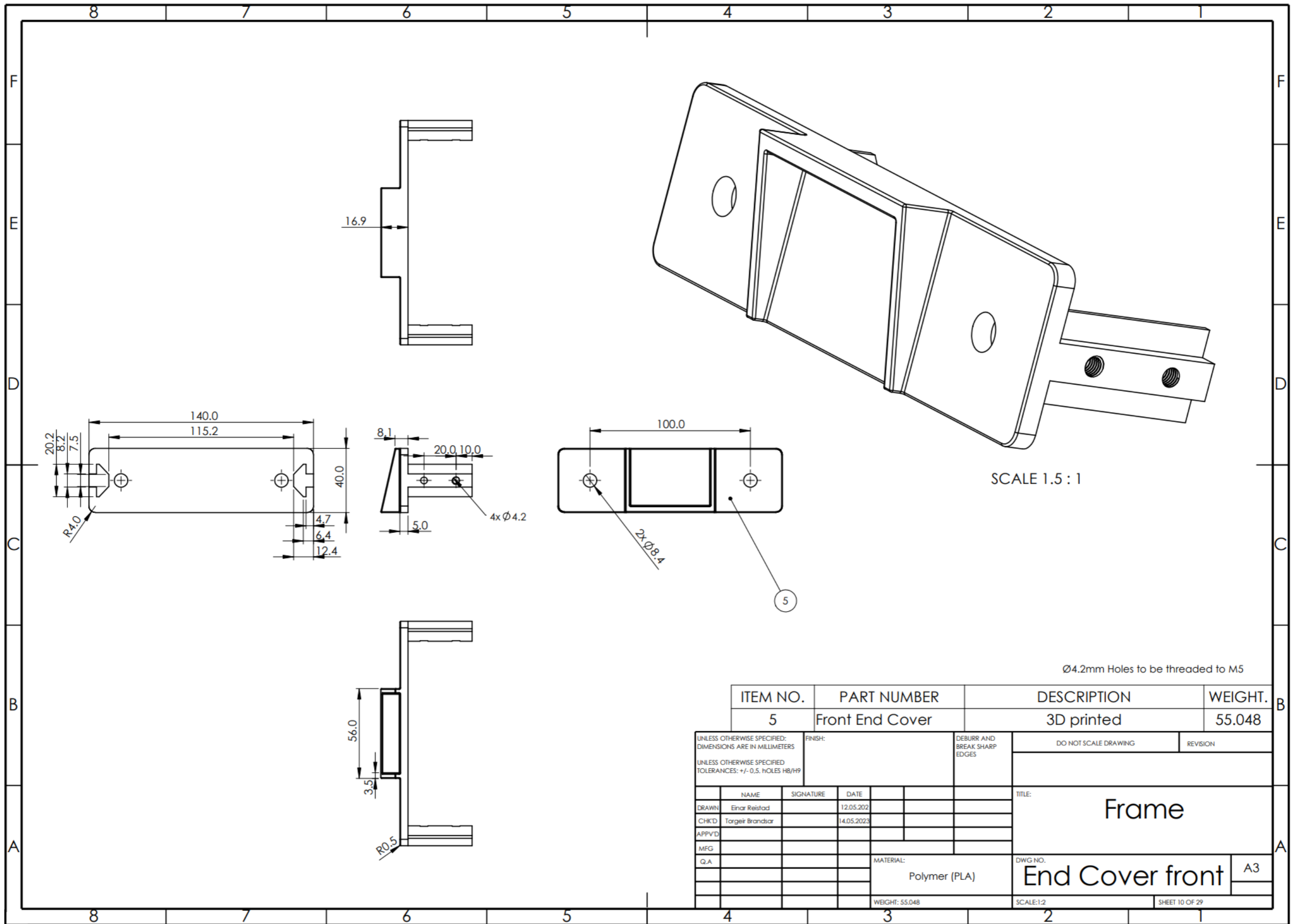
ITEM NO.	PART NUMBER	DESCRIPTION	WEIGHT.
5	Front End Cover	3D printed	55.048

UNLESS OTHERWISE SPECIFIED:
DIMENSIONS ARE IN MILLIMETERS

UNLESS OTHERWISE SPECIFIED
TOLERANCES: +/- 0.5, hOLES H8/H9

FINISH:

DEBURR AND
BREAK SHARP
EDGES

DO NOT SCALE DRAWING

REVISION

	NAME	SIGNATURE	DATE
DRAWN	Einar Reistad		12.05.202
CHK'D	Targeir Brandsar		14.05.2023
APPV'D			
MFG			
Q.A			

TITLE:

Frame

MATERIAL:
Polymer (PLA)

DWG NO.
End Cover front

A3

WEIGHT: 55.048

SCALE:1:2

SHEET 10 OF 29

58

Ø4.2mm Holes to be threaded with M5

3 × Ø4.2

2 × 8.1 ▽ 5

Ø4.2mm Holes to be threaded with M5

3

Ø4.2mm Holes to be threaded with M5
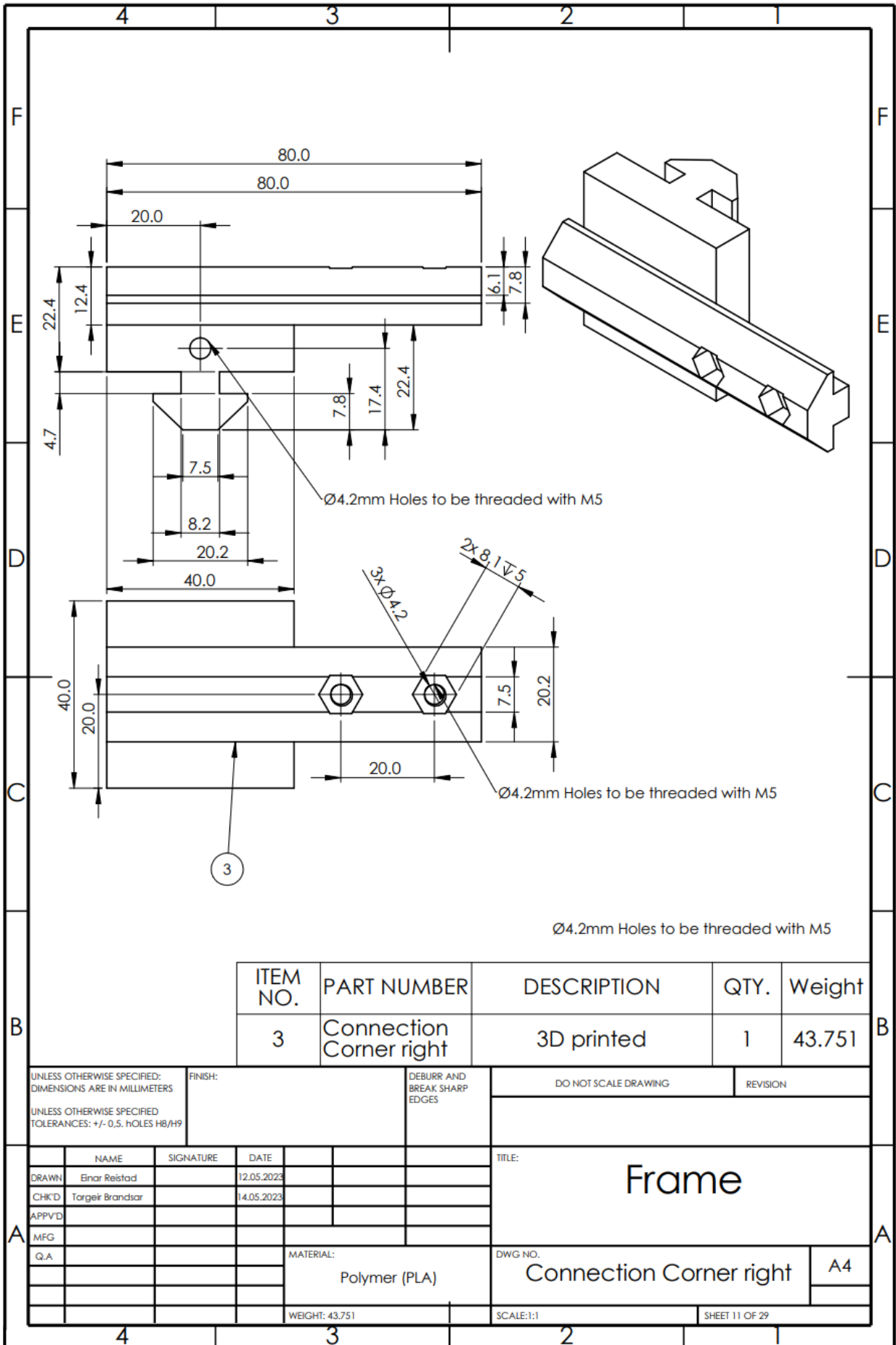
ITEM NO.	PART NUMBER	DESCRIPTION	QTY.	Weight
3	Connection Corner right	3D printed	1	43.751

	NAME	SIGNATURE	DATE
DRAWN	Einar Reistad		12.05.2023
CHK'D	Targeir Brandsar		14.05.2023
APPV'D			
MFG			
Q.A			

TITLE:

Frame

MATERIAL:
Polymer (PLA)

DWG NO.
Connection Corner right

A4

WEIGHT: 43.751

SCALE:1:1

SHEET 11 OF 29

34.8
28.8
27.1
22.4
12.4
7.8
6.1

80.0

40.0
20.2
8.2
7.5

20.0

16.9

Ø 4.2 Holes to be threaded to M5

20.2
8.2

20.0 10.0

3x Ø 4.2

Ø 4.2 Holes to be threaded to M5

Ø 4.2 Holes to be threaded to M5

40.0

Ø 4.2 Holes to be threaded to M5
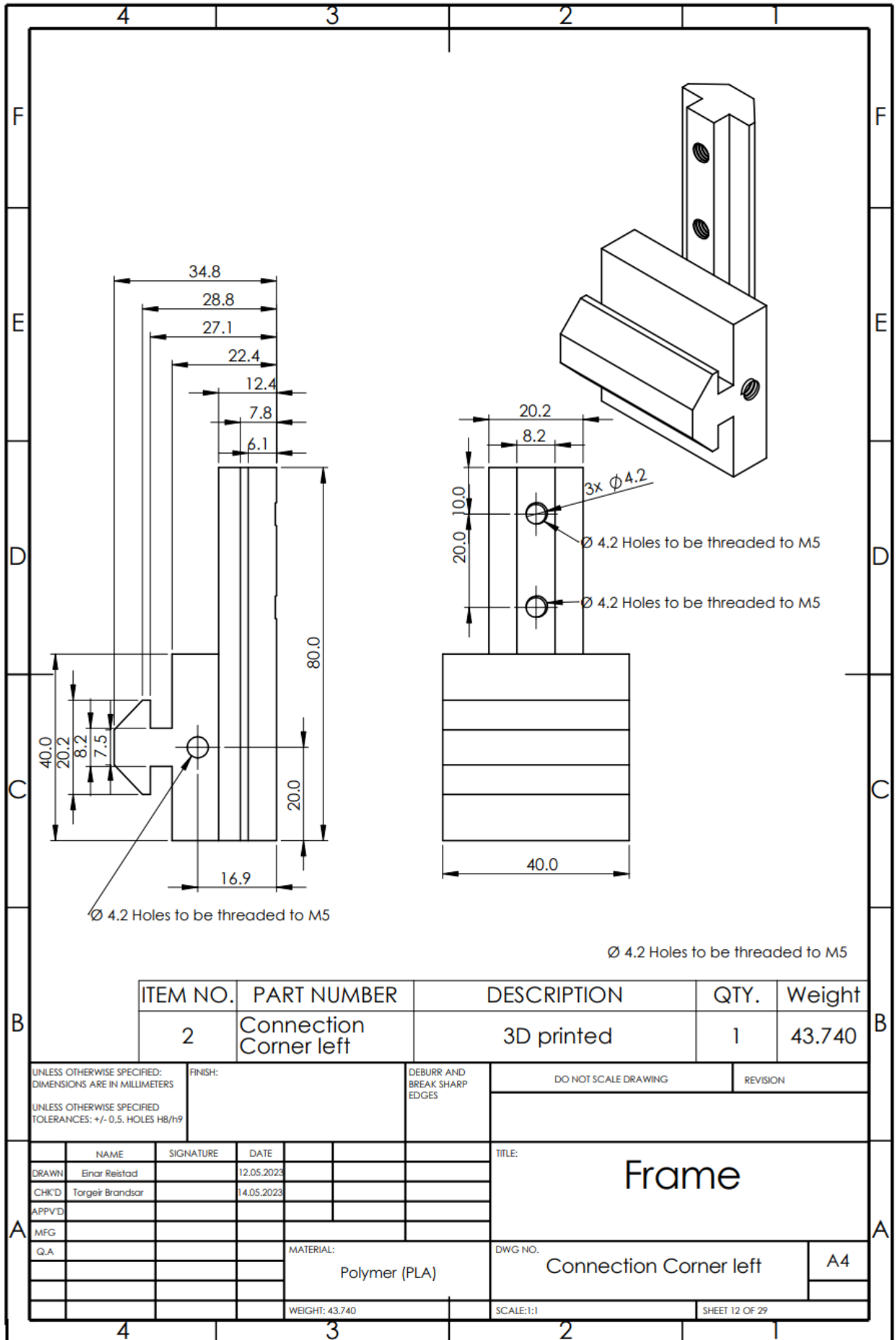
ITEM NO.	PART NUMBER	DESCRIPTION	QTY.	Weight
2	Connection Corner left	3D printed	1	43.740

	NAME	SIGNATURE	DATE
DRAWN	Einar Reistad		12.05.2023
CHK'D	Torgeir Brandsar		14.05.2023
APPV'D			
MFG			
Q.A			

TITLE:

Frame

MATERIAL:
Polymer (PLA)

DWG NO.
Connection Corner left

A4

WEIGHT: 43.740

SCALE:1:1

SHEET 12 OF 29

60
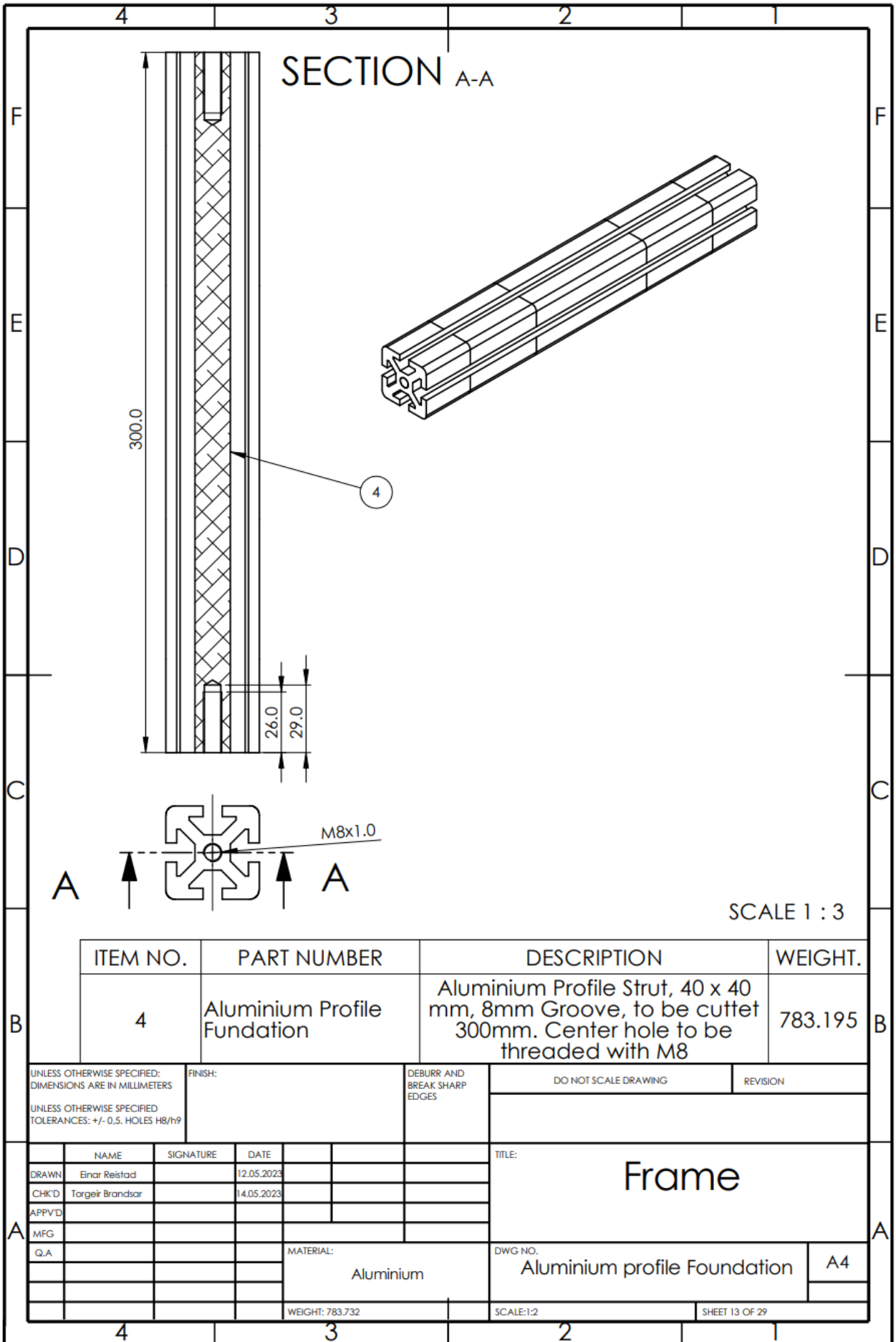
SECTION A-A

300.0

4

26.0
29.0

M8x1.0

A ← → A

SCALE 1 : 3

ITEM NO.	PART NUMBER	DESCRIPTION	WEIGHT.
4	Aluminium Profile Fundation	Aluminium Profile Strut, 40 x 40 mm, 8mm Groove, to be cuttet 300mm. Center hole to be threaded with M8	783.195

UNLESS OTHERWISE SPECIFIED:
DIMENSIONS ARE IN MILLIMETERS

UNLESS OTHERWISE SPECIFIED
TOLERANCES: +/- 0,5. HOLES H8/h9

FINISH:

DEBURR AND
BREAK SHARP
EDGES

DO NOT SCALE DRAWING

REVISION

	NAME	SIGNATURE	DATE				TITLE:	
DRAWN	Einar Reistad		12.05.2023					Frame
CHK'D	Targeir Brandsar		14.05.2023					
APPV'D								
MFG								
Q.A			MATERIAL:				DWG NO.	

Aluminium

Aluminium profile Foundation

A4

WEIGHT: 783.732

SCALE:1:2

SHEET 13 OF 29

61

346.0

12.4
4.7
20.2
8.7
2.0
8.2
40.0
40.0

ITEM NO.	PART NUMBER	DESCRIPTION	QTY.	Weight
1	Aluminium Profile Tower	Aluminium Profile Strut, 40 x 40 mm, 8mm Groove, to be cuttet 346mm	1	877.939

	NAME	SIGNATURE	DATE			
DRAWN	Einar Reistad		14.05.2023			
CHK'D	Torgeir Brandsar		14.05.2023			
APPV'D						
MFG						
Q.A						

TITLE:
Frame

MATERIAL:
Aluminium

DWG NO.
Aluminium Profile Tower

A4

WEIGHT: 877.939

SCALE:1:3
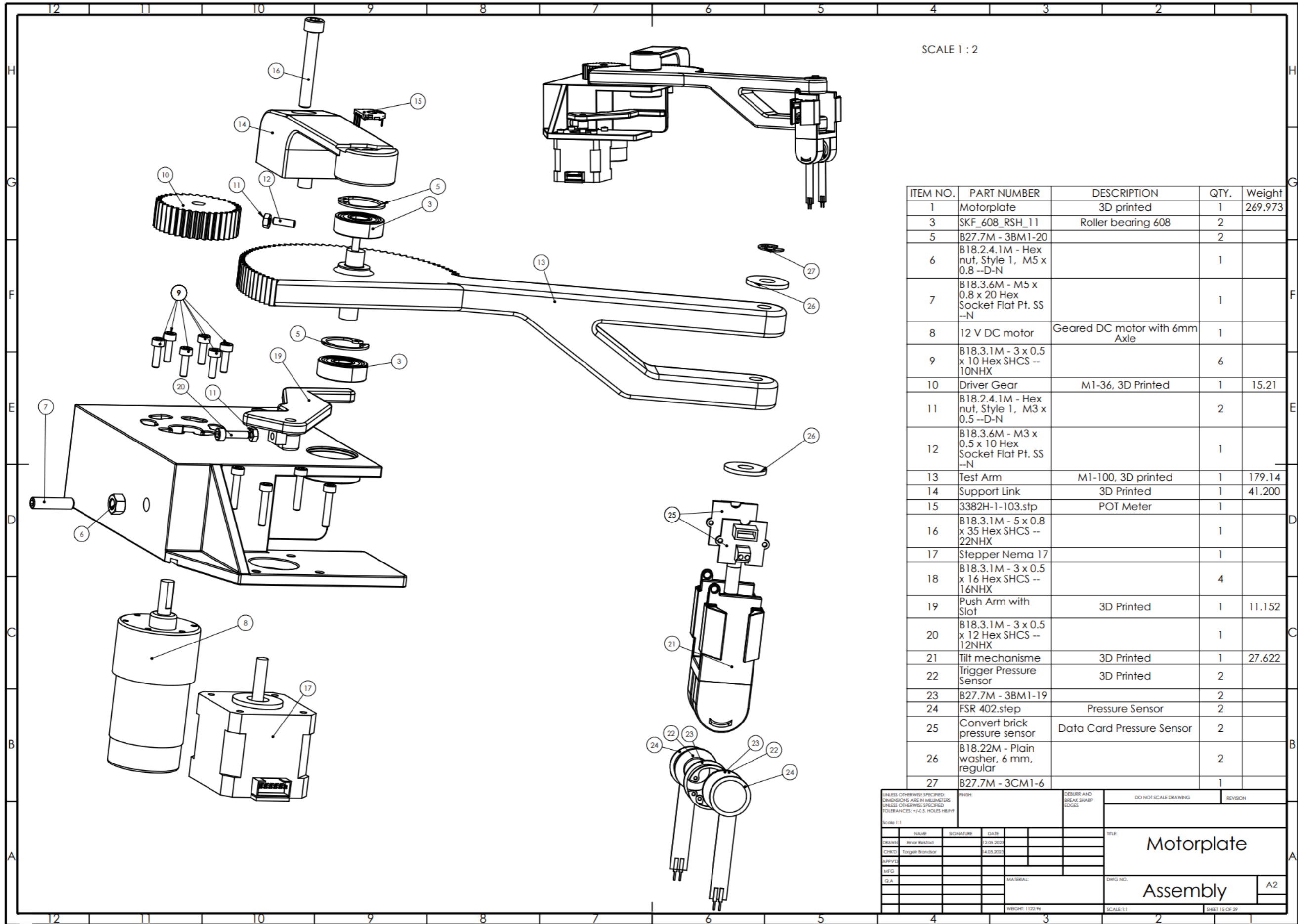
SCALE 1 : 2

ITEM NO.	PART NUMBER	DESCRIPTION	QTY.	Weight
1	Motorplate	3D printed	1	269.973
3	SKF_608_RSH_11	Roller bearing 608	2	
5	B27.7M - 3BM1-20		2	
6	B18.2.4.1M - Hex nut, Style 1, M5 x 0.8 --D-N		1	
7	B18.3.6M - M5 x 0.8 x 20 Hex Socket Flat Pt. SS --N		1	
8	12 V DC motor	Geared DC motor with 6mm Axle	1	
9	B18.3.1M - 3 x 0.5 x 10 Hex SHCS -- 10NHX		6	
10	Driver Gear	M1-36, 3D Printed	1	15.21
11	B18.2.4.1M - Hex nut, Style 1, M3 x 0.5 --D-N		2	
12	B18.3.6M - M3 x 0.5 x 10 Hex Socket Flat Pt. SS --N		1	
13	Test Arm	M1-100, 3D printed	1	179.14
14	Support Link	3D Printed	1	41.200
15	3382H-1-103.stp	POT Meter	1	
16	B18.3.1M - 5 x 0.8 x 35 Hex SHCS -- 22NHX		1	
17	Stepper Nema 17		1	
18	B18.3.1M - 3 x 0.5 x 16 Hex SHCS -- 16NHX		4	
19	Push Arm with Slot	3D Printed	1	11.152
20	B18.3.1M - 3 x 0.5 x 12 Hex SHCS -- 12NHX		1	
21	Tilt mechanisme	3D Printed	1	27.622
22	Trigger Pressure Sensor	3D Printed	2	
23	B27.7M - 3BM1-19		2	
24	FSR 402.step	Pressure Sensor	2	
25	Convert brick pressure sensor	Data Card Pressure Sensor	2	
26	B18.22M - Plain washer, 6 mm, regular		2	
27	B27.7M - 3CM1-6		1	

UNLESS OTHERWISE SPECIFIED:
DIMENSIONS ARE IN MILLIMETERS
UNLESS OTHERWISE SPECIFIED
TOLERANCES: +/-0.5. HOLES H8/f9

Scale 1:1

FINISH:

DEBURR AND BREAK SHARP EDGES

DO NOT SCALE DRAWING

REVISION

	NAME	SIGNATURE	DATE
DRAWN	Einar Reistad		12.05.202
CHK'D	Torgeir Brandsar		14.05.202
APPV'D			
MFG			
Q.A			

MATERIAL:

TITLE:

Motorplate

DWG NO.

Assembly

A2

WEIGHT: 1122.96   SCALE:1:1   SHEET 15 OF 29

SECTION A-A
SCALE 2 : 1

SECTION B-B

All external corners, edges to apply radius of 0.5
All internal corner and edges to apply radius of 0.5 withoout marked edges

ITEM NO.	PART NUMBER	DESCRIPTION	QTY.	Weight
1	Motorplate	3D printed	1	269.973

UNLESS OTHERWISE SPECIFIED:
DIMENSIONS ARE IN MILLIMETERS
UNLESS OTHERWISE SPECIFIED
TOLERANCES: +/-0.5, HOLES H8/h9

	NAME	SIGNATURE	DATE
DRAWN	Einar Reistad		13.05.2023
CHK'D	Torgeir Brandsar		14.05.2023
APPV'D			
MFG			
Q.A			

DEBURR AND BREAK SHARP EDGES
DO NOT SCALE DRAWING
REVISION

SCALE 1:1

TITLE:
Motorplate

MATERIAL:
Polymer (PLA)

DWG NO.
Motorplate

A2

WEIGHT: 269.98
SCALE:1:1
SHEET 16 OF 29

Ø6.0 THRU
8.0 6mm depht
Ø4.2 To be threaded with M5
2x Ø6.0
Edges and corner not to be applied with radius
Bottom edges of slot not to be applied with radius

64
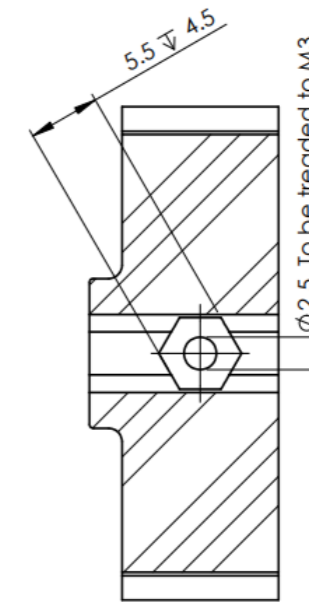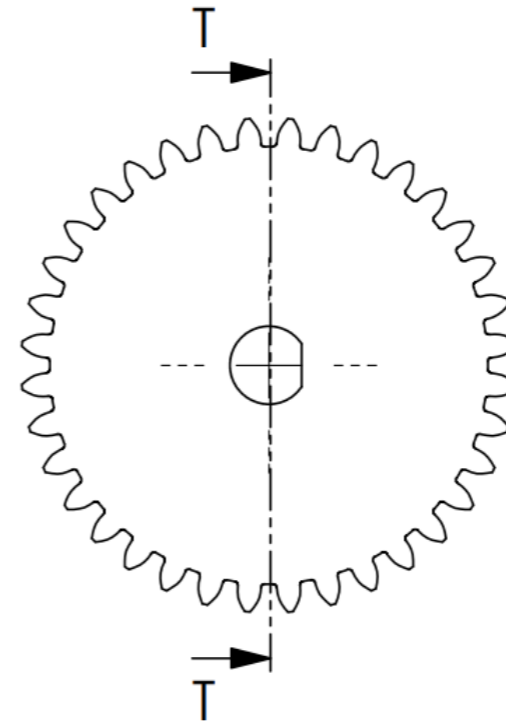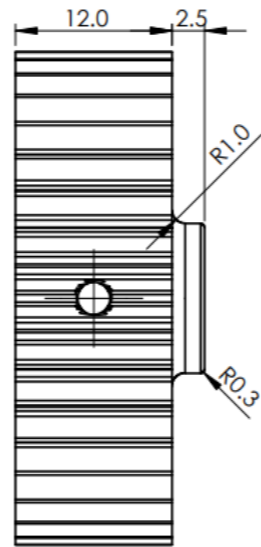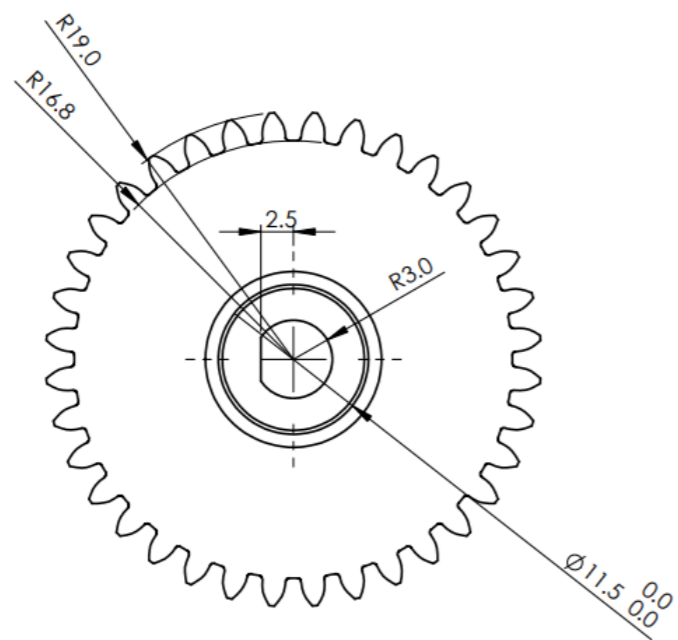
SECTION T-T
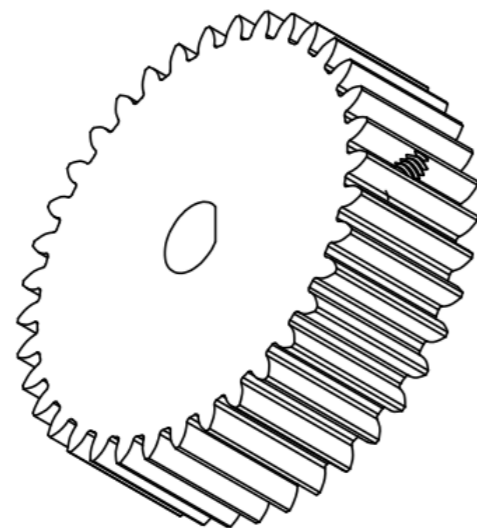
Spurs Gear data	
Module	1
Pressure angel	20
No. of Teeth	36
Pitch diameter	36
Outside diameter	38
Tooth depht	2,2
Addendum	1

ITEM NO.	PART NUMBER	DESCRIPTION	QTY.	Weight
10	Driver Gear	M1-36, 3D Printed	1	15.21

UNLESS OTHERWISE SPECIFIED:
DIMENSIONS ARE IN MILLIMETERS
UNLESS OTHERWISE SPECIFIED
TOLERANCES: +/-0.5. HOLES H8/h9

SCALE 2:1

FINISH:

DEBURR AND
BREAK SHARP
EDGES

DO NOT SCALE DRAWING

REVISION

	NAME	SIGNATURE	DATE
DRAWN	Einar Reistad		13.05.2023
CHK'D	Torgeir Brandsar		14.05.2023
APPV'D			
MFG			
Q.A			

TITLE:

Motorplate

MATERIAL:
Polymer (PLA)

DWG NO.
Driver Gear

A3

WEIGHT: 15.21

SCALE:2:1

SHEET 17 OF 29

65
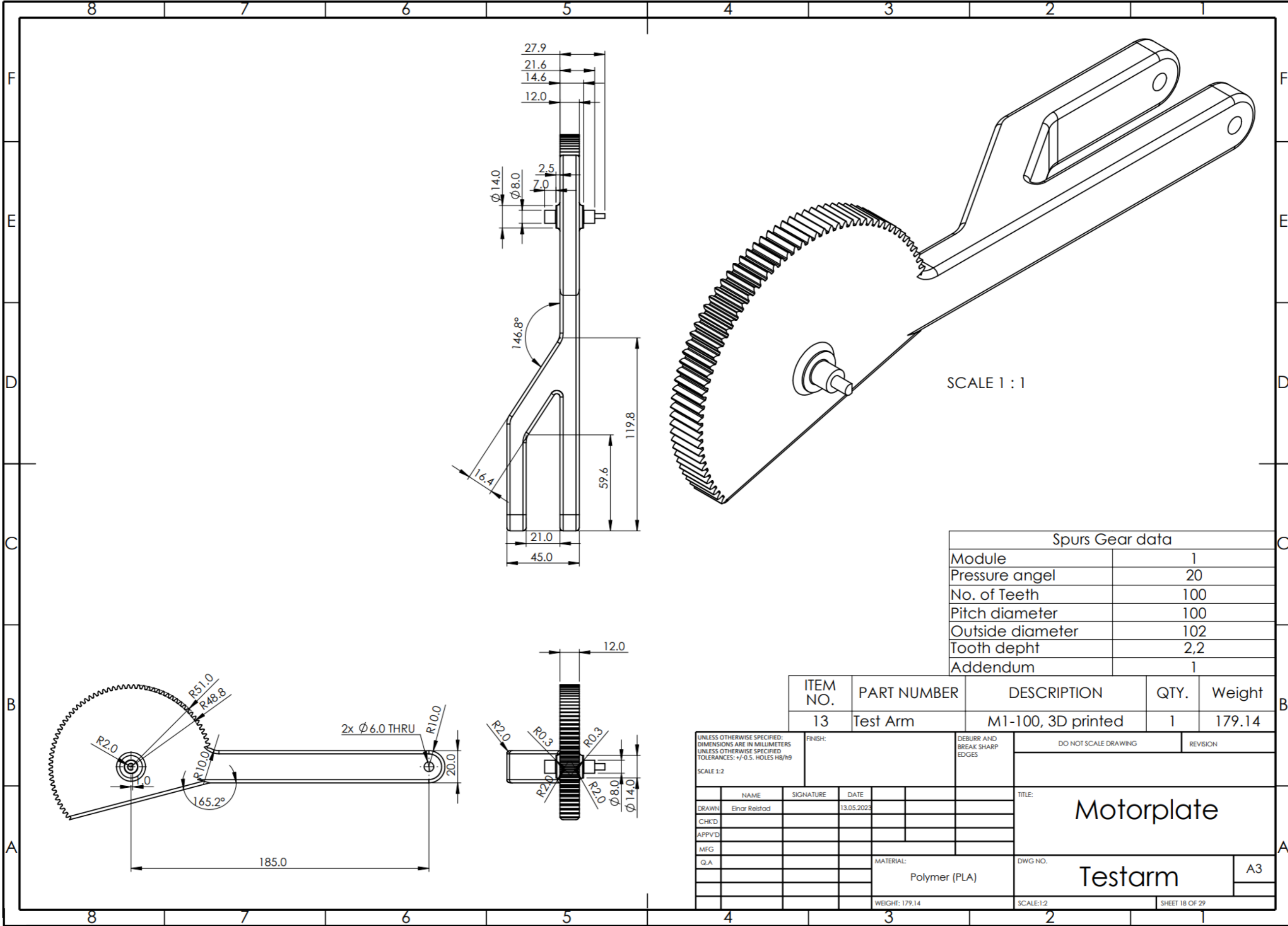
SCALE 1 : 1

Spurs Gear data	
Module	1
Pressure angel	20
No. of Teeth	100
Pitch diameter	100
Outside diameter	102
Tooth depht	2,2
Addendum	1

ITEM NO.	PART NUMBER	DESCRIPTION	QTY.	Weight
13	Test Arm	M1-100, 3D printed	1	179.14

UNLESS OTHERWISE SPECIFIED:
DIMENSIONS ARE IN MILLIMETERS
UNLESS OTHERWISE SPECIFIED
TOLERANCES: +/-0.5. HOLES H8/h9
SCALE 1:2

FINISH:

DEBURR AND
BREAK SHARP
EDGES

DO NOT SCALE DRAWING

REVISION

	NAME	SIGNATURE	DATE
DRAWN	Einar Reistad		13.05.2023
CHK'D			
APPV'D			
MFG			
Q.A			

TITLE:

Motorplate

MATERIAL:
Polymer (PLA)

DWG NO.

Testarm

A3

WEIGHT: 179.14

SCALE:1:2

SHEET 18 OF 29

66

SECTION W-W
SCALE 1 : 1

98.5
73.1
13.5
15.0
5.9
1.5
R10.0
Ø9.0
R1.0
5.0
R10.0
7.0
21.0
7.0
1.1
1.0
R1.0
11.0
Ø22.0
Ø23.3
6.0
19.0
30.0

Ø5.5 THRU
Ø5.0 THRU
4x Ø1.0 ▼1.5
16.0
R1.0
5.0
2.5
2x Ø6.0
3.0
8.0
3.0
27.0
6.5
7.5
1.2
R13.5
15.5
7.0
5.0
25.9
69.5
27.9
85.0

W

W
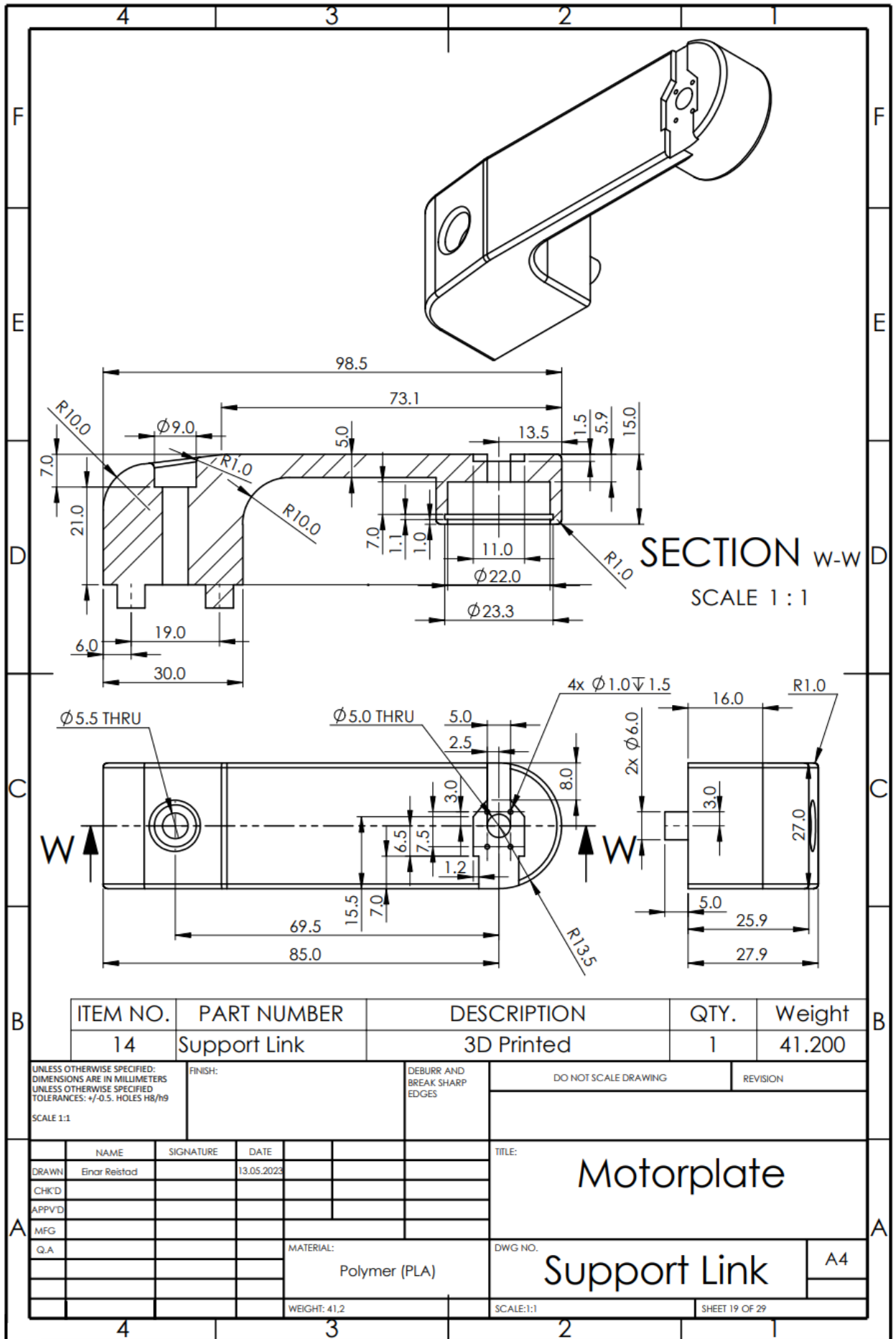
ITEM NO.	PART NUMBER	DESCRIPTION	QTY.	Weight
14	Support Link	3D Printed	1	41.200

UNLESS OTHERWISE SPECIFIED:
DIMENSIONS ARE IN MILLIMETERS
UNLESS OTHERWISE SPECIFIED
TOLERANCES: +/-0.5. HOLES H8/h9
SCALE 1:1

FINISH:

DEBURR AND
BREAK SHARP
EDGES

DO NOT SCALE DRAWING

REVISION

	NAME	SIGNATURE	DATE				TITLE:		
DRAWN	Einar Reistad		13.05.2023						
CHK'D									
APPV'D									
MFG									
Q.A									

Motorplate

MATERIAL:
Polymer (PLA)

DWG NO.

Support Link

A4

WEIGHT: 41,2

SCALE:1:1

SHEET 19 OF 29

SECTION AB-AB

19.0
17.1
160.5°
37.3°
3.0
5.1
7.0
8.5
18.1

SECTION AC-AC

26.0
24.0
10.0
21.5
20.0
No Radius

AB
12.0
3.0
2.0
3.0
AC
AB

50.1
5.0
10.8
12.0
10.0
30.0
No Radius
AA
AA

24.0
Ø19.0
Ø21.0
1.5
2.5
5.0
10.0
SECTION AA-AA
AC

24.0
9.5
20.1
15.1
1.0
1.6
13.1
2x Ø3.0 THRU
Raduius 1.0
R9.5
R7.6
R12.0
8.0

Ø19.0
Ø11.2
22

4.0
1.5
R150.6
R16.2

1
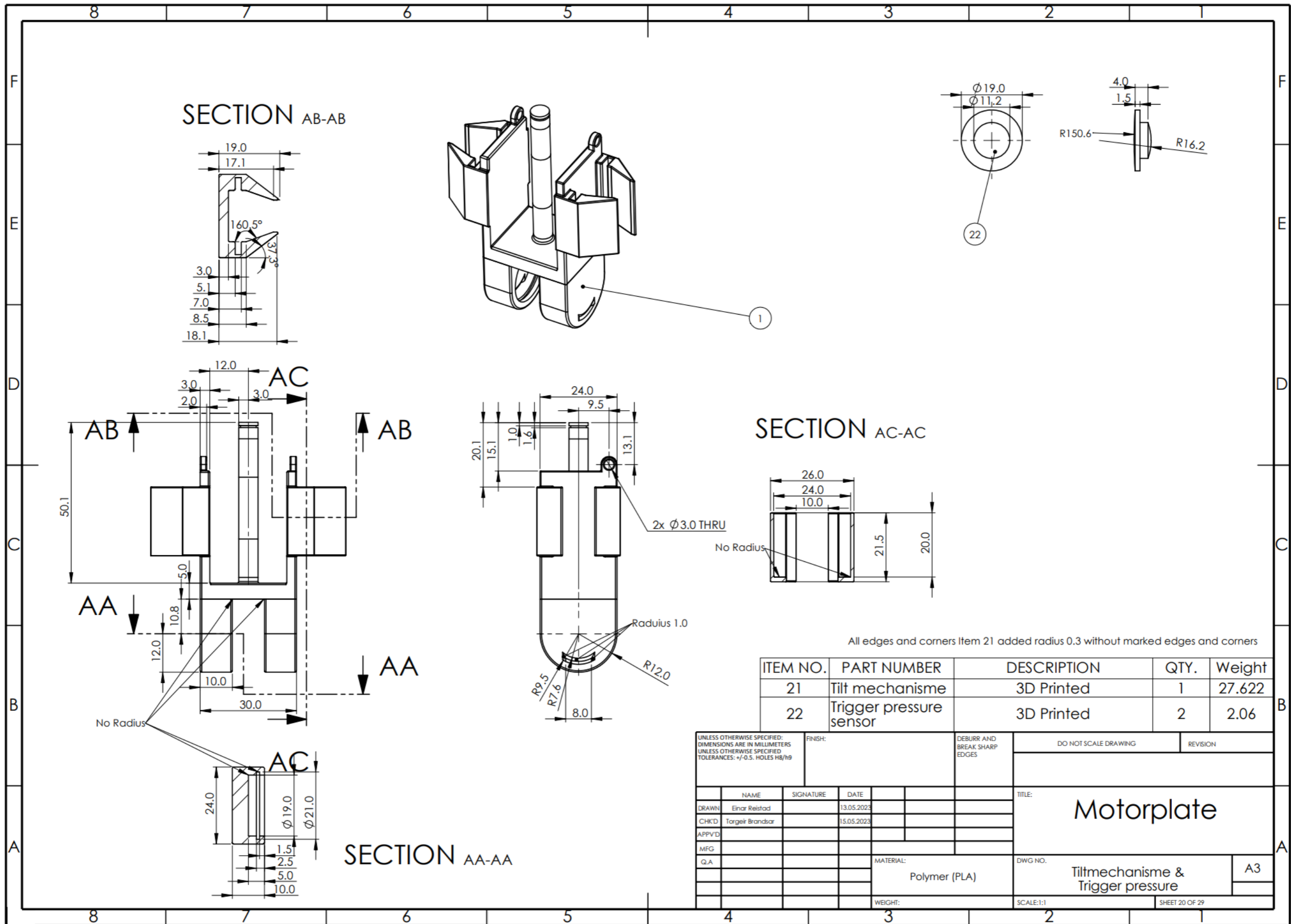
All edges and corners Item 21 added radius 0.3 without marked edges and corners

ITEM NO.	PART NUMBER	DESCRIPTION	QTY.	Weight
21	Tilt mechanisme	3D Printed	1	27.622
22	Trigger pressure sensor	3D Printed	2	2.06

ITEM NO.	PART NUMBER		DESCRIPTION	QTY.	Weight
19	Push Arm with Slot		3D Printed	1	11.152

UNLESS OTHERWISE SPECIFIED: DIMENSIONS ARE IN MILLIMETERS UNLESS OTHERWISE SPECIFIED TOLERANCES: +/-0.5. HOLES H8/h9 SCALE 1:1	FINISH:		DEBURR AND BREAK SHARP EDGES	DO NOT SCALE DRAWING		REVISION

	NAME	SIGNATURE	DATE				TITLE:
DRAWN	Einar Reistad		13.05.2023				Motorplate
CHK'D	Torgeir Brandsar		14.05.2023				
APPV'D							
MFG							
Q.A			MATERIAL: Polymer (PLA)				DWG NO. Push arm with slot
			WEIGHT: 11.152			SCALE:1:1	SHEET 21 OF 29

A4
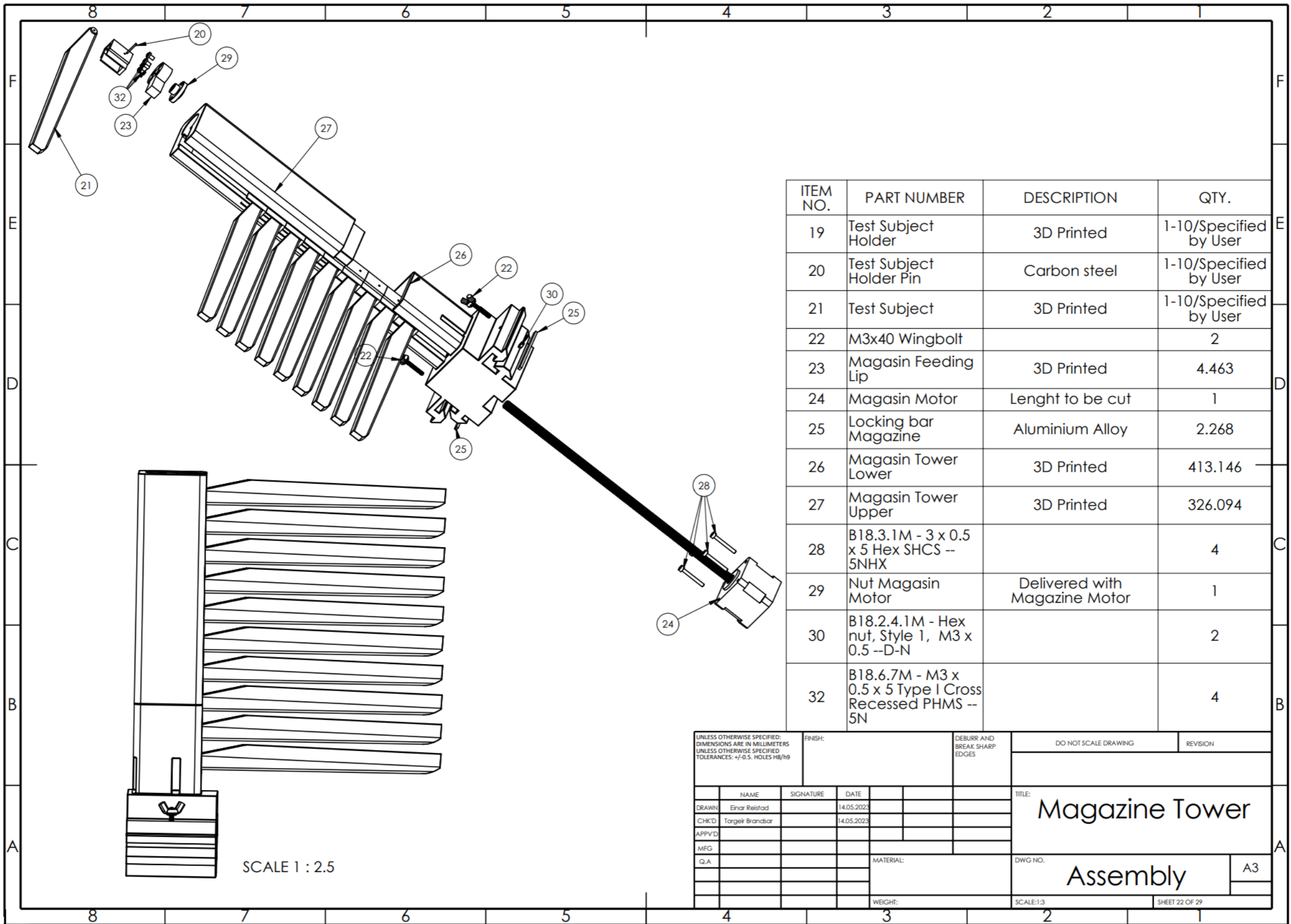
ITEM NO.	PART NUMBER	DESCRIPTION	QTY.
19	Test Subject Holder	3D Printed	1-10/Specified by User
20	Test Subject Holder Pin	Carbon steel	1-10/Specified by User
21	Test Subject	3D Printed	1-10/Specified by User
22	M3x40 Wingbolt		2
23	Magasin Feeding Lip	3D Printed	4.463
24	Magasin Motor	Lenght to be cut	1
25	Locking bar Magazine	Aluminium Alloy	2.268
26	Magasin Tower Lower	3D Printed	413.146
27	Magasin Tower Upper	3D Printed	326.094
28	B18.3.1M - 3 x 0.5 x 5 Hex SHCS -- 5NHX		4
29	Nut Magasin Motor	Delivered with Magazine Motor	1
30	B18.2.4.1M - Hex nut, Style 1, M3 x 0.5 --D-N		2
32	B18.6.7M - M3 x 0.5 x 5 Type I Cross Recessed PHMS -- 5N		4

SCALE 1 : 2.5

UNLESS OTHERWISE SPECIFIED:
DIMENSIONS ARE IN MILLIMETERS
UNLESS OTHERWISE SPECIFIED
TOLERANCES: +/-0.5. HOLES H8/h9

FINISH:

DEBURR AND BREAK SHARP EDGES

DO NOT SCALE DRAWING

REVISION

	NAME	SIGNATURE	DATE
DRAWN	Einar Reistad		14.05.2023
CHK'D	Torgeir Brandsar		14.05.2023
APPV'D			
MFG			
Q.A			

MATERIAL:

TITLE:

Magazine Tower

DWG NO.

Assembly

A3

WEIGHT:

SCALE:1:3

SHEET 22 OF 29

70

Technical drawing views with dimensions:

- R0.5
- 30.0
- 5.5
- 11.0
- 3.5
- 22.0
- 35.0
- 12.5
- 15.0
- 27.0
- 3.5
- 11.0
- 20.5
- 16.0
- R5.0

B

- 20.2
- 40.0
- Ø24.0
- 15.0
- 10.0
- 1.7
- 13.0
- 5.0
- 17.4
- 8.2
- 20.2
- 8.7
- 3.5
- 4.7
- 12.4

R0.5
R0.5

B

- 10.0
- 69.0
- 24.6
- 19.0
- 63.0
- Front
- 2.8
- 60.0

C

- 7.0
- 30.0

C

SECTION C-C

- 30.0
- 80.0
- 94.0
- 12.8
- 3.4
- 7.0
- 42.3

Back

- 24.6
- 8.0
- 29.0
- 69.0
- 40.5

- Ø3.4
- 27.8
- 4.4
- 27.8
- Ø2.5
- 3.2
- 70.0
- 43.2
- Ø22.0
- 6.0
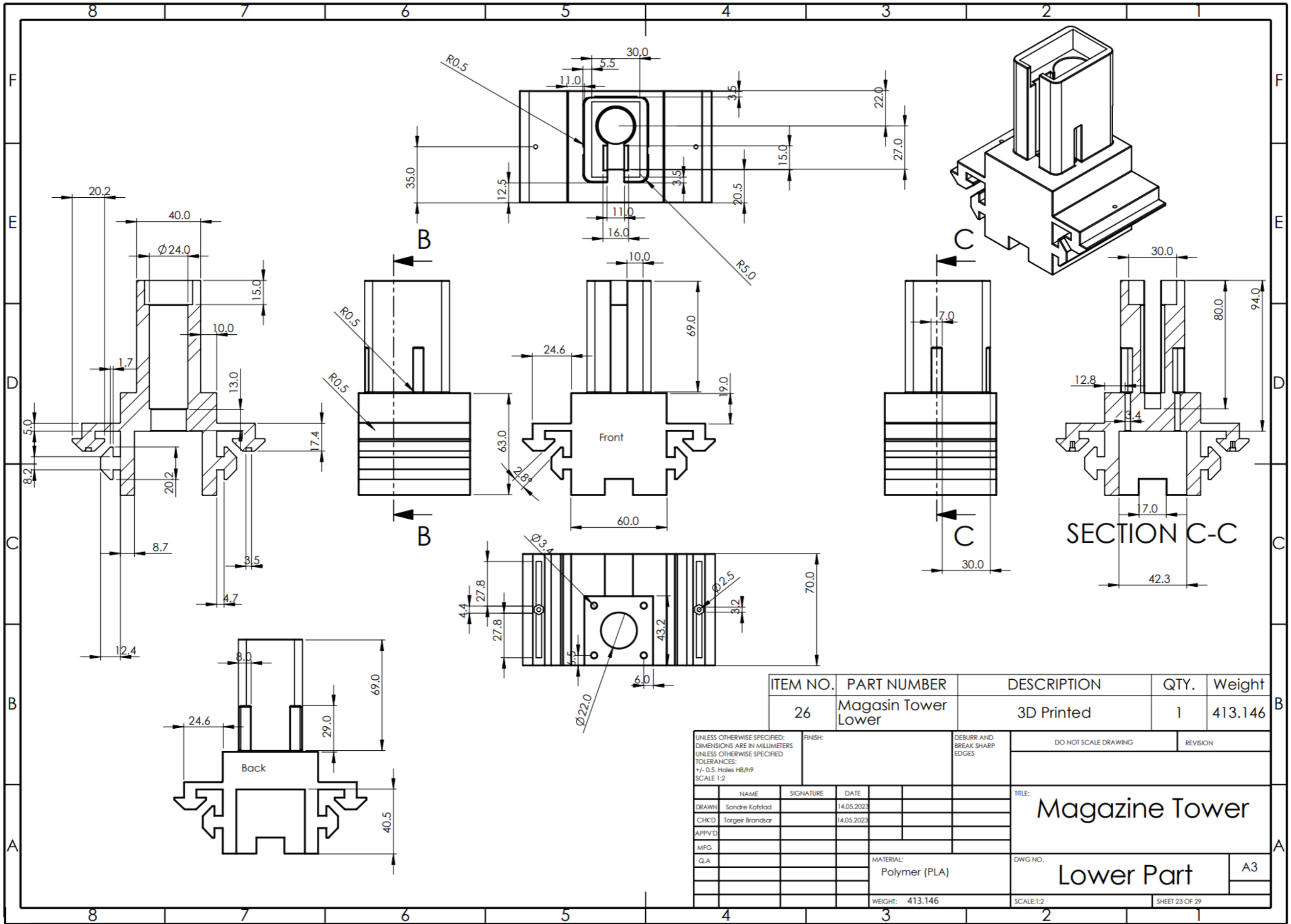
ITEM NO.	PART NUMBER	DESCRIPTION	QTY.	Weight
26	Magasin Tower Lower	3D Printed	1	413.146

UNLESS OTHERWISE SPECIFIED:
DIMENSIONS ARE IN MILLIMETERS
UNLESS OTHERWISE SPECIFIED
TOLERANCES:
+/- 0.5. Holes H8/h9
SCALE 1:2

FINISH:

DEBURR AND BREAK SHARP EDGES

DO NOT SCALE DRAWING

REVISION

	NAME	SIGNATURE	DATE
DRAWN	Sondre Kofstad		14.05.2023
CHK'D	Targeir Brandsar		14.05.2023
APPV'D			
MFG			
Q.A			

TITLE:

Magazine Tower

MATERIAL:
Polymer (PLA)

DWG NO.

Lower Part

A3

WEIGHT: 413.146

SCALE:1:2

SHEET 23 OF 29

71

15.0

4.5

29.0

47.0

3.5

R0.5

15.0

180.0

40.0

R5.0

R12.5

53.0

10.0

53.0

45.5

30.0

18.0

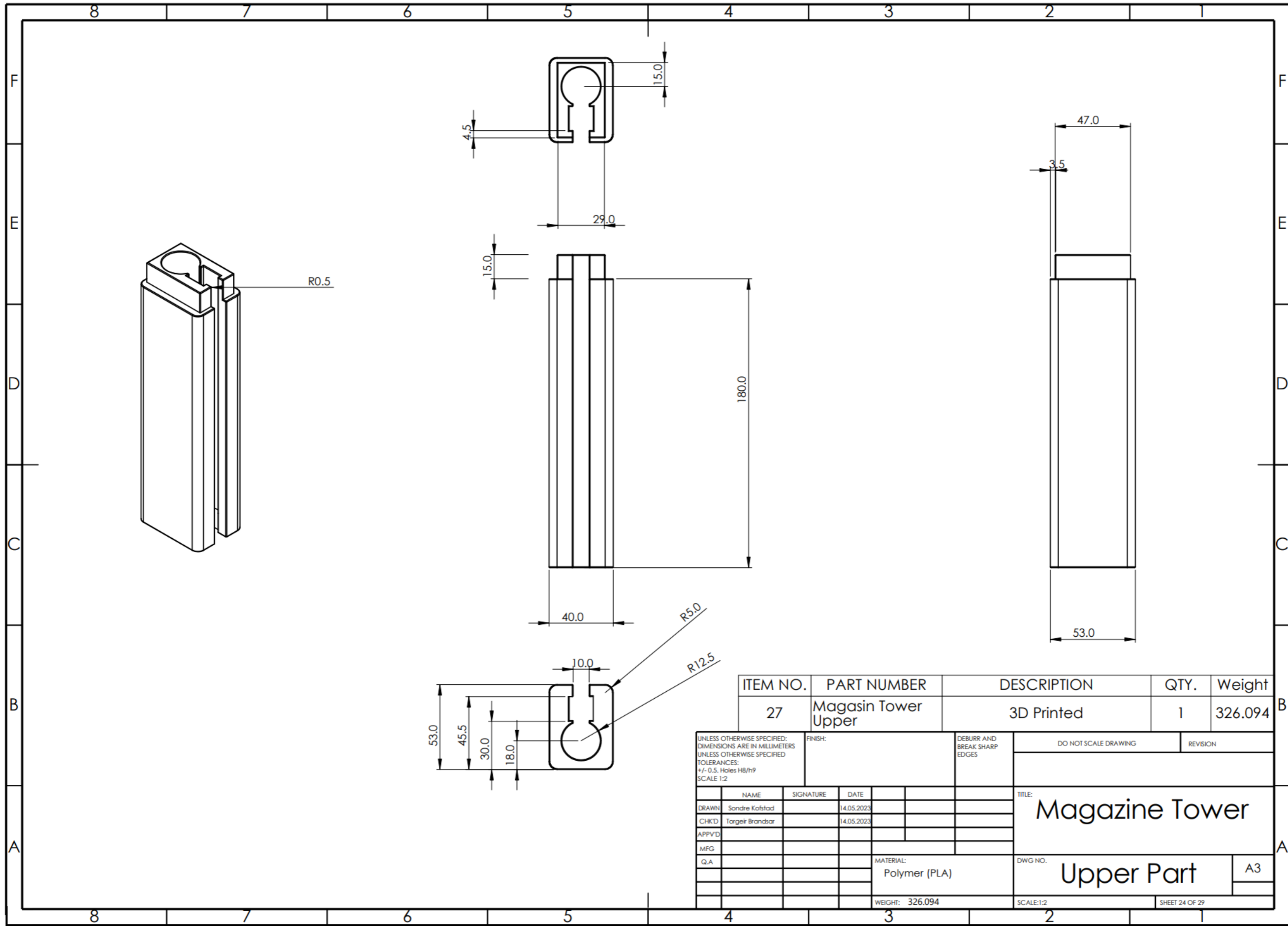| ITEM NO.	PART NUMBER	DESCRIPTION	QTY.	Weight
27	Magasin Tower Upper	3D Printed	1	326.094

UNLESS OTHERWISE SPECIFIED:
DIMENSIONS ARE IN MILLIMETERS
UNLESS OTHERWISE SPECIFIED
TOLERANCES:
+/- 0.5, Holes H8/h9
SCALE 1:2

FINISH:

DEBURR AND
BREAK SHARP
EDGES

DO NOT SCALE DRAWING

REVISION

	NAME	SIGNATURE	DATE			TITLE:
DRAWN	Sondre Kofstad		14.05.2023			
CHK'D	Torgeir Brandsar		14.05.2023			
APPV'D						
MFG						
Q.A						

Magazine Tower

MATERIAL:
Polymer (PLA)

DWG NO.

Upper Part

A3

WEIGHT: 326.094

SCALE:1:2

SHEET 24 OF 29

	4	3	2	1

R12.0
Ø6.0
R3.0
Ø3.4

11.3
10.0

45°

27.0
Ø24.0

A
A

10.5

SECTION A-A

5.5
1.9

Ø10.1
1.0

Ø22.1

16.1
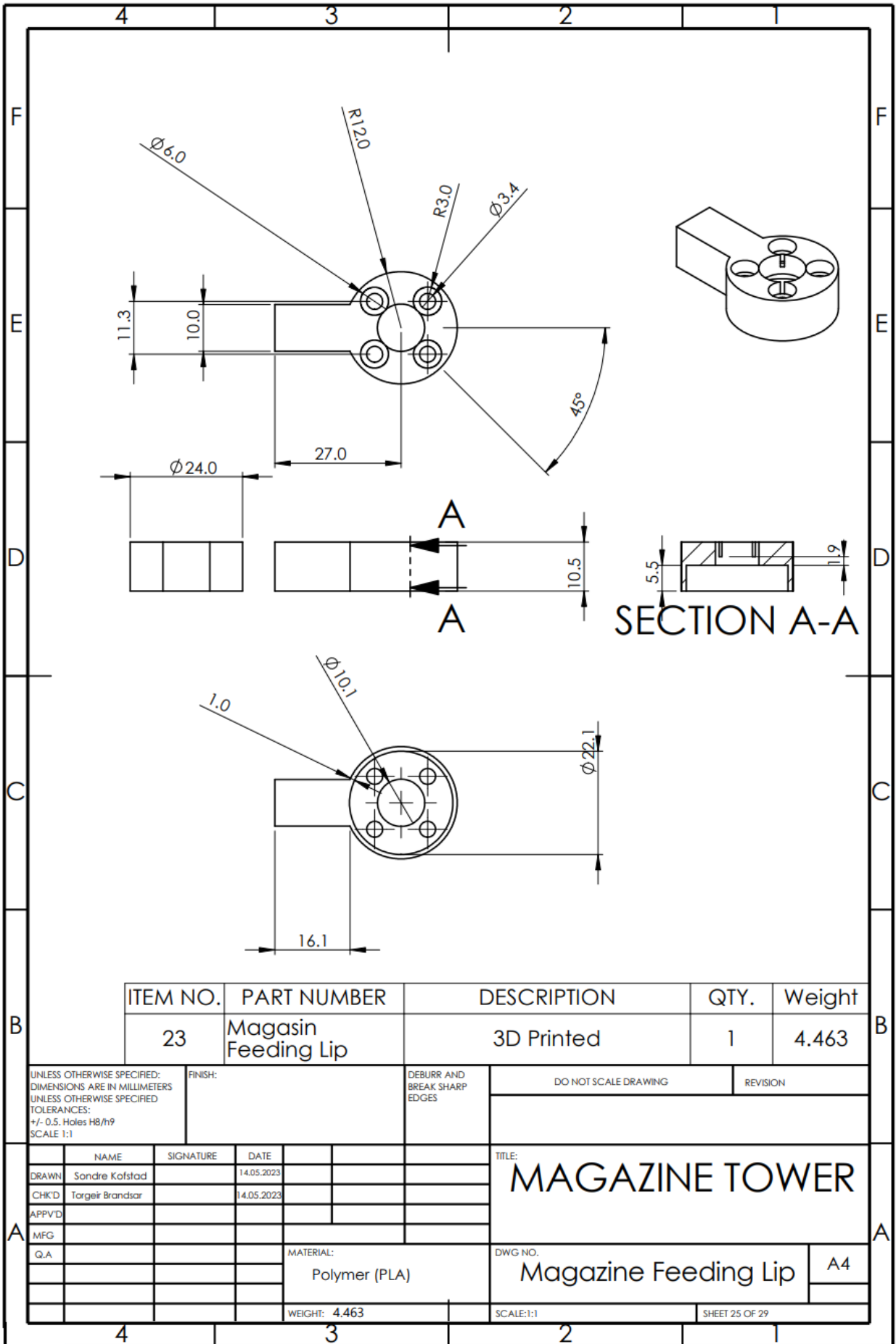
ITEM NO.	PART NUMBER	DESCRIPTION	QTY.	Weight
23	Magasin Feeding Lip	3D Printed	1	4.463

UNLESS OTHERWISE SPECIFIED:
DIMENSIONS ARE IN MILLIMETERS
UNLESS OTHERWISE SPECIFIED
TOLERANCES:
+/- 0.5. Holes H8/h9
SCALE 1:1

FINISH:

DEBURR AND BREAK SHARP EDGES

DO NOT SCALE DRAWING

REVISION

	NAME	SIGNATURE	DATE
DRAWN	Sondre Kofstad		14.05.2023
CHK'D	Torgeir Brandsar		14.05.2023
APPV'D			
MFG			
Q.A			

TITLE:
MAGAZINE TOWER

MATERIAL:
Polymer (PLA)

DWG NO.
Magazine Feeding Lip

A4

WEIGHT: 4.463

SCALE:1:1

SHEET 25 OF 29

73

2.0

3.5

60.0

ITEM NO.	PART NUMBER	DESCRIPTION	QTY.	Weight
25	Locking bar Magazine	Aluminium Alloy	2	1.134

UNLESS OTHERWISE SPECIFIED:
DIMENSIONS ARE IN MILLIMETERS
UNLESS OTHERWISE SPECIFIED
TOLERANCES:
+/- 0.5. Holes H8/h9
SCALE 2:1

FINISH:

DEBURR AND
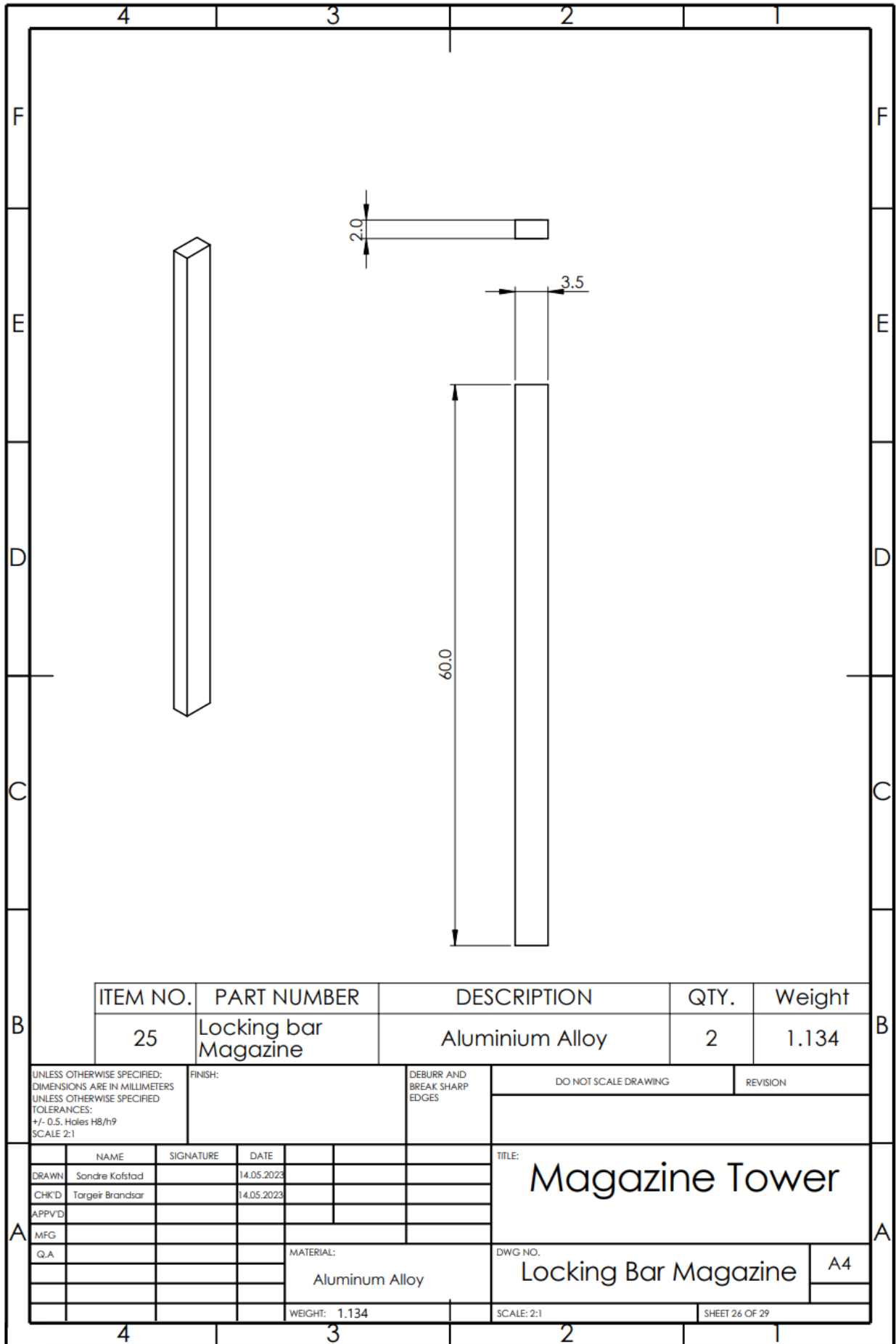BREAK SHARP
EDGES

DO NOT SCALE DRAWING

REVISION

	NAME	SIGNATURE	DATE
DRAWN	Sondre Kofstad		14.05.2023
CHK'D	Targeir Brandsar		14.05.2023
APPV'D			
MFG			
Q.A			

TITLE:

Magazine Tower

MATERIAL:
Aluminum Alloy

DWG NO.
Locking Bar Magazine

A4

WEIGHT: 1.134

SCALE: 2:1

SHEET 26 OF 29
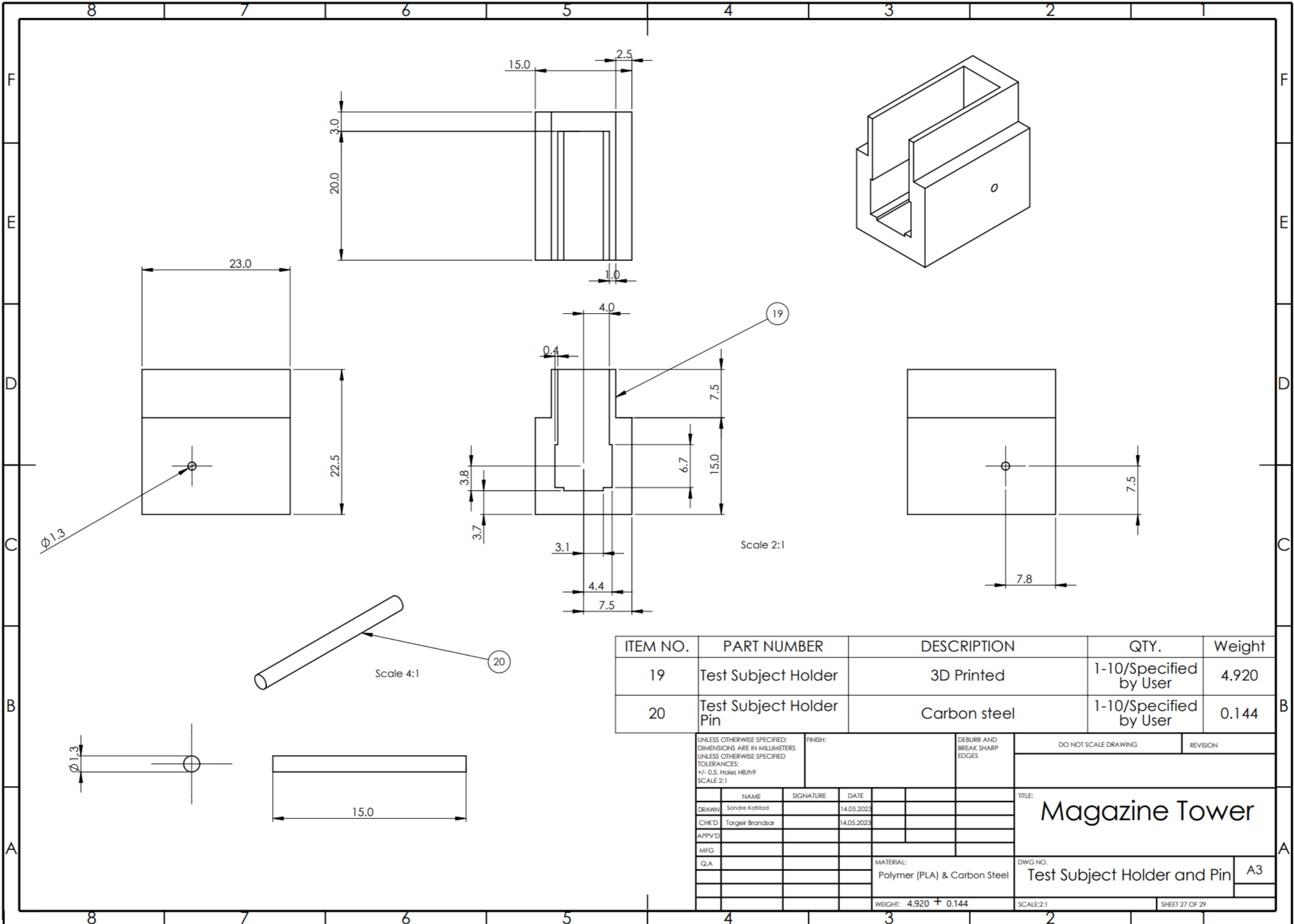
ITEM NO.	PART NUMBER	DESCRIPTION	QTY.	Weight
19	Test Subject Holder	3D Printed	1-10/Specified by User	4.920
20	Test Subject Holder Pin	Carbon steel	1-10/Specified by User	0.144

Scale 2:1

Scale 4:1

	NAME	SIGNATURE	DATE		TITLE:
DRAWN	Sondre Kofstad		14.05.2023		Magazine Tower
CHK'D	Torgeir Brandsar		14.05.2023		
APPV'D					
MFG					
Q.A					

MATERIAL:
Polymer (PLA) & Carbon Steel

DWG NO.
Test Subject Holder and Pin

A3

WEIGHT: 4.920 + 0.144

SCALE:2:1

DETAIL A
SCALE 2 : 1

R0.2

151.8

200.6

ITEM NO.	PART NUMBER	DESCRIPTION	QTY.	Weight
21	Test Subject	3D Printed	1	26.868

UNLESS OTHERWISE SPECIFIED:
DIMENSIONS ARE IN MILLIMETERS
UNLESS OTHERWISE SPECIFIED
TOLERANCES:
+/- 0.5. Holes H8/h9
SCALE 1:2

FINISH:

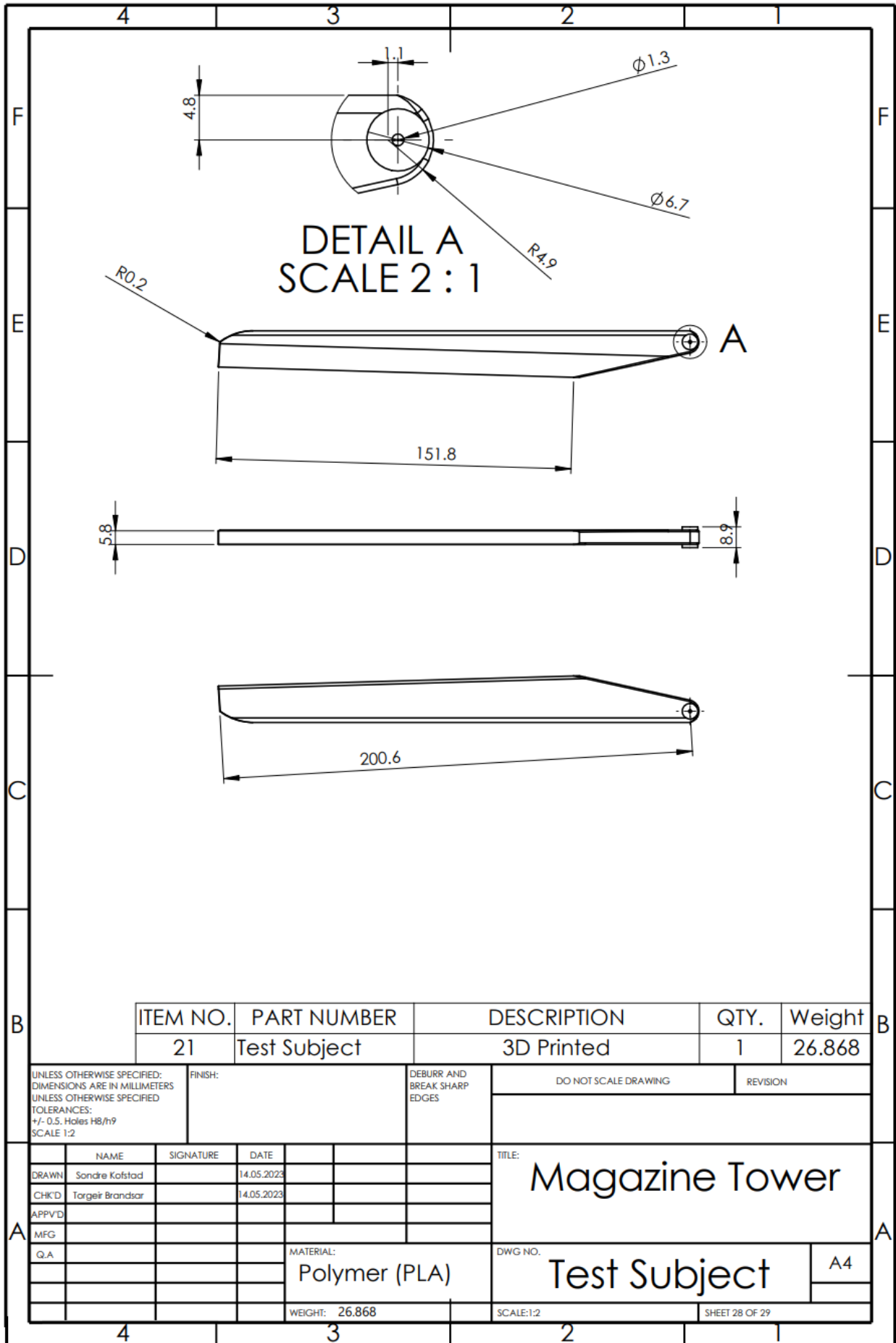DEBURR AND
BREAK SHARP
EDGES

DO NOT SCALE DRAWING

REVISION

	NAME	SIGNATURE	DATE
DRAWN	Sondre Kofstad		14.05.2023
CHK'D	Torgeir Brandsar		14.05.2023
APPV'D			
MFG			
Q.A			

TITLE:

Magazine Tower

MATERIAL:
Polymer (PLA)

DWG NO.
Test Subject

A4

WEIGHT: 26.868

SCALE:1:2

SHEET 28 OF 29

SCALE 2 : 1

312.0

(24)

(29)

SCALE 1 : 3
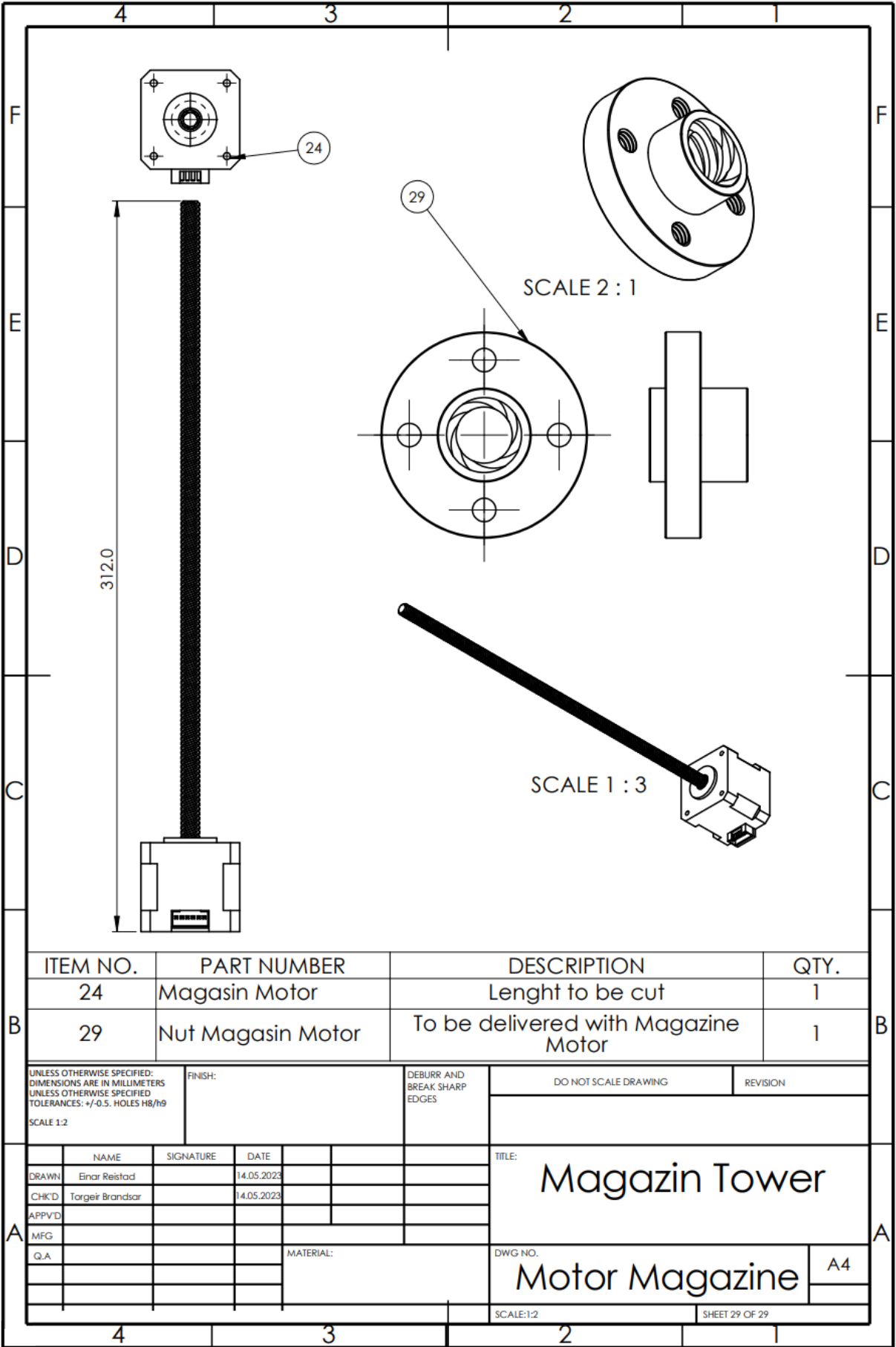
ITEM NO.	PART NUMBER	DESCRIPTION	QTY.
24	Magasin Motor	Lenght to be cut	1
29	Nut Magasin Motor	To be delivered with Magazine Motor	1

UNLESS OTHERWISE SPECIFIED:
DIMENSIONS ARE IN MILLIMETERS
UNLESS OTHERWISE SPECIFIED
TOLERANCES: +/-0.5. HOLES H8/h9

SCALE 1:2

FINISH:

DEBURR AND
BREAK SHARP
EDGES

DO NOT SCALE DRAWING

REVISION

	NAME	SIGNATURE	DATE
DRAWN	Einar Reistad		14.05.2023
CHK'D	Targeir Brandsar		14.05.2023
APPV'D			
MFG			
Q.A			

MATERIAL:

TITLE:

Magazin Tower

DWG NO.

Motor Magazine

A4

SCALE:1:2   SHEET 29 OF 29

Table 3:

Credits and references for downloaded parts used in the assembly.

Item no.	Module	Function	Description
8	Electric Box	Switch	Push Button, downloaded, and used without modification (CrabCad, 2023).
1 4	Frame	Alu- profile	Alu profile, design based on profile from RS Components (RS Components, u.d.).
15	Motor Plate	Pot- meter	Bourns Potentiometer 3382-1-103, downloaded and used without modification (DigiKey, u.d.)
8	Motor Plate	DC- motor	Designed according to Metal DC Geared Motor w/Encoder-12V 251RPM 18Kg.cm (DFROBOT, 2023).
3	Motor Plate	SKF 608	SKF Bearing 608, downloaded, and used without modification (SKF, u.d.).
17	Motor Plate	Nema 17 Ejector motor	Nema 17, downloaded, and used without modification (GrabCad, 2023).
22	Motor Plate	Trigger Pressure Sensor	FSR402, downloaded model and used without modification (CrabCad, 2019).
10	Motor Plate	Driver Gear	M1-36 Gear used as base model, modified thickness, and hole for axle (Kedjeteknik, n.d., p. 1).
13	Motor Plate	Test arm	M1- 100 Gear used as base model, modified into test arm (Kedjeteknik, n.d., p. 2).
24 29	Magazine	Magazine motor /Nut	Nema 17, used as base model (GrabCad, 2023), modified with threaded axle and nut according to Iverntech Nema 17 with integrated 300mm T8 Lead Screw (amazon, u.d.).
21	Magazine Tower	Test Subject	800mm Rotor Blade, used as a basis model and modified to fit our purpose (CrabCad, 2012).

3.5 Mechanics calculation of von Mises criterion for the tilt mechanism

It is required to establish some material properties to calculate whether the tilt mechanism will fail or not. The selection of parts of the prototype is all printed in polylactic acid (PLA) using fused deposition modeling (FDM). Polylactic acid is a biopolymer, one of the thermoplastics and ductile (MatWeb, 2023). However, depending on how it is printed with regard to the filament's angle, width and height, the properties can transition from ductile to brittle (Rajpurohit & Dave, 2018). Here it is assumed that PLA has a yield strength of 26 MPa, which is within the typical range of values for PLA (MatWeb, 2023).

Figure 18 shows the tilt mechanism and an idealized, simplified model. It is assumed that the maximum force applied to the test subject is 5N, but it should handle up to 10N. The normal forces are a result of the tilt mechanisms being connected to the test arm.
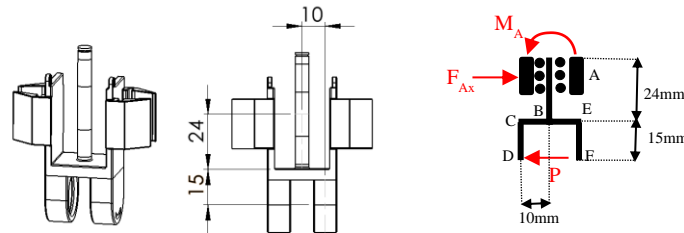

Figure 18 Tilt mechanism simplified to idealized model for mechanics calculation.

The equilibrium equations (22) are used to calculate the unknown normal forces F_{Ax} and M_A:

$$\sum F_x = 0 = F_{Ax} - P \iff F_{Ax} = P$$

$$\sum F_z = 0 \iff F_z = 0$$

$$\sum M_A^{\circlearrowleft} = 0 = P * z_1 - M_A \iff M_A = P * z_1 \iff M_A = 39 * P \ Nmm$$

The calculation above gives the reactionary forces in the system. Before making the shear and moment diagrams, it is necessary to calculate the force in a cut in the intersections of the segments A-B, B-C, C-D, B-E and E-F:
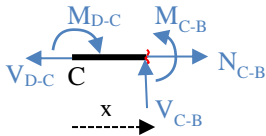
System
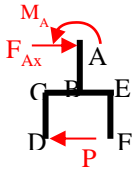
D-C
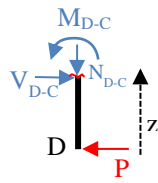
$$\sum F_X = 0 = V_{D-C} - P \iff V_{D-C} = P$$

$$\sum F_z = 0 = N_{D-C} \qquad \iff N_{D-C} = 0$$

$$\sum M_{D-C}^{\circlearrowleft} = 0 = zP - M_{D-C} \iff M_{D-C} = z_2 P$$

C-B

$$\sum F_x = 0 = -V_{D-C} + N_{C-B} \iff$$
$$N_{C-B} = V_{D-C} = P$$

$$\sum F_z = 0 = V_{C-B} \iff$$
$$V_{C-B} = 0$$

$$\sum M_B^{\circlearrowleft} = 0 = M_{D-C} - M_{C-B}$$
$$\iff M_{C-B} = M_{D-C}$$

A-B
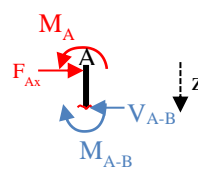
$$\sum F_x = 0 = F_{Ax} - V_{A-B} \iff$$
$$V_{A-B} = F_{Ax} = P$$

$$\sum F_z = 0$$

$$\sum M_C^{\circlearrowleft} = 0 =$$
$$M_{A-B} - M_A + z_1 V_{A-B} \iff$$
$$M_{A-B} = M_A - z_1 V_{A-B}$$

B-A-E (T-section)
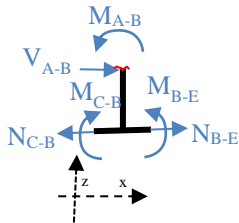
From the FBD it is obvious that $M_{B-E} = N_{B-E} = 0$:

$$\sum F_x = 0 = N_{B-E} - N_{C-B} + V_{A-B} \iff$$
$$0 = 0 - N_{C-B} + V_{A-B} \iff$$
$$V_{A-B} = N_{C-B} = P$$

$$\sum F_z = 0$$

$$\sum M_B^{\circlearrowleft} = 0 = M_{C-B} - M_{B-E} - M_{A-B} + zV_{A-B} \iff$$
$$M_{C-B} - 0 - M_{A-B} + zV_{A-B} = 0 \iff$$
$$M_{A-B} = M_{C-B} + z_1 V_{A-B} = M_{D-C} + z_1 P = P(z_1 + Z_2)$$

The shear- and moment diagrams shown in Figure 19 is drawn by using the results from the calculation above:

Moment *(Units is in N, mm and Nmm)*   **Shear**   **Axial**
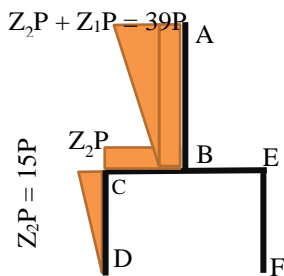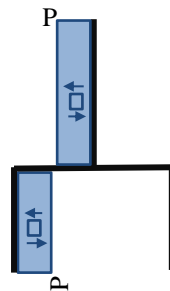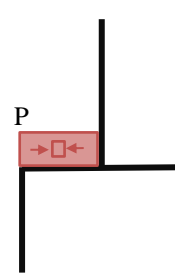
Figure 19 Shear and moment diagram for the tilt mechanism.

First, the cross-section area is smallest (radius r = 2mm) between point A and B (A-B). Secondly, the diagrams show the moment force is greatest in point A and the share force is equal in the segment A-B and C-D. Therefore, the stress of point A will be calculated, because the cross-section area is smallest in A-B and the moment force is greatest in point A.

Here the equations (20) is used to calculate the normal stress σ_z and the second moment of area is looked up in Bell (2014):

$$I_y = \frac{\pi r^4}{4}$$

$$\sigma_x = \frac{M}{I_y} z + \frac{N}{A} = \frac{39 * P}{\frac{\pi r^4}{4}} z + \frac{0}{A} = \frac{4 * 39 * P \ Nmm}{\pi * (3 \ mm)^4} * 3mm = 1.84 * P \frac{N}{mm^2}$$

Setting the test force P equal to 5N yields 9.2 MPa. This is probably somewhat conservative, because the reaction forces F_{ax} is set between the two actually connecting points with the test arm, making the arm longer and thus also the moment.

Equation (21) is used to calculate the shear stress and the first moment of area is looked up in Bell (2014, p.110):

$$\tau = \frac{VS}{I_y b} = \frac{P \frac{4r^3}{3\pi}}{\frac{\pi r^4}{4} 2r} = \frac{8P}{3\pi^2 r^2} = 0.03 * P \frac{N}{mm}$$

Setting P equal to 5N yields a shear force of 0.15 MPa. The principal stresses can then be calculated by combining these two results and the equation (19):

$$\sigma_{1,2} = \frac{\sigma_x + \sigma_z}{2} \pm \sqrt{\left(\frac{\sigma_x - \sigma_z}{2}\right)^2 + \tau^2} = \frac{9.2 \ \text{MPa} + 0}{2} \pm \sqrt{\left(\frac{9.2 \ \text{MPa} - 0}{2}\right)^2 + (0.15 \ MPa)^2}$$

$$= 4.6 \ MPa \pm \sqrt{21.18} \iff$$

$$\sigma_1 = 9.2 \ MPa \ and \ \sigma_2 = 0 \ MPa$$

The principal stresses can then be inserted into the Von Mises stress formula (18):

$$\sigma_j = \sqrt{\sigma_1^2 + \sigma_2^2 - \sigma_1^2 \sigma_2^2} = \sqrt{(9.2 \ \text{MPa})^2} = 9.2 \ MPa$$

Dividing the Von Mises stress formula gives the safety factor:

$$safety\ factor = \frac{f_y}{\sigma_j} = \frac{26\ MPa}{9.2\ MPa} = 2.8$$

The result shows that it satisfies a safety factor of 2.8. As it is not dangerous if any parts on the machine fail, this should be considered more than good enough for the tilt mechanism.

3.6 Finite Element Method (FEM), choice of material and dimensioning

By using finite element method analysis (FEM), we can verify our calculations and make design changes to prevent failure in the machine's parts due to high stress. This can also help reduce material consumption, production time, and energy usage. The analysis performed was static, with fixed geometry in areas with no room for movement and bearing support in areas with movement. Components were subjected to maximum forces according to design criteria, with the direction of forces applied according to the direction of strain on faces or connections exposed during a test sequence.

All components were tested, with more thorough testing performed on the most critical components to identify potential faults in design and material choice. The software used for the analysis was SolidWorks simulation that has a FEM analysis tool integrated into the software.

3.6.1 FEM Analysis of the tilt mechanism

To check the calculation done for the tilt mechanism von Mises stress is simulated, in addition displacement has also been simulated.

Fixture and external loads

The tilt mechanism is applied with fixed support at the areas of the axle that are in contact with the test arm, as shown in Figure 20 marked with green arrows. The force of 5N from the test subject is applied to the area in the tilt mechanism that will be in contact with the test subject, i.e. where the pressure pads are placed.
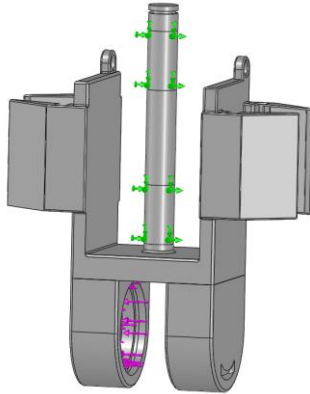
Figure 20 The FEM analysis set up for the tilt mechanism. The green arrow shows the fixed support against the test arm and the pink arrows shows the forces applied to the tilt mechanism.

The set up:

- Material: PLA
- Static analysis
- Fixed support
- Applied test force of 5N with 90° direction of the area of the tilt mechanism

Mesh

The analysis was done by dividing the part of the model with high levels of stress into a mesh with smaller elements, by using mesh control. First a coarse mesh for the whole model was created. This gives a much quicker analysis than a FEM examination with smaller mesh size.

Then the areas with the highest stress were identified and mesh control applied. Figure 21 shows this applied to the tilt mechanism. Element sizes for the mesh in the mesh control areas were decreased until the highest simulated stress level started to converge.
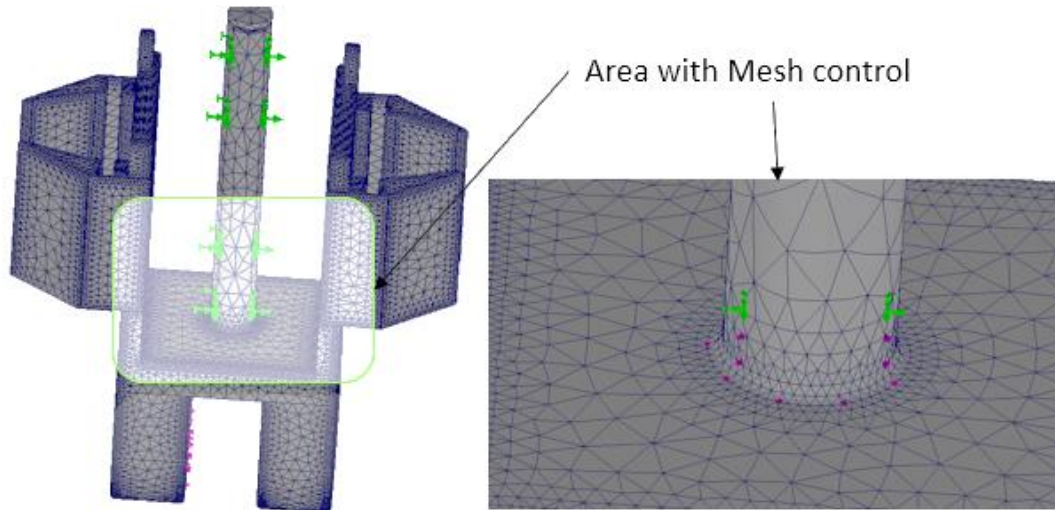
Figure 21 Standard mesh and area with mesh control marked with pink cubes.

Figure 22 Mesh details and Figure 23 contains details about the mesh and mesh control for the tilt mechanism.

One can see that the percentage of the aspect ratio is 98.7% and that the Jacobian is below 3.

Mesh Details

Study name	Test 4 Tilt Mechanisme* (-Default-)
DetailsMesh type	Solid Mesh
Mesher Used	Curvature-based mesh
Jacobian points for High quality mesh	16 points
Mesh Control	Defined
Max Element Size	1.90693 mm
Min Element Size	0.191342 mm
Mesh quality	High
Total nodes	939670
Total elements	617127
Maximum Aspect Ratio	8.1511
Percentage of elements with Aspect Ratio < 3	98.7
Percentage of elements with Aspect Ratio > 10	0
Percentage of distorted elements	0
Number of distorted elements	0
Time to complete mesh(hh:mm:ss)	00:01:10
Computer name	ZENBOOK

Mesh Control Details

Study name	Test 4 Tilt Mechanisme* (-Default-)
Mesh type	Solid Mesh
Entities	1 edge(s), 1 face(s)
Units	mm
Size	0.715097
Ratio	1.4
Identifier	4

Figure 22 Mesh details.   *Figure 23 Mesh control details.*

Figure 24 show probes inserted around the stress area which reads Jacobian value from 1 to 1.388. From these values one can argue that the mesh is of high quality.
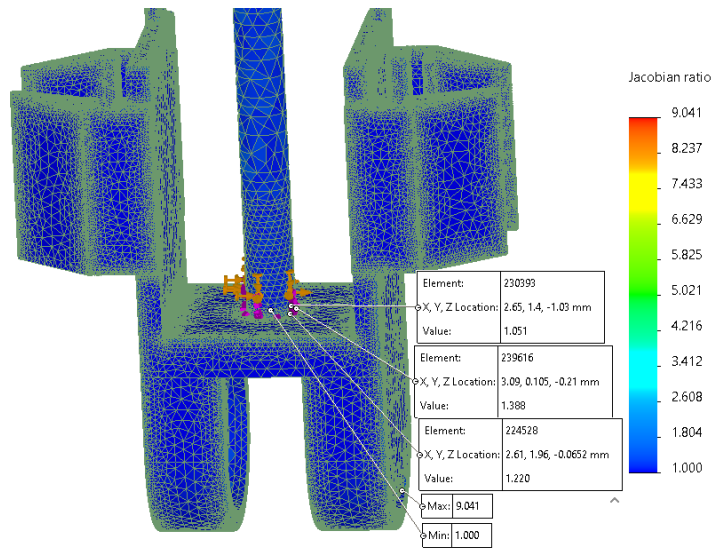
Figure 24 Probes to measure Jacobian.

Analysis of Stress

Figure 25 show the result of the von Mises stress plot simulation. Blue and cold colors are areas with less stress and warm red colors are higher stress. The highest stress is at the foot of the cylinder that connects the tilt mechanism to the test arm.
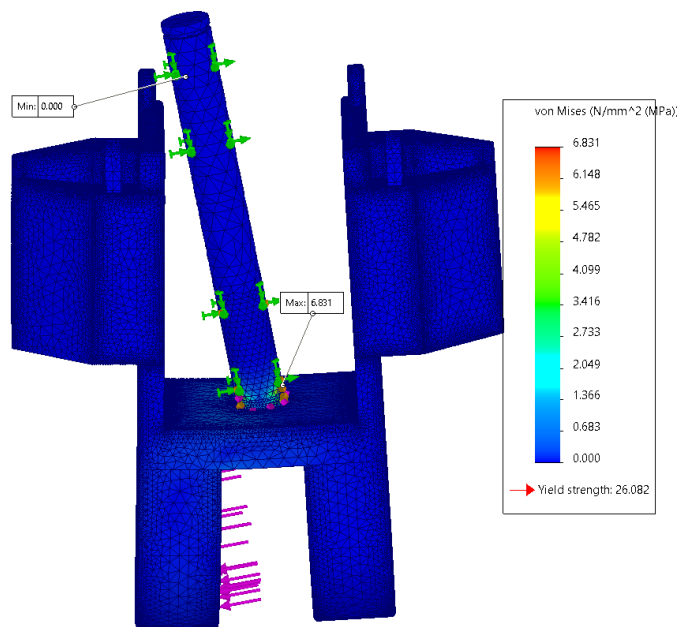
Figure 25 Tilt mechanism. Stress plot von Mises.

From the Stress plot in Figure 25 one can see that the maximum von Mises stress is 6.831 MPa and Figure 26 show the convergence of stress.
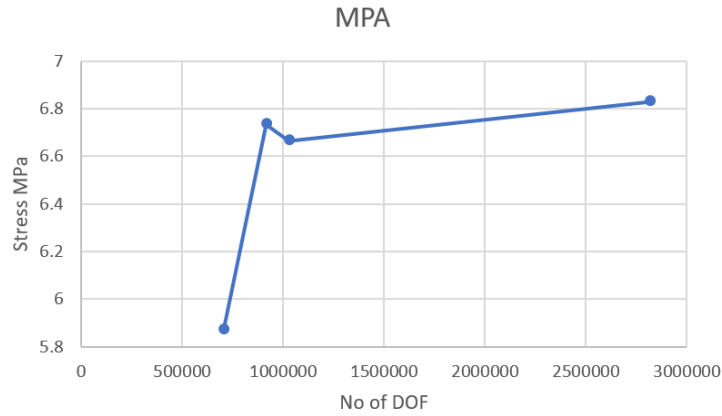
Figure 26 Convergence of stress vs No of DOF for tilt mechanism.

Displacement

The displacement plot shows the displacement for the part when exposed to the stress. In this case, the maximum displacement is 0.069mm as shown in Figure 27, and this deemed as acceptable.
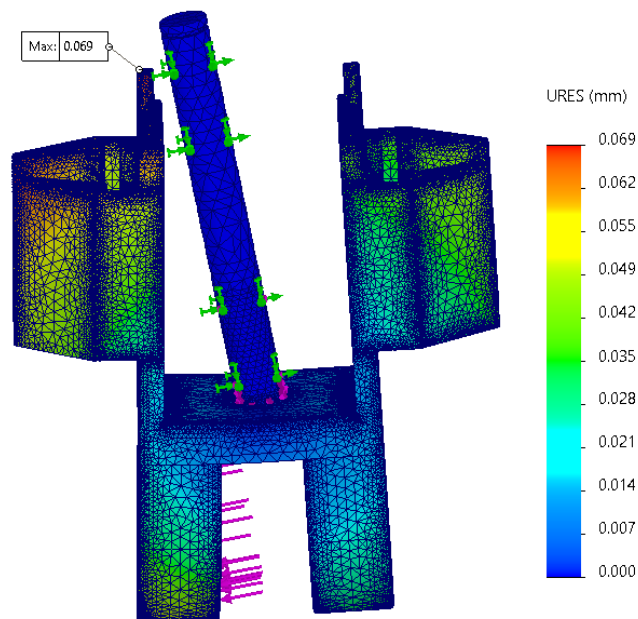
Figure 27 Displacement plot.

Conclusion

The maximum stress for the tilt mechanism is 6.831 MPa which is below the hand calculated maximum stress of 9.2 MPa (see 3.5). Maximum Yield strength for PLA material 26 MPa.

86

The tilt mechanism will handle the forces during designed test criteria of 5N for the test machine with a safety factor of:

$$safety\ factor = \frac{f_y}{\sigma_j} = \frac{26\ MPa}{6.831\ MPa} \approx 3.8$$

If one wish to identify the limitation in lifetime due to fatigue of the part, it will also be necessary to do some lifetime calculation/simulation during different frequencies with this stress level.

3.6.2 FEM Analysis of the test arm

Simulation of the test arm is shown in Figure 28. The SolidWorks CAD model has been derived from a gear CAD model downloaded from Ingenjörsfirman Kedjeteknik AB (Kedjeteknik, n.d., p. 2). The purpose of the test arm is to transfer rotation movement from the DC motor into oscillating movements of tilt mechanism that will give test force against the test subject. Between the test arm and driving gear there will a gear ratio from the difference in gear sizes.

The set up:
- Material: PLA
- Static analysis
- Fixed support on tooth
- Bearing support axle
- Simulated force with remote load
- Applied test force: 5N
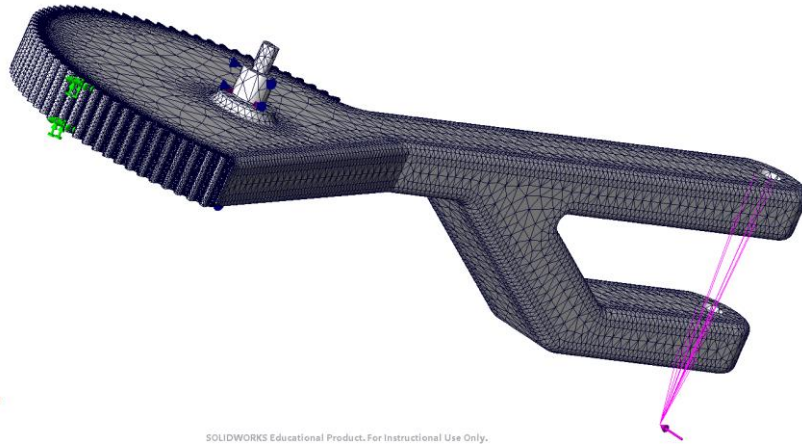
Figure 28 Test arm with applied standard curvature mesh.

Fixture and external load

Fixed geometry is added at one side of the tooth face, presented with green arrows. Bearing support is added at the top and bottom axle, shown as blue cones. Remote load is added at the test arm to simulate forces against the tilt mechanism and shown as pink arrow and pink lines in Figure 28.

Mesh

A standard curvature mesh was applied to the model. Mesh control was set at the radius in bottom of the axles, and at the face of the tooth that has been given fixed geometry as the highest stress was simulated in this area. Figure 29 show the mesh control.
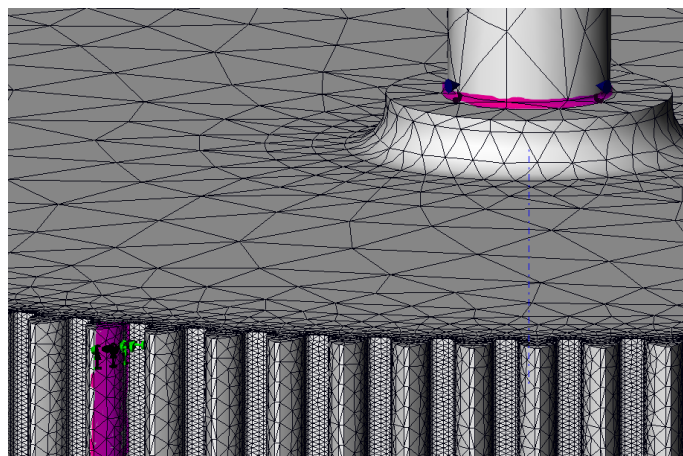
Figure 29 Applied mesh control, pink areas.

Figure 30 Mesh details.	*Figure 31 Mesh control details.*

Figure 30 and Figure 31 display the details of the mesh. The quality can be evaluated by looking at the aspect ratio which is 99.4%, so this can be considered as a high-quality mesh.

Analysis of Stress

From the stress plot one can read that the maximum von Mises stress is 5.079 MPa.
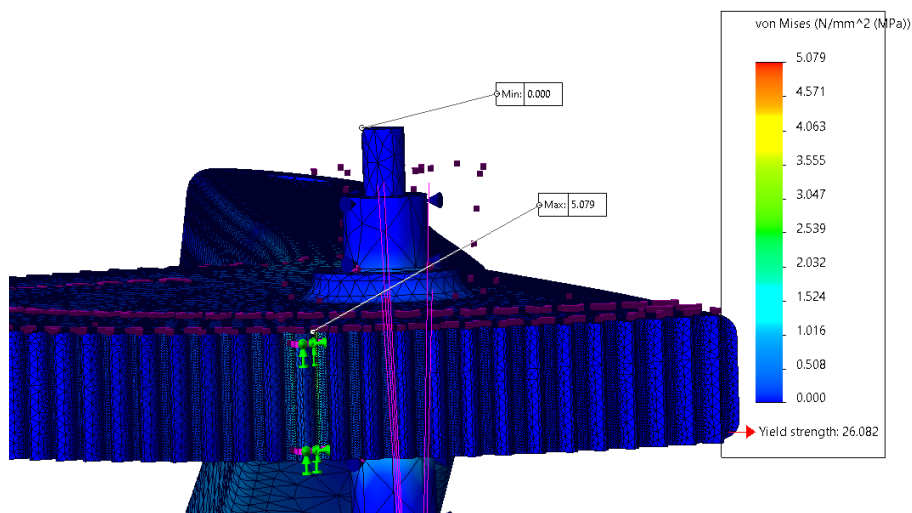
Figure 32 Test arm stress plot.

One can see in Figure 32, after probes were placed around the area with the highest stress, that the peak value of stress is due to a stress singularity because of the sharp edge. Thus, the highest value from the von Mises stress plot should be used.

Displacement

To check the maximum displacement, a simulation was plotted presented in Figure 33. In this case the maximum displacement is 0.309mm which is deemed acceptable.
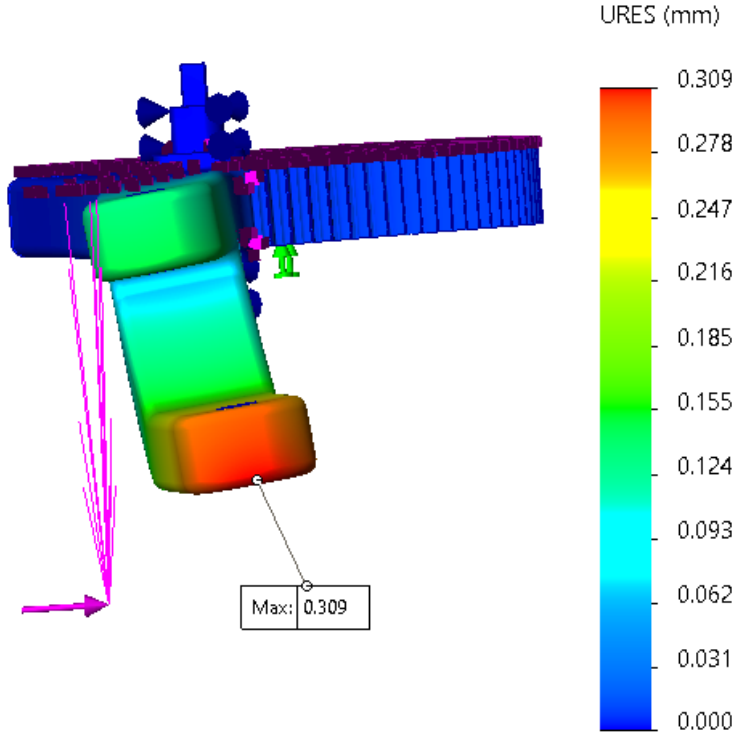
Figure 33 Displacement of test arm.

Reaction forces

Checked Reaction forces in the tooth to be 18.351N Figure 34.

Figure 34 Reaction forces for test arm.

Conclusion

Maximum stress appeared in the edge of the tooth with a stress of 5.079 MPa, which was not expected. An explanation is that this spot became a stress singularity, which was verified by

placing probes in the area around the suspected singularity, see Figure 35. The Maximum stress from the plot was not so much higher than probed result, so in calculation the highest result will be used.
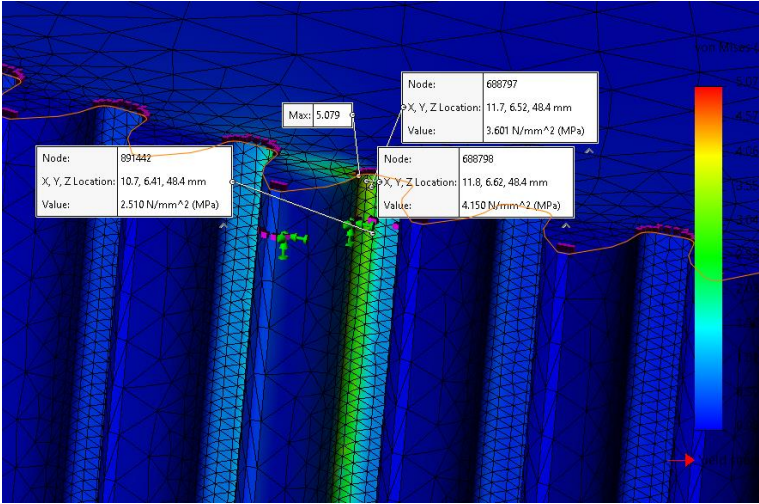
Figure 35 Readout Stress with probes.

It was performed four simulations with an increase of mesh quality and applied mesh control at the faces with the highest stress, results are shown in Figure 36.
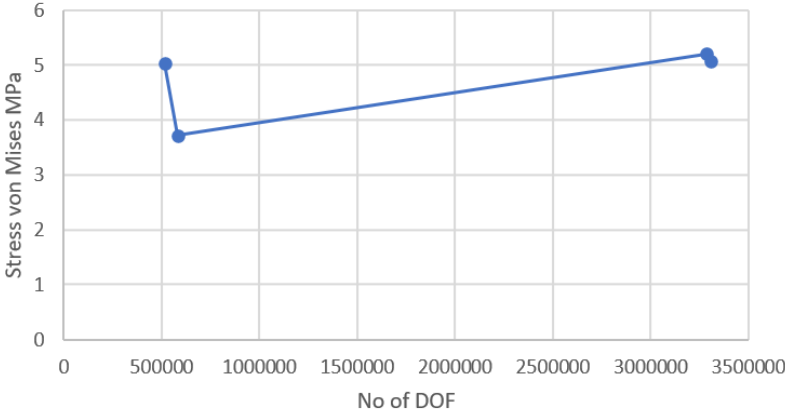
Figure 36 Convergence of stress vs No of DOF for test arm.

A displacement of 0.309mm at the lowest "point" on the test arm. Since the Yield strength for this material is 26 MPa, it is not needed to change the material to a stronger type, and we get an acceptable safety factor:

$$safety\ factor = \frac{f_y}{\sigma_j} = \frac{26\ MPa}{5.079\ MPa} \approx 5.1$$

If one wish to identify the limitation in lifetime due to fatigue of the part, it will also be necessary to do some lifetime calculation/simulation during different frequencies of the test arm and also for wear and tear in the teeth area.

3.6.3 FEM analysis of the driver gear

The model has been designed in SolidWorks CAD part, the gear model has been used is as a basic model and remodeled for this purpose have been downloaded from Ingenjörsfirman Kedjeteknik AB (Kedjeteknik, n.d., p. 1). The driver gear's purpose is to transfer rotation movement from the DC motor into test arm gear face. There is a setscrew hole located between two teeth to secure the driver gear to the axle of DC motor. The construction is assessed to be weakest at this point hence, the force in the simulation will be applied to this area, and to avoid stress singularity in threads they will be altered as Cosmetic threads in CAD part of SolidWorks.

Set up data:
- Material: PLA
- Static analysis
- Fixed support in axle hole
- Applied test force: 18.5N, from calculation in 3.7.2, and reaction forces in Figure 34.
- Applied cosmetic thread to avoid stress singularity

Fixture and external loads

Fixed geometry was added to the hole for the DC motor's axle, is shown with green arrows, and applied force at the face of the tooth that receives the reaction force from the test arm, shown in the figure with pink arrows Figure 37.
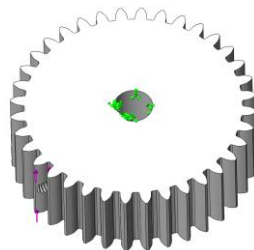
Figure 37 Fixture and external load.

Mesh

Standard curvature mesh was applied to the model in general and mesh control was added at in the area of the tooth where the force was applied (shown as pink arrows in Figure 38).
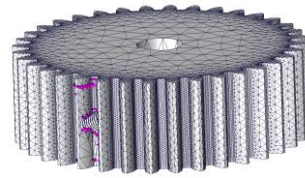
Figure 38 Applied mesh.

The mesh quality is summarized in Figure 39 and Figure 40. The aspect ratio is 99.7% so the mesh quality is high.

Mesh Details	
Study name	Test 4 Driver Gear* (-Default-)
DetailsMesh type	Solid Mesh
Mesher Used	Curvature-based mesh
Jacobian points for High quality mesh	16 points
Mesh Control	Defined
Max Element Size	1 mm
Min Element Size	0.2 mm
Mesh quality	High
Total nodes	1072636
Total elements	752106
Maximum Aspect Ratio	5.4054
Percentage of elements with Aspect Ratio < 3	99.7
Percentage of elements with Aspect Ratio > 10	0
Percentage of distorted elements	0
Number of distorted elements	0
Time to complete mesh(hh:mm:ss)	00:01:20
Computer name	ZENBOOK

Mesh Control Details	
Study name	Test 4 Driver Gear* (-Default-)
Mesh type	Solid Mesh
Entities	3 face(s)
Units	mm
Size	2
Ratio	1.4
Identifier	1

Figure 39 Detail of mesh.   *Figure 40 Details of mesh control.*

Analysis of stress

The stress plot in Figure 41 shows a max stress value of 5.815 MPa.
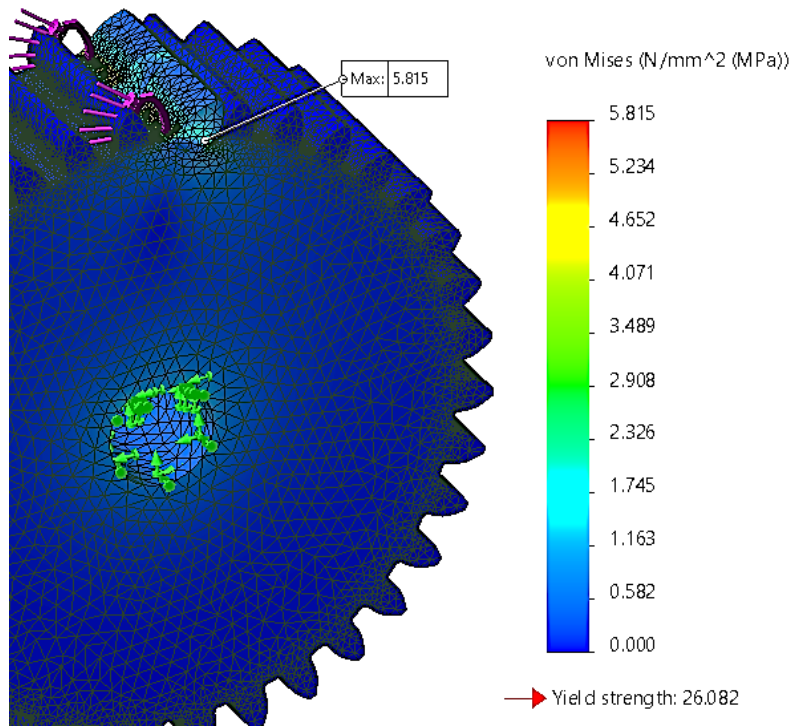
Figure 41 Driver gear, von Mises stress plot from FEM analysis.

Probes were placed around areas where the highest stress where marked. They show that the highest value of stress is the same as read out from von Mises stress plot. Figure 42 shows the placement of the probes.
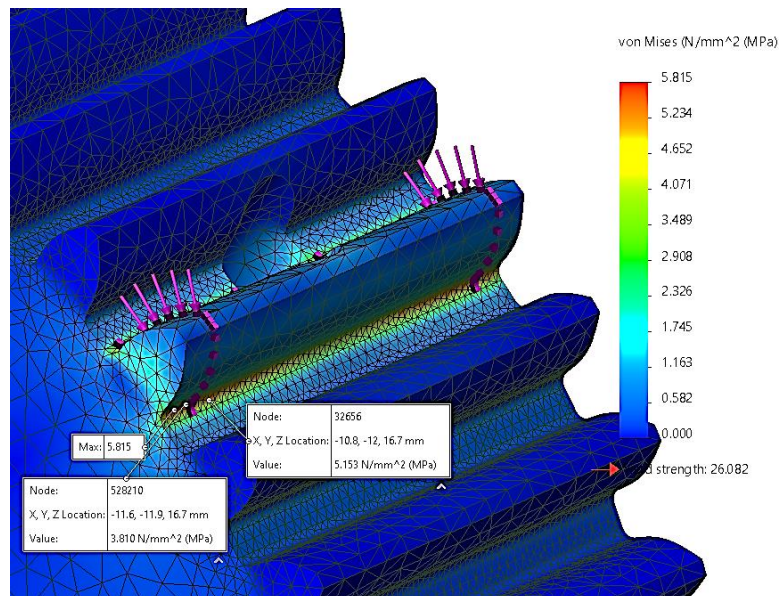
Figure 42 Driver gear. Stress readout with probes.
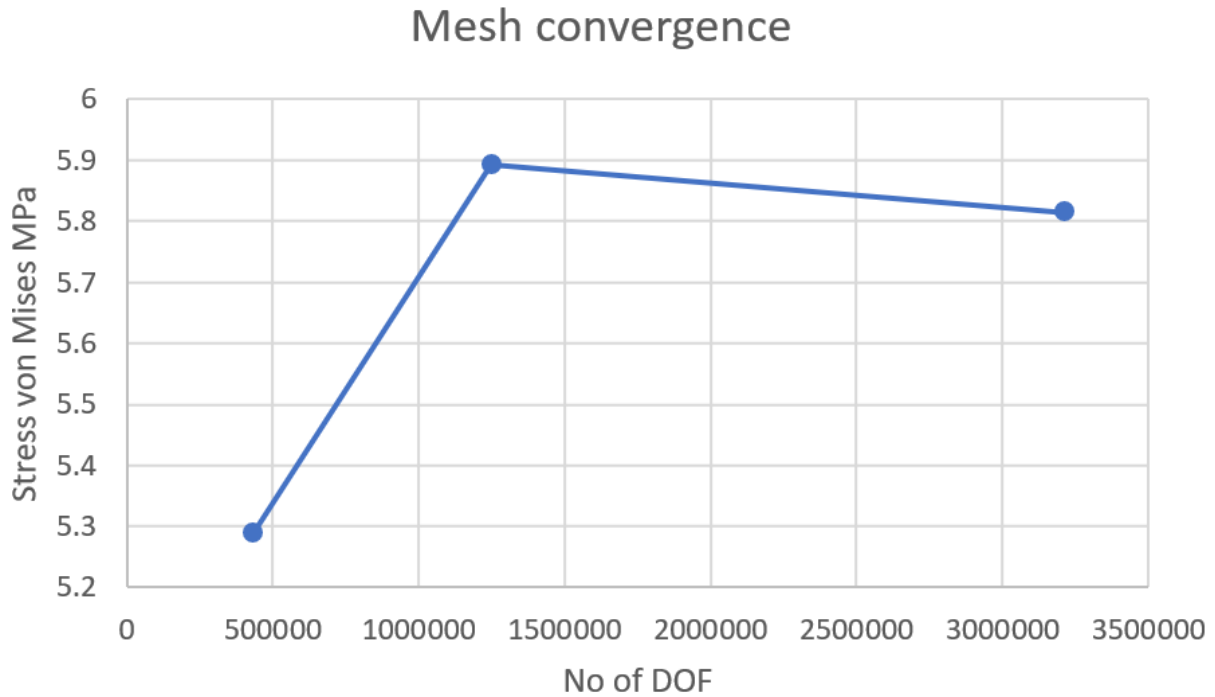
Figure 43 Stress vs No of DOF for driver gear.

The value of stress vs number of DOF shows that the convergence, this gives the indication that there are no stress singularities in the model.

Displacement

Figure 44 shows the displacement plot for the driving gear. The maximum displacement is 0.008mm, which is deemed acceptable.
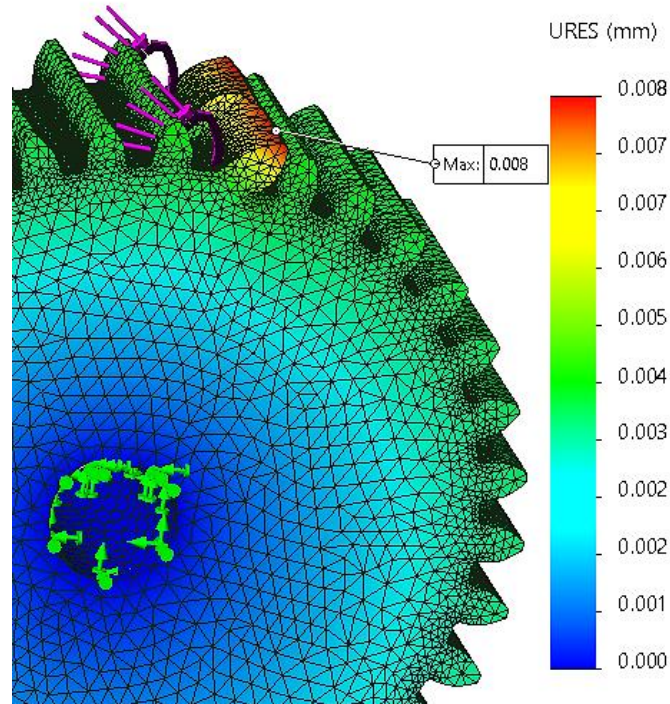
Figure 44 Driving gear, displacement plot.

Conclusion

The maximum stress observed was of 5,815 MPa and appears at the bottom of the tooth in the fillet radius. This was verified with two probes placed in the area around where there would most possibly be a singularity, see Figure 42. Further it was performed three simulations with an increasing mesh quality and mesh control were applied at the faces with highest stress. The result was a displacement of 0.008mm at the top of the tooth. Since the Yield strength for this material is 26 MPa it is no need to change to a stronger material:

$$safety\ factor = \frac{f_y}{\sigma_j} = \frac{26\ MPa}{5.815\ .MPa} \approx 4.45$$

3.7 Electrical motor selection

In section 2.6 it is shown that essential parameters for selecting an electrical motor is the load torque, second moment of area of the load and angular velocity. Determining these parameters is sufficient to calculate requirements for the motor's second moment of area, torque, and

power. This section will make an estimate of these values and then compare various motors on the market that meets these requirements. This section will focus on the motor driving the test arm as this is the most crucial part.

3.7.1 Inertia matching for motor driving test arm

The second moment of area of the load (which is the "test subject") will vary as tests can be run on many possible test subjects with different geometries. For simplicity, a rectangular geometry is used in the calculations, which cross-section and dimensions are shown in Figure 45. The equation for the second moment of area for this rectangle is $I_z = \frac{hb^4}{12}$ (Bell, 2014, p. 409).
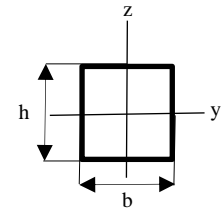
Figure 45 Dimensions of a rectangle's second moment of area.

The dimensions h and b will be different for the type of test subject, but some assumptions about the probable dimensions of a test subject can be made. Assuming that the length of the test subject is 200 mm, then a quite large cross-section would be a breadth and height (b = h), which are 20% of the test subject's length, i.e., 40 mm. The assumption here describes a test subject with a large cross-section and second moment of area, thus it should be a conservative assumption. The second area's moment of this test subject can then be calculated $I_z = \frac{hb^3}{12} = \frac{h^4}{12} = \frac{(40\ mm)^4}{12} = 213\ 333\ mm^4 = 2.13 * 10^{-7}\ m^4$

.

The required second moment of area of the motor can be found by setting I_z as I_L and setting the gearing ratio to $n = 2.7n_m$, in equation (12). Here 2.7 is the gearing ratio of the gear on the motor shaft (76 teeth) and the testing arm (204 teeth). In addition, it is necessary to consider the gearing ratio of any gearing box the motor is delivered with, referred to as n_m. The necessary second moment of area of the motor is thus to be greater than $\frac{213\ 333\ mm^4}{2.7^2 n^2} =$

$\frac{29\ 264\ mm^4}{n^2}$. If the motor's given second moment of area takes into account the gear ratio, then the required second moment of area is 29 264 mm^2.

3.7.2 Torque requirement for the motor driving the test arm

The load torque is the easiest parameter to calculate. It is assumed that 10N force is to be applied to the test subject. This is twice the force applied in an article performing fatigue testing on similar test subjects (Zawadzki, et al., 2022), and should thus suffice. With the chosen design, the test arm has a length of 185 mm from where the test arm is in contact with the test subject to the fulcrum.
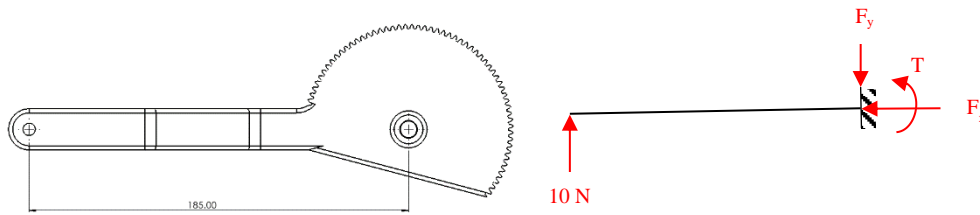
Figure 46 Simplifying test arm (dimensions in mm).

Assuming a load of 10 N on the test arm, as shown in Figure 46, one can calculate the torque production in a static situation. It is obvious that the force F_x is zero in this case, F_z is 10 N and the torque equals $T_L = Fr = 10\,N * 185\,mm = 1850\,Nmm = 1.85\,Nm$. Inserting this in the equation (14) and with the gearing ratio of 2.7 (between test arm and the gear on the electric motor shaft):

$$T_m > \frac{T_L}{n} \Longleftrightarrow T_m > \frac{1.85\,Nm}{2.7} \Longleftrightarrow$$

$$T_m > 0.69\,Nm$$

Assuming that the torque given by the motor is taking into account the motor's own gearbox, then the max torque output of the motor should be greater than 0.7 Nm.

3.7.3 Power requirement motor driving test arm

The power requirement is given by equation (16):

$$P = \omega T_L = 2 * \pi * (RPM\,\frac{1\,min}{60\,s}) * T_L$$

Torque (T_L) was calculated in section 3.7.2 above, but the RPM is yet to be specified. A higher RPM means that the test can be run faster. In a similar project where they made such a test machine, the RPM in one of the cases was 75 (Zawadzki, et al., 2022, p. 273). Entering this RPM and the torque into the equation gives a power requirement of:

$$P = 2 * \pi * \left(\frac{75 \; RPM}{60 \frac{s}{min}} \right) * (0.69 \; Nm) = 5.2 \; W$$

Thus, the motor is expected to be needing slightly above 5.2W. At a voltage of 5V this is about 1 ampere current and 1.7A at 3V. This means it is possible to power it with a Raspberry PI as they have GPIO pins that provide a voltage of 3.3V and 5V (Raspberry Pi Fundation, 2023).

3.7.4 Conclusion: motor driving test arm

Table 3 summarizes the motor requirements laid out in sections 2.6.1, 2.6.2 and 2.6.3. Type in the table means whether the motor should have characteristics close to the values or greater than the values.

<div align="center">

Table 4:

Motor requirements.

Requirement	Type	Value
Second moment of area	Close to	29 264 mm^2
Torque	Greater than	0.7 Nm
Power	Greater than	5.2 W

</div>

DC motor has been chosen as the motor type for the test arm, because: it is easier to calculate the power the DC motor uses than to calculate the power that a stepper motor uses (see section 2.5.2), DC motors have a more favorable price than servomotors and it is desirable to have a motor that can rotate several times as the design have its own gearing mechanism that requires more than one rotation (see section 3.3). There are a lot of DC electrical motors available on the consumer market. Table 5 compares some motors on the market. The values in the table are the standard values given, but in most cases, the datasheets show that more torque can be gained with the cost of lower RPM. This is better reflected by the power of the

motor since motors that have high torque and RPM have a higher power rating. The second moment of area was not given for the motors, thus this is not considered in the comparison.

Table 5:

DC motors comparison.

Model	Maximum Output torque (Nm)	Power (W)	Motor shaft diameter	RPM	Relative Price
Metal DC Geared Motor w/Encoder - 12V 251RPM 18Kg.cm	1.8	84	6	251	0.4
DC 24V 35W Mini DC Gear Motor Metal Speed Adjustable Large Torque Motor CW/CCW(24V 600rpm)	0.98	35	8	100	0.5
RS PRO Brushed Geared DC Geared Motor, 19.8 W, 12 V, 98 Ncm, 120 rpm, 6mm Shaft Diameter	0.98	19.8	6	120	0.7
RS PRO Brushed Geared, 7.92 W, 12 V dc, 98 Ncm, 19 rpm, 6mm Shaft Diameter	0.98	7.92	6	19	0.7
Micromotors Geared, 8 W, 12 V dc, 1 Nm, 9 rpm, 6mm Shaft Diameter	1	8	6	9	0.8
RS PRO Brushed Geared, 7 W, 12 V dc, 1.2 Nm, 8 rpm, 6mm Shaft Diameter	1.2	7	6	8	0.8
RS PRO Brushed Geared, 12.8 W, 12 V dc, 98 Ncm, 71 rpm, 6mm Shaft Diameter	0.98	12.8	6	71	0.8
RS PRO Brushed Geared, 41.3 W, 12 V dc, 1.8 Nm, 116 rpm, 8mm Shaft Diameter	1.8	41.3	8	116	0.9
RS PRO Brushed Geared, 7.92 W, 12 V dc, 98 Ncm, 99 rpm, 6mm Shaft Diameter	2.9	41.3	8	11	1.0
Crouzet Brushed Geared, 3 W, 12 V dc, 2 Nm, 2.9 rpm, 6mm Shaft Diameter	2	3	6	2.9	1.7

Of these different DC motors in Table 5, the Metal DC Geared Motor w/Encoder - 12V 251RPM 18Kg.cm was chosen for the project.

3.7.5 Other motors: magazine driver and test subject ejector

In addition to the motor driving the test arm, there is also a need for a motor to eject test subjects and one to move test subjects upward in the magazine. None of these motors will be under any significant load, thus no calculations are done for these two motors.

A stepper motor can be controlled open-loop, that is one can control its position without any feedback from the motor through an encoder (Bolton, 2019). This makes it a favorable choice for the motor that moves the test subjects in the magazine.

Test subjects are to be ejected by an arm controlled by a third electric motor. This motor will not be put under much load. A weak stepper motor or a simple DC motor with a mechanism that decouples the arm when it rotates too much so it doesn't break will work fine here.

3.8 Production methods

3.8.1 Additive rapid prototyping: fused-deposition modeling (3D-printing)

The 3D-printed pieces are an important part of the prototype. The frame is built up of aluminum profiles bound together with 3D-printed end covers and corner connections. They are fastened to the aluminum profiles with screws, which in turn hold the frame together. The magazine tower had to be split in two due to limitations in printing dimensions on the Prusa i3 mk3 printer. The other printed parts are the feeder lip, tilt mechanism, test arm, driver gear, support link, ejector arm, frame for the PSU and the electrical box.

Mostly everything was printed with the "quality" setting in the Prusa Slicer software and achieved the desired tolerances. In some cases, the CAD-files were slightly adjusted to avoid a too tight fit between two parts. Especially the parts that slides into the aluminum profiles were adjusted, but this was mainly because the procured aluminum profiles deviated slightly from the CAD models. Another brand of aluminum profiles with slightly different geometry was initially intended to be procured for the prototype, making the CAD model slightly different than the actual profile.

3.8.2 Circular saw: miter saw

The aluminum profiles were cut with a miter saw. The profiles are made of a light-weight aluminum alloy material which is quite soft. Both saw blades suited for cutting aluminum and steel and saw blades intended for woodcutting were used. Due to the fact that only a limited number of cuts had to be made and that the aluminum profile was thin (40x40 mm) and

somewhat hollowed out, cutting with a saw blade intended for wood was successful as well. This is however not recommended as it causes excessive wear on the blade.

Figure 47 Cutting aluminium profile with miter saw.

3.8.3 Drill

Holes in the aluminum profiles had to be made in order to mount the profiles with the 3D-printed parts. This was done by preinstalling the 3D-printed plastic on the aluminum profile and making a mark in the middle of the plastic hole on the aluminum. Metal bits with an outer layer of titanium nitride or titanium carbonitride were used. In all 13 holes had to be made. Both hand drills and press drills were used with success. The holes were drilled in accordance with the dimensions in Table 2, making them ready for threading. An alternative to this is to drill a wider hole through the entire aluminum profile and tighten it with a washer and nut on the opposite side. However, this alternative will not be suitable for all of the screw holes due to the design.

3.8.4 Angle grinder

An angle grinder was used to cut screws to length and as well as the threaded rod of one of the stepper motors. A cutting disc for stainless steel was used. The cutting was done by measuring the screw or rod and fasten it in a bench vice before cutting. As an alternative to the angle grinder, one can use a bow file.

3.8.5 Adhesives

Contact adhesive was applied to the lower part and upper part of the magazine. The adhesive was given about 3 minutes to dry. The lower and upper part was then pressed together with manual power and then held together in a vice for 5 minutes. The result was that the two parts adhered strongly together. This procedure can vary between different manufacturers and types.

3.8.6 Soldering

Soldering was mainly used to connect wires. On some wires, soldering was used to add female or male connections, which made it possible to connect the wires to the breadboard.

3.8.7 Threading and use of various hand tools

A threading tool was used to thread the various screw holes to fit the applicable machine screw. An alternative to this would be to use self-drilling screws. This alternative would also remove the need to drill holes. It would, however, be important to find screws with the correct length, at least if used without a pilot hole.

Pliers or multitool has been used throughout the assembly of the machine. It comes in handy in a variety of ways, like inserting jumper wires in a crowded breadboard or removing support filament on 3D-printed parts.

Files, rubbing blocks and sandpaper were used to smooth out dents and unevenness in both aluminum and plastic. It was also used to slightly widen holes and other tight fits in the 3D-printed plastics when the printed dimensions proved to be too small.

Screw drivers with appropriate bits, hex keys, spanners or other tools for fastening were used as required by the chosen bolts and nuts.

3.9 Electronics and wiring diagrams

Wiring and circuit diagram are discussed in this section. Each part of the electrical system is explained in isolation and in the last subsection the whole diagram is shown and discussed.

3.9.1 MCP3008

MCP3008 (U1) is connected to the Raspberry Pi 4's (J1) pins as shown in the diagram (CS/SHDN, Din, Dout and CLK). It is through these connections that the digital signal is sent to the Raspberry Pi 4. It also receives signals from A4, A5, R5, U4 and U5 at its channels 5, 4, 3, 1 and 2, respectively. Power is supplied to U1 from the power supply's 3.3V and it is connected to the power supply's ground (alternatively, it can power by connecting to Raspberry Pi's 3.3V and GND).
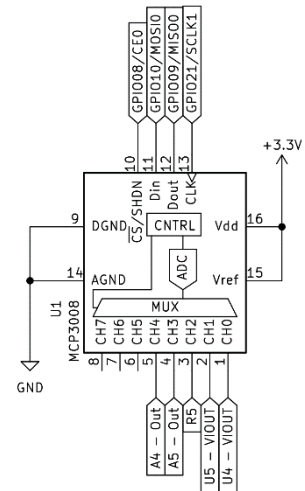
Figure 48 MCP3008 wiring.

3.9.2 Motor, voltage sensor and current sensor for test arm

The DC geared motor is connected to the Raspberry Pi 4 (J1) via the DC motor driver (A6). The motor driver is connected to the 12V power supply through 9-36V and PGND. OUT1 is connected to the motors negative and the OUT2 to positive. The motor driver is connected to the Raspberry Pi via COM, IN1, IN2 and PWM which is connected to ground, GPIO16, -17 and -18/PWM0 respectively. The encoder on the motor is powered by 5V and sends signals to GPIO14 and 15 on the Raspberry Pi.

The ampere sensor (U5) and voltage sensor (U4) are both connected to the power supply via 5V and ground. The ampere sensor is connected in series with the motor, whilst the voltage sensor is connected in parallel. Both the voltage sensor and ampere sensor produce an analog output which is respectively connected to channel 0 and 1 on the analog to digital converter (U1).
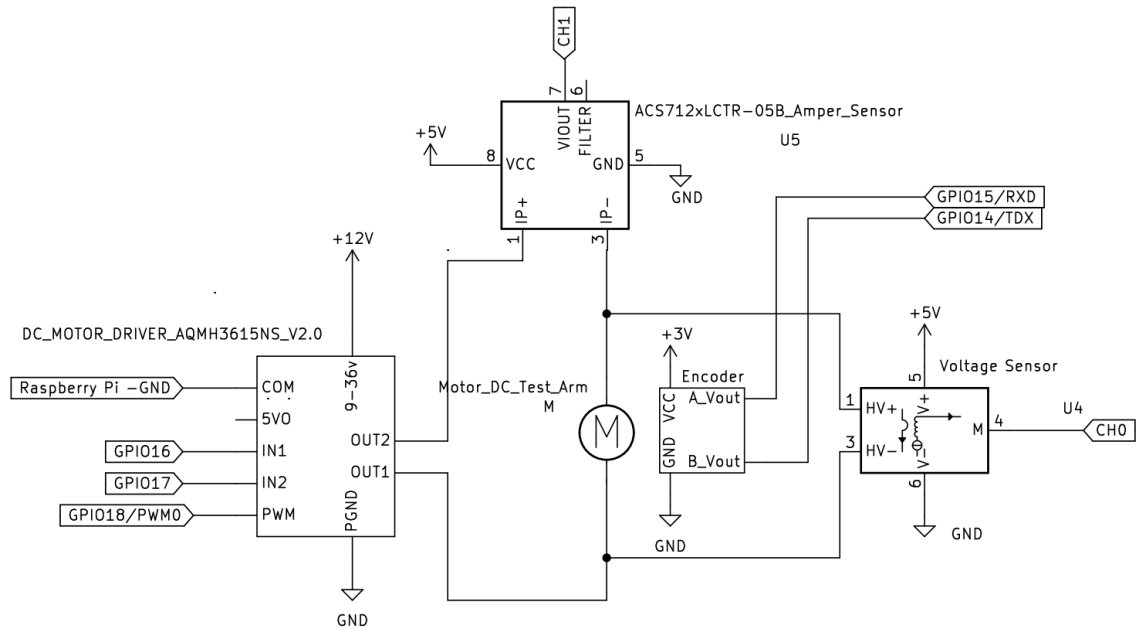
Figure 49 test arm DC Motors electronics.

3.9.3 Stepper motors

The stepper motors (M2 and M3) are connected to the driver via four wires. 4 to 1A, 1 to 2A, 3 to 1B and 2 to 2B. The drivers (A2 and A3) are connected to the power supply unit via 12-volt and ground. A capacitor of 100uF is connected between these wires. The drivers are also connected to 5-volt power and to ground on the Raspberry Pi 4 (J1). The STEP and DIR pins are connected to GPIO 6 and 4 for the stepper motor controlling the magazine and GPIO 19 and 20 for the motor controlling the ejector. All the MSX inputs are not connected, therefore the motors are in their full step mode. RESET and SLEEP are connected together and also to 3,3-volts setting their conditions to HIGH. This, along with the ENABLE input kept at LOW, maintains the driver active at all times.
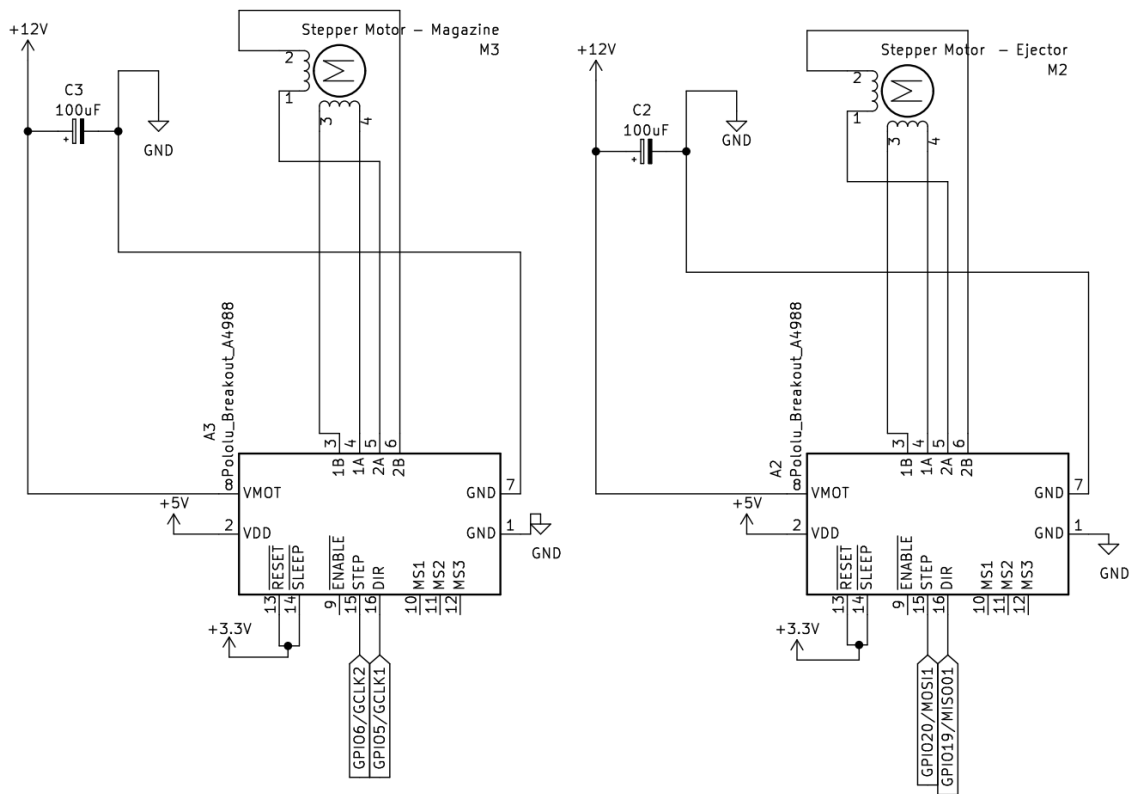
Figure 50 Stepper motors electronics.

3.9.4 Force/pressure sensors

The force/pressure sensors (A4 and A5) are connected to the 5V output from the power supply (VCC) and to the power supply's ground (GND). The out signal (Out) is connected to the MCP3008's (U1) channels 3 and 5 (CH3 and CH4).
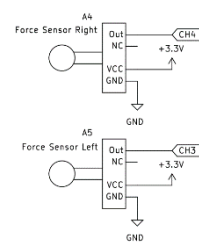
Figure 51 Force Sensors wiring.

3.9.5 Potentiometer

The potentiometer (RV1) is wired into the 5V output from the power supply and to its GND (1 and 3). The output signal (3) is connected to the channel 2 (CH2) of the MCP3008 (U1), which then delivers the voltage (and thus the position of the test arm) to the Raspberry Pi 4 (J1).
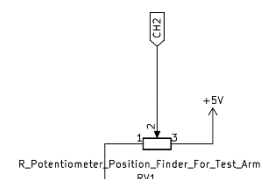
Figure 52 Potentiometer wiring.

106

3.9.6 Buttons and lights

Figure 53 shows the wiring of the two buttons "Start/Restart" and "Start/Pause" to GPIO26 and GPIO27, respectively. It also shows the four LED lights, green 1, green 2, orange and red. The LED lights are connected respectively to GPIO22, GPIO23, GPIO24 and GPIO25.
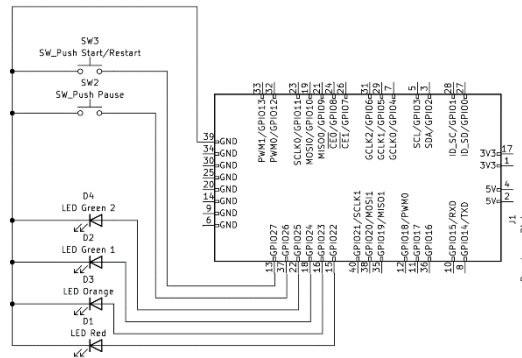
Figure 53 Buttons and LED lights.

3.9.7 Power supply unit (PSU) and fuses

The machine is supplied with electrical power from a power supply unit (PSU) designed for personal computers. These have a pinout called ATX which is explained in 2.9.7. In this bachelor thesis, a Seasonic 400W ATX Power Supply (100 → 240V AC Input, 3.3V Output) or Corsair CV450 has been used. The main sets of components (stepper motors, test motors and microcontroller) are in parallel circuits and each circuit should have an appropriate fuse, as shown in Figure 54.
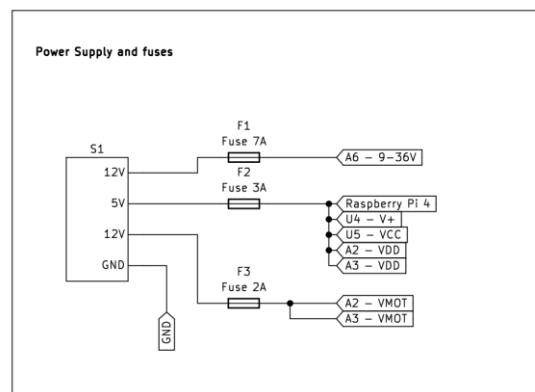
Figure 54 Circuit: Power Supply.

Table 6 shows the requirements for the fuses shown in Figure 54. These requirements are based on the limits laid out in the datasheets of the components.

Table 6:

Fuses requirements

COMPONENT	CODE	#	FUSE	REFERENCE
RASPBERRY PI 4	J1	1	3 A	https://thepihut.com/blogs/raspberry-pi-tutorials/how-do-i-power-my-raspberry-pi
STEPPER DRIVER CARD	A2,A3	2	3 A	https://www.pololu.com/file/0J450/a4988_DMOS_microstepping_driver_with_translator.pdf
DC VOLT TRANSFORMER	A1	1	Connect to raspberry pi	https://www.mantech.co.za/Datasheets/Products/Voltage%20Sensor-170640_SGT.pdf
FORCE SENSORS	A4,A5	2	Connect to raspberry pi	
POTENTIOMETER	RV1	1	Connect to raspberry pi	
DC_MOTOR_DRIVER_AQMH3615NS_V2.0	A6	1	8A	Base on motors stall current: https://wiki.dfrobot.com/12V_DC_Motor_122_rpm_w_Encoder_SKU__FIT0403
VOLTAGE SENSOR	U4	1	Connect to raspberry pi	
AMPER SENSOR	U5	1	Connect to raspberry pi	
MCP3008	U1	1	Connect to raspberry pi	

3.9.8 Wiring

Most of the component utilizes lower currents (1A or lower) and can be connected with normal jumper wires. However, the DC motor for the test arm is as much 7A (DFROBOT, 2023) and thus a wire with a cross-sectional area of at least 4 mm^2 is needed (see 2.9.9), here a RK-7 will be more than sufficient with its 6 mm^2.

3.9.9 The whole wiring diagram

Figure 55 shows the whole electrical wiring, except the wiring from the PSU's 5V into the USB-C port of the Raspberry Pi. The box in the upper left corner shows the PSU, fuses and how it is connected to all the various components in the system. As it shows, there are a lot of parallel connections. Most of the components are connected to the 5V, except the motors that are connected to the 12V and the DC voltage converter that is connected to both the 5V and the 3.3V.

In the center of the diagram is the Raspberry Pi. This is the microcontroller that controls all the motors, lights, and buttons and processes all the sensor inputs. The connections to the various IC and cards go into the Raspberry Pi's numerous GPIO pins. In some cases, the

choice is arbitrary. In other cases, it is determined by requirements for the various IC and cards.

Over the Raspberry Pi, two stepper motors and their control cards are shown. This is the motor for the ejector arm and for the magazine.

Left for the Raspberry Pi are the various buttons and LED lights. Further left are the ADC and the force sensors. The ADC is connected to the force sensor, the potentiometer (below it in the diagram), the voltmeter and the amperemeter.

Below the Raspberry Pi is the DC motor controlling the test arm, the voltmeter and the amperemeter. On the right is a DC voltage converter needed for converting the 5V signal from the DC motor encoder into 3.3V signal that can be received by the Raspberry Pi.
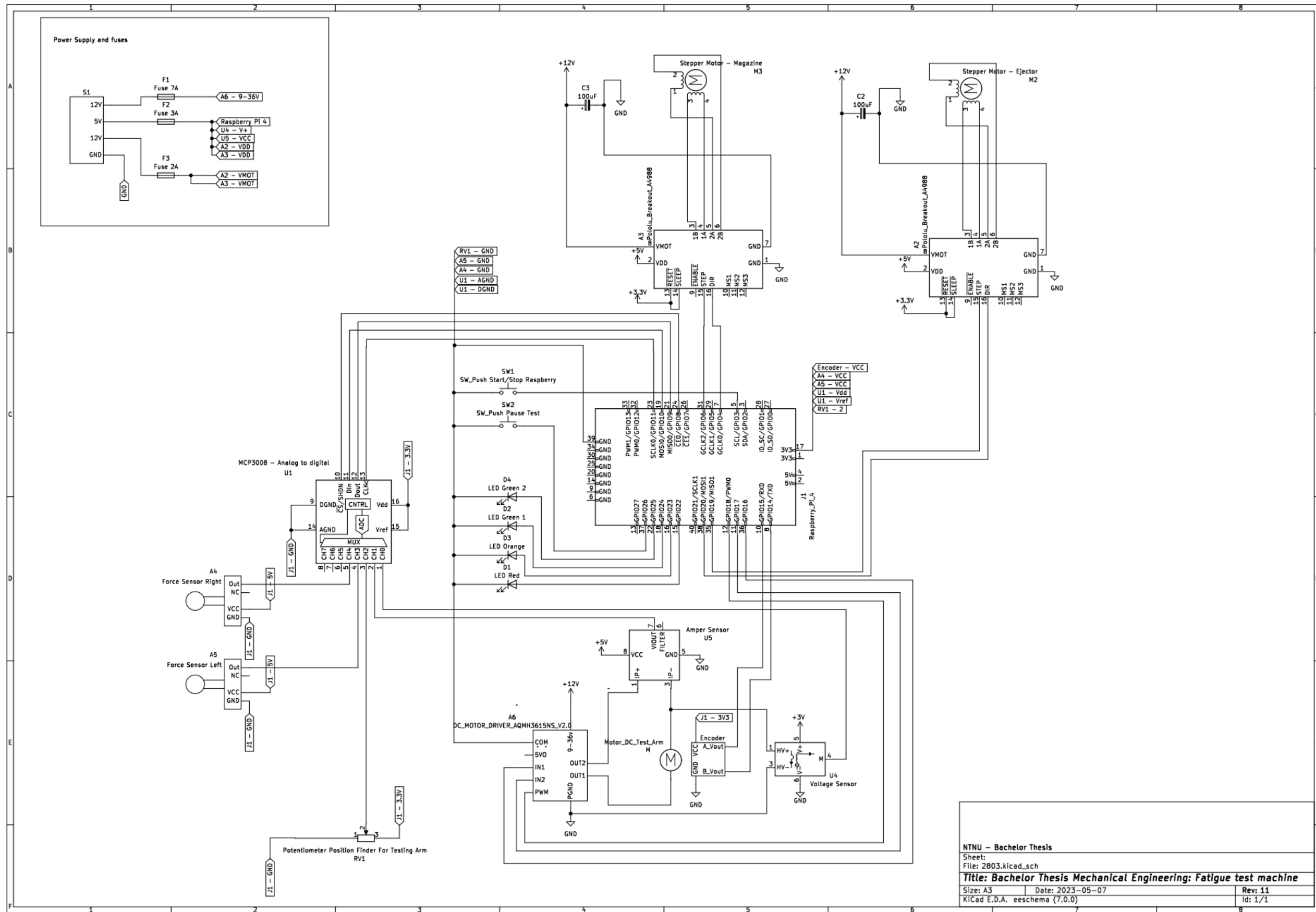
Figure 55 Whole wiring diagram.

110

The voltage in the system is fairly easily determined as almost all of the main set of components are connected in parallel. The voltage in parallel connections is equal and equal to the voltage of the total voltage, i.e. the voltage of the power source (Gomeringer, et al., 2017, p. 54). Thus, the voltage in each parallel connection connected to the same voltage output of the PSU is equal to each other and equal to the voltage rating of that PSU output (3.3V, 5V or 12V).

The table below shows the total current needed for the most current intensive subsystems based on the datasheets. It shows that a total current of above 13A is needed (the other components draw a negligible amount of current). This is far below the current that can be provided by the PSU, which is up to 36A for 12V, and 20A for 5V or 3.3V (SHWETA COMPUTERS, 2023).

Table 7:

Current needed by the most current intensive subsystems

SUBSYSTEM	CURRENT	VOLTAGE
RASPBERRY PI 4 B	3A	5V
NEMA 17 STEPPER MOTOR	1.33 A	2.8V
NEMA 17 STEPPER MOTOR WITH AXEL	1.5 A	3.3 V
METAL DC GEARED MOTOR DF ROBOT 12 V 251 RPM	7A	12V

The fuses shown in the top left of the Figure 55 are particularly important since the PSU can provide more than ten times the current needed by some of the components.

3.10 Software, programming and mechatronics

There are three steps in using the machine, as illustrated in Figure 56. Each of them involves using software:

1. A test plan must be set up in a software user interface and transferred to a USB stick.
2. The USB stick with the test plan is inserted into the test machine's USB slot, which then executes the plan. The execution and control of the machine is done with software.
3. When the tests are finished, the results are written to the USB, which then needs to be analyzed with software.
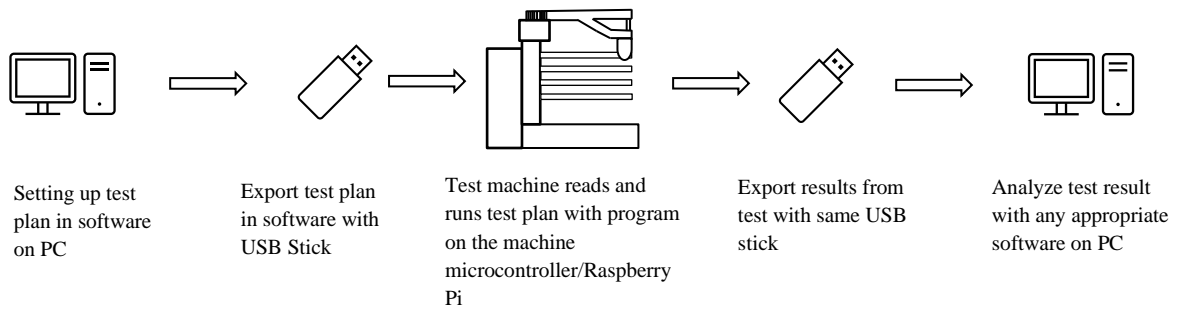
Figure 56 The three steps of using the fatigue testing machine.

For steps 1 and 2, a new software has been written and will be explained in the following sections.

For step 3, the output is written to CSV files to the USB stick and can therefore easily be read by any data analyzing software or with a programming language (such as Excel, Power BI, Tableau, R, Python, MatLab etc.). It is therefore not necessary to make new software for analyzing the output as there is a multitude of existing products that already can do this, and the user can choose after their own preference.

3.10.1 Software for setting up test

A graphical user interface (GUI) has been made to set up the tests. The Software uses the .NET framework and is written in C#. The GUI has been made using Windows Presentation Forms (see (Microsoft, 2023)). The program is made for Windows 10/11 and is started by double-clicking an executable file (.exe). This will bring up the interface shown in Figure 57.
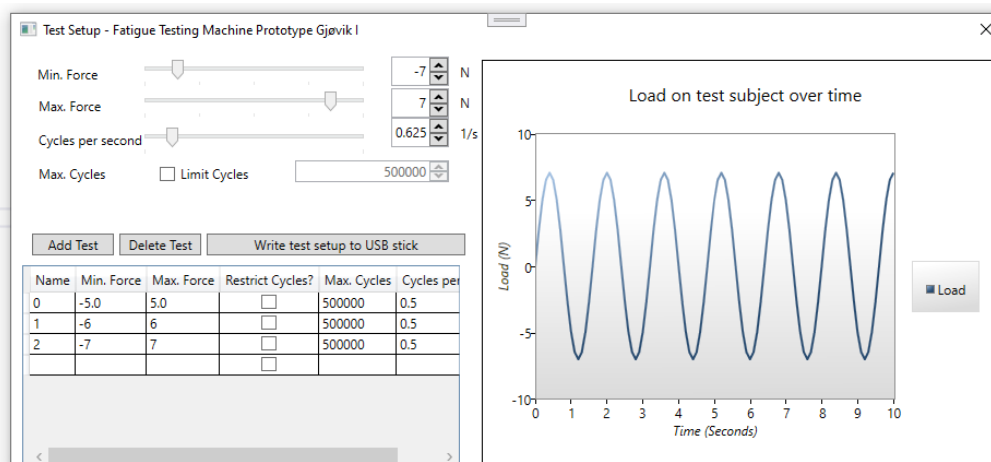
Figure 57 Test setup program.

The program's user interface (UI) should be quite self-explanatory. One sets the min and max force of the test, the speed (cycles per second), whether the machine should stop after a number of cycles (Limit Cycles) and then click "Add Test" to add the test run to the testing plan. "Delete Test" can be used to remove tests from the testing plan. When finished, click "Write test setup to USB stick" and save it to a USB stick for insertion into the test machine. The test file saved to the USB stick is in a JSON data format.

3.10.2 Machine software

Machine software refers here to the code on the fatigue testing machine that is used to control the machine. The machine software is written in Python and runs on the Raspbian operative system installed on a Raspberry Pi 4B.

The program consists of 7 Python files which can be found in appendix 8.2. At startup, initiated by turning on the PSU, the Raspbian runs the file called "Main.py", which starts the fatigue testing program. This is done by changing some of the Raspbians configuration files (Hymel, 2023), more precisely by adding "python {insert path of main.py file}/Main.py &" before "exit 0" to the "/etc/rc.local" file.

At the start of the program, the green light "ON/OFF" turns on. The program then starts searching for a USB stick with a test plan. It chooses the most recent file with a valid test plan format, as defined by the program described in section 3.10.1. If a file is not found, then the orange light starts blinking. By clicking the "Start/Resume" button, it will again try to load a test plan. If it successfully loads a test plan, then the green "Running/Pause" light starts blinking.

Clicking the "Resume/Pause" button when the green "Start/Resume" light is blinking will start the test. Starting the test involves reading the first test in the test plan. It will then apply cyclic load to the test subject until failure. After failure, the DC motor in the test arm centers the arm, the stepper motor in the magazine moves the failed test subject up and then the machine ejects it with the ejector motor. The number of cycles is then written on the USB stick in a csv. file format, before the machine continues to the next test in the testing plan.

At finishing the last test, it turns off the ON/OFF light. The machine can be started again at a new test by clicking the ON/OFF button twice.

Figure 58 illustrates the description of how the program works above. Boxes represent different states, boxes processes and the triangles conditions in the program.
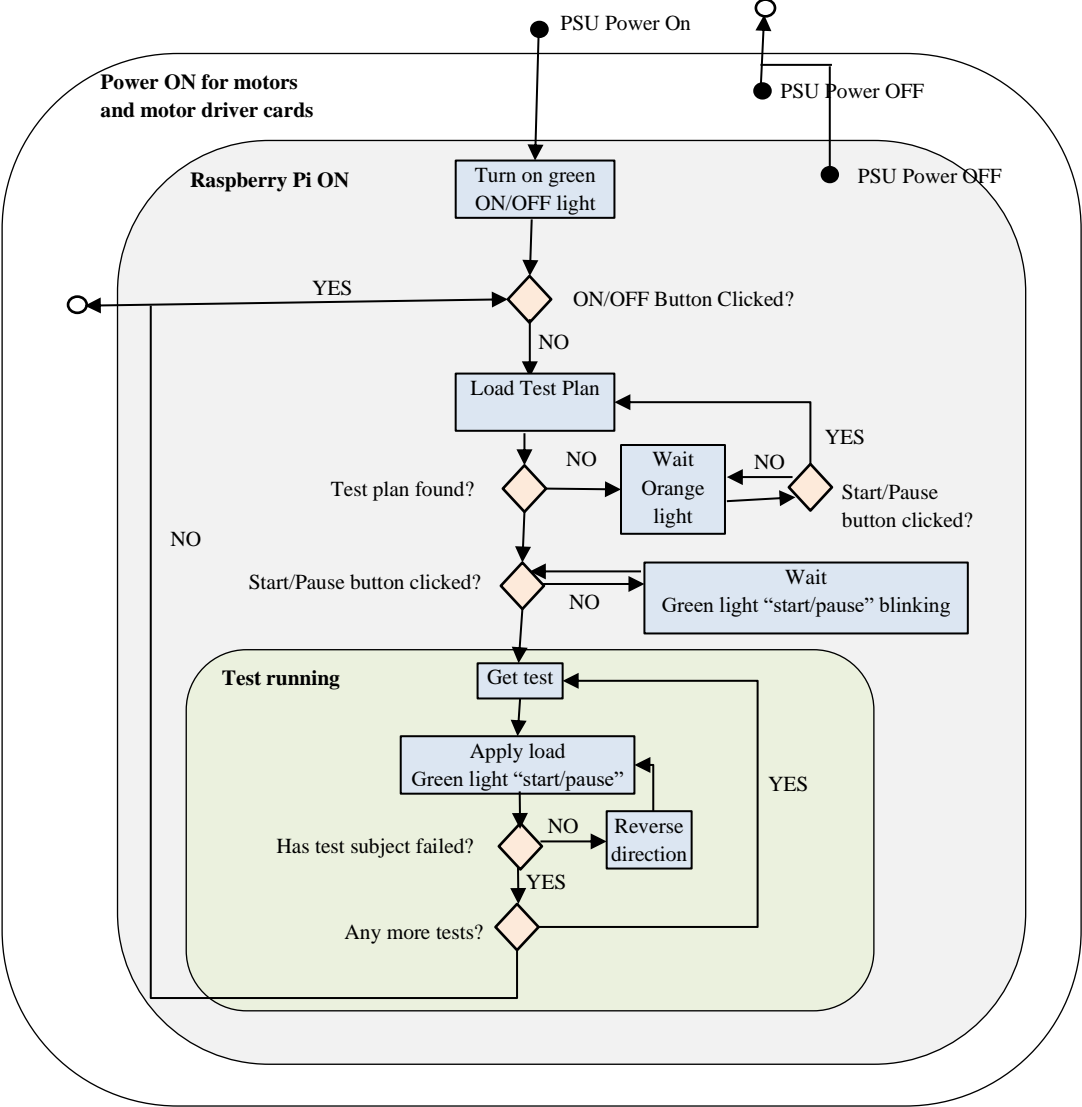
Figure 58 Diagram describing the program and its states.

3.10.3 Force Sensor Calibration

The force/pressure sensors were calibrated by adding 0.1, 0.3, 0.6, 0.9 and 1 kg weights on the force sensor pad and then taking 50 readings from the MCP3008 with 0.1s between each reading. The weights were translated into force by multiplying with the gravity acceleration of 9.81. The results of these measurements are shown in Figure 59, where Vout is the out signal from the MCP3008 read by the Raspberry Pi microcontroller.

114

Force sensor out signal vs. force applied to sensor

$$Force = 1E\text{-}07 * e^{19.91 * Vout}$$
$$R^2 = 0.5746$$
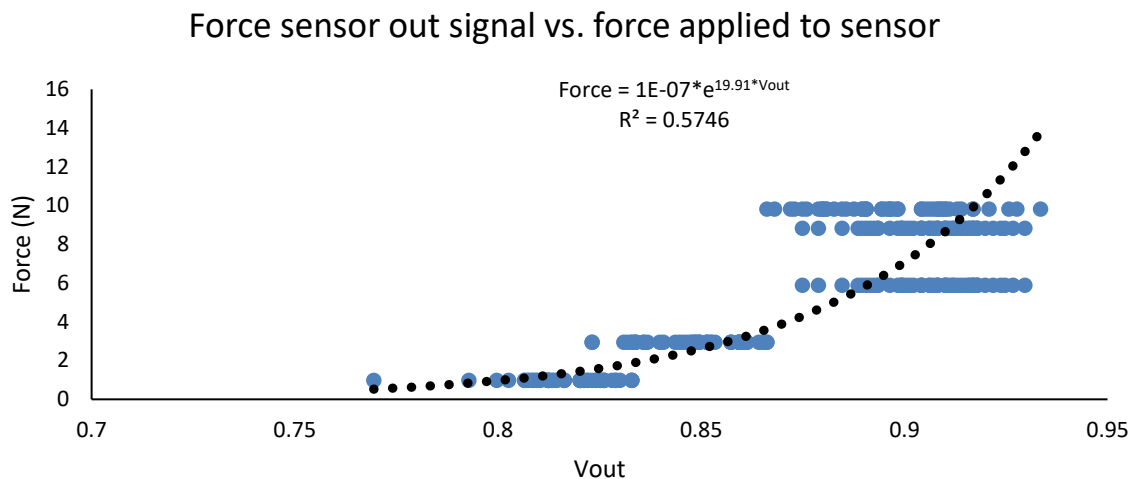
Figure 59 Force sensor calibration.

A good sensor is sensitive to what is measured and insensitive to all other factors (Jonsdottir, 2016, p. 21). The characteristic curve is estimated with an OLS regression with a logarithm transformation so that the force applied to the sensor is expressed as an exponential functional of the signal read from the MCP3008. This regression equation is shown in the top right corner of Figure 59. However, the equation has a low R^2 and thus not explaining the variance in the data very well (Løvås, 2005, p. 289). A plainer way to explain the problem is that there is a lot of overlap in the reading of the signal from the sensor at different forces. In other words, it is not a very good sensor due to high variance/noise in measurements and non-linear sensor characteristics.

A possible way to improve the sensor is suggested by the datasheet and would involve dropping the small chip that was delivered with the pressure pad and instead use a low resistance of 3kΩ between the pressure pad and an amplifier (Interlink Electronics, 2017, p. 3). According to the datasheet, this should give a more linear and thus more favorable characteristic of the sensor.

4 Prototype and results

4.1 General description

Figure 60 shows the prototype (version T) made in this bachelor thesis. Two prototypes were made (T and E) in total, with some variations on the handling of the electronics and cables. The following sections will describe the prototype and what was learned from building and testing it. It has not been carried out comprehensive testing of the machine. Therefore, the assessments in this chapter are considerations based on a general impression and on functional testing.
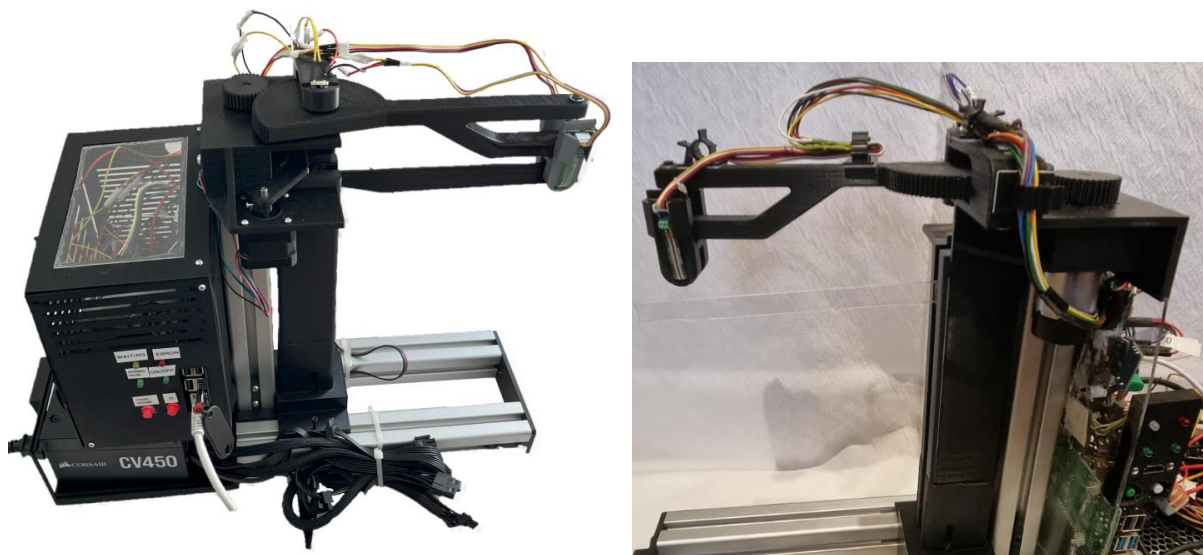
Figure 60 Picture of the prototypes T (left) and E (right) of a desktop-sized fatigue testing machine.

4.2 Electronics and sensors

4.2.1 Stepper motors

The stepper motors and the electronics for controlling the stepper motors worked well. They were easily controlled precisely and reliably with the microcontroller. The control was achieved when using "full step", thus even better control could have been attained by using the other stepping conditions (see 2.9.4), but the "full step" option was sufficient for moving the next test subject up and ejecting the old one.

4.2.2 DC Motor and controlling of the test arm

Control over the test arm proved to be difficult. A tolerable level of control was achieved, but a high level of control was not achieved even though the motor ran at a very low rate (PWM set to 0.1, which corresponds to 10 %). At this low PWM the test arm was still moving fast, making the test sequence somewhat sharp and it reduced the overall precision. The motor was easily controlled with the motor driver card, but there were circumstances where the motor ran out of control. The issue was not obviously code related. It was still possible to control and perform the test with the test arm, but due to the relatively high minimum speed, the testing scheme was rather abrupt, and a very accurate control was not achieved. In addition, returning the test arm to the center was in many cases off by about 1-2° degrees.

4.2.3 Potentiometer

Calculating the angle of the test arm with the potentiometer worked well, but there was some fluctuation in the values, so they had to be averaged to reduce the noise. Overall, it worked well.

4.2.4 Force sensor

The left and right force sensor worked. However, testing shows that they have an unfortunate sensor characteristic in regard to linearity and variance (see 3.10.3). Otherwise, they worked consistently.

4.2.5 Ampere- and voltmeter

The voltmeter only gave readings when the motor turned in one direction. The amperemeter gave readings, but they were constant whether or not the engine was turning. In conclusion, these electronic parts did not satisfy the requirements.

4.2.6 User interface

The panel with switches and LEDs for controlling and observing the different states of the machine functioned well. This is an important feature of the machine as it is the main man-machine interface. This interface also includes the process of setting up the test parameters and uploading them to the microcontroller.

4.3 Design

4.3.1 The frame

The frame of the machine has been an aspect that worked well for its purpose. It serves as an attachment for all operating parts in a space-efficient way. The PSU, electrical box and motors are positioned rather close to each other, simplifying the connections between these three stations and enhancing the overall tidiness of the machine. To the extent the machine has been tested, the frame has proven to withstand the load of running fatigue tests. The frame also gives an impression of a platform that is stable and rigid despite being rather light weight and fairly easy to build.

4.3.2 The magazine

The magazine works as intended in most areas. It can be adjusted in accordance with the length of the test subjects within the limitations and it can withstand the load transferred to it during fatigue testing. Even though comprehensive testing has not been carried out, it seems like the magazine motor will have no problem handling a full magazine of test subjects. A problem with the magazine has arisen when test subjects break far from the magazine. This can lead to the test subject and test holder tilting and getting stuck when reaching the top of

118

the magazine screw. If this happens, the ejector arm is unable to remove the finished test subject.

4.3.3 The tilt mechanism and test arm

In the testing of the fatigue testing machine, it often happened that the test subject was not loaded correctly into the tilt mechanism. This problem was a combination of the tilt mechanism not being very wide and the control of the test arm not beeing reliable to center the arm correctly. Widening the distance between the force sensors in the tilt mechanism would solve this issue.

The test arm was strong enough to handle the forces of a fatigue testing sequence. On the other hand, the dimensions of the test arm set limitations on the size of the test subjects. If larger test subjects are to be used, the test arm has to be longer. Also, the gap on the tilt mechanism has to be deeper and the opening in the motor plate where the ejector arm operates has to be higher.

4.3.4 Gearing

The gearing worked fine, but a higher gearing ratio would have helped in gaining better control over the test arm. This would also reduce the torque needed from the motor.

4.3.5 Cable management

The cable management differed somewhat between prototype T and E. Figure 61 shows prototype E, which has much better management of the cables than prototype T shown to the left in Figure 61. Prototype E achieves this through the use of strips and various cable fasteners. Prototype T has the advantage that cables are protected by a box, but a combination of these two approaches and a smaller electrical box would be ideal.
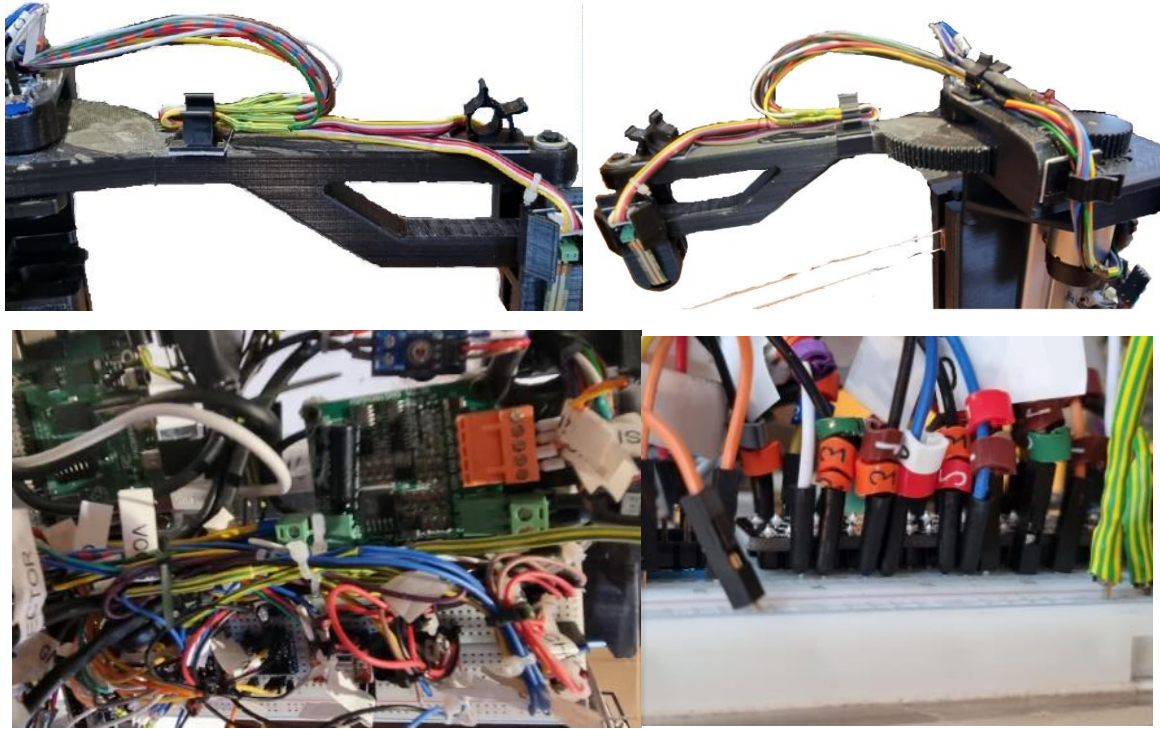
Figure 61 The two top images show the wiring on the test arm (seen from right and left side). The two bottom images show breadboard and motor drivers.

5 Discussion and limitations

5.1 A short comment on procurement, COVID, supply chains and availability of Raspberry Pi

Procurement of electronics for the project has been challenging, with long delivery times, especially for the Raspberry Pi. The availability of the Raspberry Pi has been scarce and very much limited to what could be bought on the second-hand market. The manufacturer of the Raspberry Pi has had issues with their supply chains after the COVID pandemic, and it is first expected to be widely available again in the second half of 2023 (Upton, 2022). In hindsight, a cheaper and more easily acquired microcontroller should have been chosen, given the situation at the start of this project.

5.2 Environmental concerns and ethics

UN's sustainability goal 12 concerns consumption and production, wherein recycling of electronics and widgets is an important policy. Since the test machine is made of thermoplastic and aluminum, it is quite recyclable. Aluminum can be melted and recycled. The plastic used is thermoplastic and can in theory be recycled. However, since fatigue testing machines are not something that ever will be mass produced, the environmental impact is negligible. If the machine actually could help in better design and improved lifetime of various 3D-printed widgets, then it has a potential for a net positive environmental impact.

Regarding ethics this project should also be unproblematic. A common definition of ethics is that ethics relates to the teaching of how to treat one's fellow man. Very simplified, ethics/morality is all about not to do harm onto others. There is very little potential for the fatigue testing machine to do any harm to anyone, except obvious a risk of fire, crush injury, electric shock damage and similar situations that can occur with any electronic appliances that can be bought at a local mall selling such thing. In conclusion, there should not be any ethical issues related to this bachelor thesis other than warning successors about potential risks.

5.3   Results from testing the prototype

This section summarizes what was learned about the design from building and testing the prototype.

5.3.1 What did work?

The prototype demonstrated that a lot of features worked well with the design. Some of these are:

- Stepper motors for ejector arm and magazine worked well with good precision and control from the microcontroller.

- The potentiometer performed as intended and gave sensible readings.

- The user interface functioned in an effective way, despite being simple.

- The frame and the test arm were both stable and solid.

- The tilt mechanism worked well in ensuring a perpendicular force vector on the pressure sensors.

- The magazine performed well in most scenarios.

- The electrical box managed to hide a large portion of the electrical components.

5.3.2 What did not work?

The prototype also revealed some flaws with the design:

- Precise control of the test arm was not achieved due to the motor and gearing.

- Ampere- and voltmeter readings did not work when motor runs both directions.

- Force sensor characteristics were problematic.

- Physical limitations on the test subject due to test arm, tilt mechanism and motor plate.

- Cable management could be better.

- Broken test subjects got stuck when they fractured too far away from the test subject holder because they tipped forward.

5.4 Improvements of the design and further work

5.4.1 Making the motor plate compatible Nema 17 stepper motor

The DC motor was not ideal for operating and controlling the test arm. More precise and less harsh operation is desired in this operation. The use of a stepper motor or servo motor would presumably be a more eligible choice. Stepper motors are, as discussed earlier in the thesis, easily controllable with high-resolution steps. A servomotor is a linear or rotary actuator that gives high precision control of speed or position due to sensor feedback. It often has a limited range of physical stops. A drawback of the use of a servomotor is that it requires a rather complex controller (Gastreich, 2018).

Only minor changes are needed to the motor plate design to make it compatible with other motors of comparable sizes. Figure 62 shows the changed dimension on a modified design of the motor plate. The modifications make it possible to use NEMA 17 stepper motor to control the test arm instead of the motor Metal DC Geared Motor w/Encoder - 12V 251RPM 18Kg.cm. Similar changes can be made to use a servo motor. Thus, implementing this small change will make it possible to replace the existing motor with a stepper motor that will give better control over the test arm.
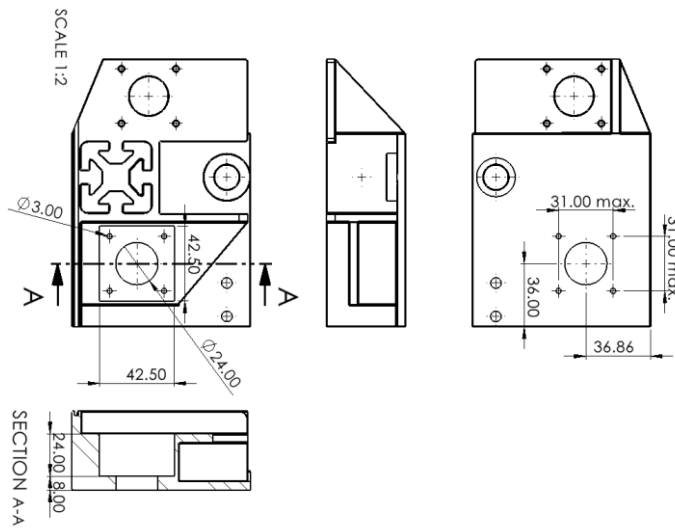
Figure 62 Modified design of motor plate for using NEMA 17 stepper motor to control test arm.

5.4.2 Widening the tilt mechanism

Centering the test arm so that the test subjects fit nicely into the tilt mechanism proved difficult with the current design. Part of this was due to a lack of accurate control over the test arm, but also due to the gap being very narrow in the tilt mechanism. Figure 63 shows a modified design with a broadened gap between the holders for the pressure sensors.
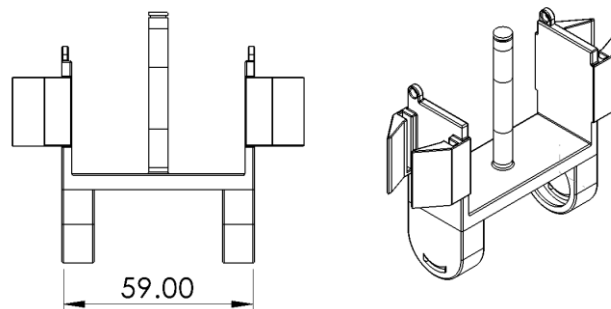
Figure 63 Modified tilt mechanism.

5.4.3 Modules

Multiple modules can be done for the tilt mechanism, test arm and driver gear to perform other modes of fatigue testing (e.g. mechanism that applies axial forces and torsion etc.).

124

5.4.4 Electronic components and further testing

The reading from the voltmeter only worked in one direction. A possible solution is to use two, one dedicated to each way the motor can spin. The amperemeter showed constant reading, so either the component was defective, or the actual current was constant and only the voltage changed. These components need further testing.

The force sensors exhibited a measuring characteristic that resulted in low precision in the readings obtained from the sensors. As discussed in previous sections, adjusting some of the resistances in the circuit or the input voltage may improve the characteristic of the sensor. Be that as it may, high quality readings of actually applied force on the test arm probably require procurement of higher quality components more suited for the purpose.

5.4.5 Gravity based ejection

The design can probably be changed so that the test subject is ejected by using gravity, thus eliminating the need for the motor controlling the ejector arm. This would require a slight change to the motor plate and the magazine so that a sloop or track is made where the old test subject can fall down and away from the machine.

5.4.6 Material choice

The machine is mainly built with aluminum profiles and FDM parts in PLA. The aluminum profiles have functioned as the main frame parts. Aluminum is not a very strong metal, but for this project, it has been strong enough. It is also a rather inexpensive material and has the advantage of being easy to cut, drill and grind without expensive equipment. As an alternative, it could likely be possible to use 3D-printed bars instead of aluminum if this is desired. If one desires to scale the machine up so that larger and stronger plastics can be tested, aluminum bars would possibly still be sufficient in the frame.

The 3D-printed parts are required to connect the frame together, to be a platform or shelter for other components as well as to provide parts directly involved in the fatigue test itself. The FDM parts on the machine are exposed to forces generated through fatigue testing. Simulations, calculations and functional tests have shown that the parts can handle the load. Some of the parts have been of special concern as they are exposed to large forces. This has

been the case for the small and fine gear teeth of the test arm and driving gear, which has been evaluated thoroughly and found to be capable of the task. If one desires to scale the machine up to conduct fatigue testing on larger and stronger plastics, it is recommended to perform new calculations and simulations on the FDM parts and make improvements if needed.

6   Conclusion

In this bachelor thesis, a desktop-sized fatigue testing machine has been designed. It can be argued that the machine is relatively easy to build. All CAD files, drawings and program code files have been made available open source through an open Google Drive link. Therefore, the overall goal of this bachelor thesis has been achieved. Furthermore, prototypes were built and tested. However, the building of the prototype revealed some flaws with the design. Fixes for these flaws have been discussed in sections 4 and 5.

Besides the overall goal of designing and building a prototype for a desktop-sized fatigue testing machine with open-source code and design, seven more concrete subgoals were also stipulated in the introduction of this thesis. These seven subgoals were only partly achieved:

1. The machine was not able to read the force applied on the test subject from the power drawn due to a problem with the sensors.

2. The machine was able to count the number of cycles of applied force to the test subject, but it was only able to measure the force applied to the force sensor with low accuracy due to nonlinearity in sensor characteristics and a high degree of noise/variance in the measurements. However, this is more likely a result of cheap, low-quality components and could be solved by investing in higher quality and more suited sensors.

3. The machine has a functional design and is decently user-friendly. It automatically reads test plans from a software made for it and that automatically outputs the output data from the tests.

4. In designing machine mechanics, FEM analysis, wiring diagrams, CAD modeling and production method theory; were utilized. Thus, the design was based on engineering principles and theory.

5. Given access to FDM and availability to procure some of the basic parts and some of the tools, it should be fairly easy to build the machine. Especially since all drawings, CAD files and program code have been made available.

6. The machine is able to change test subjects automatically without manual replacement.

7. The prototype has been tested in this bachelor thesis and the design has been evaluated. However, more testing could have been done and several iterations of the prototype would have been beneficial to improve the design further.

In conclusion, 5 of 7 subgoals were achieved and subgoal two was partly achieved. Subgoal 1 was not accomplished. However, the overall goal was achieved, and a working design was produced. Some small changes to the design by performing a topology optimization of the model would reduce the consumption of material and lessen the production time, current consumption, and wear and tear of production equipment, resulting in a total lower production cost at the end of the product. Procurement of higher quality electronic components is needed to make it a fully operational fatigue testing machine and a more suitable motor for controlling the test arm should be installed.

7 Glossary

Ordinary least square (OLS)   Common statistical method used in regression analysis to achieve best fit to a dataset (Løvås, 2005, p. 273).

Pulse-with-modulation (PMW)   Changing the average DC voltage by turning the voltage on (high) and off (low) in fast pulses, the longer time between each on pulse the lower the average voltage (Bolton, 2019, p. 98). By varying how long the pulses remains in a off condition, one can simulate a voltage control, i.e. achieve the same effect as one would if one could control the voltage directly.

Prusa Slicer software   Prusa Slicer Software is Prusa's software that converts STL files into G-Code readable by the Prusa 3D-printer.

Topology optimization   To find the best design of material use for s specific design criteria as load, and size of design, for to reduce material consumption and be able to achieve the stiffness of construction (Kurowski, 2020, p. 587).

References

Agnihotri, N., n.d. *RPi Python Programming 16: Analog output and software PWM.* [Online]
Available at: https://www.engineersgarage.com/articles-raspberry-pi-python-software-pwm-led-fading/
[Accessed 2 april 2022].

Aksdal, A., 2003. *Elektriske anlegg: Industri og motorinstallasjoner.* [Online]
Available at:
https://www.nb.no/items/5d11462f52bded9fe16b4678a7eb2b87?page=3&searchText=elektro
motorer
[Accessed 20 Oktober 2022].

Alciatore, D. G., 2019. *Introduction to Mechatronics and Measurement Systems.* 5. ed. New
York: McGraw-Hill Education.

Allegro MicroSystems LLC, 2014. *A4988 Datasheet(PDF) 1 Page - Allegro MicroSystems.*
[Online]
Available at: https://html.alldatasheet.com/html-pdf/455036/ALLEGRO/A4988/292/1/A4988.html
[Accessed 15 April 2023].

Allegro MicroSystems, LLC, n.d. *A4988 - DMOS Microstepping Driver with Translator.*
[Online]
Available at:
https://www.pololu.com/file/0J450/a4988_DMOS_microstepping_driver_with_translator.pdf
[Accessed 5 mai 2023].

amazon, n.d. *3D Printer Motors.* [Online]
Available at: https://www.amazon.com/Iverntech-NEMA-17-Stepper-Motor/dp/B07D6GC4C4?th=1
[Accessed 4 April 2023].

Anon., 2020. *Wikimedia Commons.* [Online]
Available at: https://commons.wikimedia.org/wiki/File:Roller_Bearing_(PSF).png
[Accessed 16 May 2023].

Bell, K., 2014. *Konstruksjonsmekanikk: Del I Likevektslære.* Bergen: Fagbokforlaget.

Bell, K., 2014. *Konstruksjonsmekanikk: Del II Fasthetslære.* 2 ed. Bergen: Fagbokforlaget.

Bolton, W., 2019. *Mechatronics: Electronic control systems in mechanical and electrical
engineering.* Harlow, UK: Pearson Educational Limited.

Bourns, n.d. *3382 - 12 mm Rotary Position Sensor.* [Online]
Available at: https://docs.rs-online.com/7fb0/0900766b8119b40e.pdf
[Accessed 6 april 2023].

Brush, K., 2019. *TechTarget.* [Online]
Available at: https://www.techtarget.com/searchsoftwarequality/definition/finite-element-analysis-FEA
[Accessed 16 March 2023].

Callister, W. D. & Rethwisch, D. G., 2010. *Materials Science and Engineering an Introduction.* USA: Wiley.

Collins, D., 2014. *Inertia Matching: Why Perfect Isn't Always Best.* [Online]
Available at: https://www.linearmotiontips.com/inertia-matching-perfect-isnt-always-best/

Corrosionpedia, 2019. *Material Selection.* [Online]
Available at: https://www.corrosionpedia.com/definition/6939/material-selection
[Accessed 21 may 2023].

CrabCad, 2012. *Library.* [Online]
Available at: https://grabcad.com/library/800mm-rotor-blade
[Accessed 3 February 2023].

CrabCad, 2019. *Library.* [Online]
Available at: https://grabcad.com/library/fsr402-1
[Accessed 4 April 2023].

CrabCad, 2023. *Library.* [Online]
Available at: https://grabcad.com/library/push-button-54
[Accessed 4 April 2023].

Dahlvig, G., 1991. *Konstruksjonselementer.* 2 ed. Asker: Gyldendal Norsk Forlag AS 2000.

Dassault Systems, 2021. *Meshing.* [Online]
Available at: https://help.solidworks.com/2021/english/SolidWorks/cworks/c_meshing.htm

DFROBOT, 2023. *Metal DC Geared Motor w/Encoder - 12V 122RPM 38Kg.cm.* [Online]
Available at: https://www.dfrobot.com/product-1210.html
[Accessed 2 April 2023].

DFRobot, n.d. *15A Single DC Motor Driver - Product WIKI.* [Online]
Available at: https://wiki.dfrobot.com/15A_Single_DC_Motor_Driver_SKU__DRI0042
[Accessed 03 april 2023].

DiCola, T., 2016. *MCP3008.* [Online]
Available at: https://learn.adafruit.com/raspberry-pi-analog-to-digital-converters/mcp3008
[Accessed 14 March 2023].

DigiKey, n.d. *Potentiometer.* [Online]
Available at: https://www.digikey.no/no/products/detail/bourns-inc/3382H-1-103/2080233
[Accessed 4 April 2023].

DNV-GL, 2016. *Høgskulen på Vestlandet.* [Online]
Available at:
https://home.hvl.no/ansatte/tct/FTP/H2022%20Marinteknisk%20Analyse/SESAM/SESAM%
20UM%20Brukermanualer/GeniE_UM_Vol_3.pdf
[Accessed 16 March 2023].

EUR-Lex, 2014. *EUR-Lex.* [Online]
Available at: https://eur-lex.europa.eu/legal-content/EN/TXT/PDF/?uri=CELEX:32014L0032
[Accessed 19 May 2023].

Falck-Ytter, H., 2014. *Materialteknologi Del 1 Grunnlag.* Oslo: Gyldendal Undervisning.

Gastreich, W., 2018. *What is a servo motor and how it works?.* [Online]
Available at: https://realpars.com/servo-motor/
[Accessed 19 mai 2023].

Gomeringer, R., Heinzler, M., Kilgus, R. & Menges, V., 2017. *Mechanical and metal trades handbook.* Haan-Gruiten: Verlag Europa-Lehrmittel.

Grabcad, 2019. *Library.* [Online]
Available at: https://grabcad.com/library/fsr402-1
[Accessed 3 April 2023].

GrabCad, 2023. *Library.* [Online]
Available at: https://grabcad.com/library/stepper-nema17-2
[Accessed 4 April 2023].

Hufford, T., 2015. *Welder.* [Online]
Available at: https://www.thefabricator.com/thewelder/article/cuttingweldprep/cutting-metal-with-cutting-wheels
[Accessed 16 May 2023].

Hughes, A. & Drury, B., 2019. *Electric motors and drives: Fundamentals, Types and Applications.* Oxford: Elsevier Ltd..

Hymel, S., 2023. *How to Run a Raspberry Pi Program on Startup.* [Online]
Available at: https://learn.sparkfun.com/tutorials/how-to-run-a-raspberry-pi-program-on-startup/all
[Accessed 8 May 2023].

Ignatowitz, E., 2021. *Prosesskjemi.* 2 ed. OSLO: Gyldendal Norsk Forlag AS.

Interlink Electronics, 2017. *FSR 400 Series.* [Online]
Available at:
https://cdn2.hubspot.net/hubfs/3899023/Interlinkelectronics%20November2017/Docs/Datasheet_FSR.pdf
[Accessed 14 March 2023].

Jonsdottir, H., 2016. *Usikkerhet og støy i målinger.* Bergen: Fagbokforlaget.

Kalpakjian, S. & Schmid, S. R., 2014. *Manufacturing Engineering and Technology.*
Singapore: Pearsons Education Inc..

Kedjeteknik, n.d. *Gir i 3D.* [Online]
Available at: https://www.kedjeteknik.se/kugghjul-3d
[Accessed 18 May 2023].

Knight, B., 2023. *Understanding Inertia Ratio and Its Effect On Machine Performance White
Paper.* [Online]
Available at: https://us.mitsubishielectric.com/fa/en/support/technical-support/knowledge-
base/getdocument/?docid=3E26SJWH3ZZR-41-13086

Kozierko, C. M., 2001. *Power Good Signal.* [Online]
Available at:
https://web.archive.org/web/20190131063020/http://www.pcguide.com/ref/power/sup/funcPo
werGood-c.html
[Accessed 7 May 2023].

Kurowski, P. M., 2020. *Engineering Analysis with SolidWorks Simulation 2020.* 1 ed. Kansas:
SDC Publications.

Lackey, B., 2023. *Servo Motor vs Stepper Motor: Which is right for your application?.*
[Online]
Available at: https://www.motionsolutions.com/servo-motor-vs-stepper-motor-right-
application/

Last Minute Engineers, n.d. *Control Stepper Motor with A4988 Driver Module & Arduino.*
[Online]
Available at: https://lastminuteengineers.com/a4988-stepper-motor-driver-arduino-tutorial/
[Accessed 7 mai 2023].

Lewotsky, K., 2015. *Understanding the Mysteries of Inertia Mismatch.* [Online]
Available at: https://www.automate.org/industry-insights/understanding-the-mysteries-of-
inertia-mismatch

Leyton Fasteners, n.d. *Technicak Information.* [Online]
Available at: https://leytonfasteners.co.uk/bolt-setscrew-information/
[Accessed 9 May 2023].

Loctite, n.d. *Loctite 401 Instant Aghesive.* [Online]
Available at: https://www.henkel-adhesives.com/sk/en/product/instant-
adhesives/loctite_401.html
[Accessed 25 April 2023].

Løvås, G. G., 2005. *Statistikk: for universiteter og høgskoler.* 2 ed. Oslo: Universitetsforlaget.

MatWeb, 2023. *Overview of materials for Polylactic Acid (PLA) Biopolymer.* [Online]
Available at:
https://www.matweb.com/search/DataSheet.aspx?MatGUID=ab96a4c0655c4018a8785ac403
1b9278
[Accessed 12 May 2023].

McCrum, N. G., Buckley, C. P. & Bucknall, C. B., 1997. *Principles of Polymer Engineering.*
Oxford, United Kingdom: Oxford University Press.

Microchip, 2008. *MCP3004/3008.* [Online]
Available at: https://cdn-shop.adafruit.com/datasheets/MCP3008.pdf
[Accessed 2023 March 2014].

Microsoft, 2023. [Online]
Available at: https://learn.microsoft.com/en-
us/dotnet/desktop/wpf/overview/?view=netdesktop-7.0
[Accessed 26 March 2023].

MiSUMi, 2014. *Technical Data.* [Online]
Available at: https://uk.misumi-ec.com/pdf/fa/2014/P1_2297-2298_F80_EN.pdf
[Accessed 17 May 2023].

Mobley, K. R., 2001. *Plant Engineer's Handbook.* Woburn: Butterworth-Heinemann.

Ninive, P. H., 2018. *Introduksjon til elementmetoden TEK2001.* [Online]
Available at: https://learn-eu-central-1-prod-fleet01-
xythos.content.blackboardcdn.com/5def77a38a2f7/1497798?X-Blackboard-S3-Bucket=learn-
eu-central-1-prod-fleet01-xythos&X-Blackboard-Expiration=1681246800000&X-
Blackboard-Signature=Il8K%2Fhyz%2B3PRZcje%2FW0ltCrBEEy4FBD

NTN, n.d. *Sliding bearings.* [Online]
Available at: https://www.ntnglobal.com/en/products/slidingbearing.html
[Accessed 16 May 2023].

OurPCB, n.d. *What is Motor Driver: A complete Guide and More!.* [Online]
Available at: https://www.ourpcb.com/what-is-motor-driver.html
[Accessed 25 mars 2023].

Prusa Reserach, 2023. *Original Prusa i3 MK3S+ kit.* [Online]
Available at: https://www.prusa3d.com/product/original-prusa-i3-mk3s-kit-
3/?gclid=Cj0KCQjwla-hBhD7ARIsAM9tQKs0oWMJRvqAOzSH7ZncBhoSunR1yISFzPC9-
qnfvOEnE4i2ylwEecMaArUwEALw_wcB#Specs
[Accessed 4 April 2023].

Quest International, n.d. *The Negative Environmental Impacts of Offshoring.* [Online]
Available at: https://www.questinc.com/company/blog-posts/impacts-of-offshoring
[Accessed 21 May 2023].

Rajpurohit, S. R. & Dave, H. K., 2018. Effect of process parameters on tensile strenght of FDM printed PLA part. *Rapid prototyping journal,* 24(8), pp. 1317-1324.

Raspberry Pi Fundation, 2023. *GPIO pins.* [Online]
Available at: https://projects.raspberrypi.org/en/projects/physical-computing/1

Raspberry Pi Ltd., 2019. *Raspberry Pi 4 Model B.* [Online]
Available at: https://datasheets.raspberrypi.com/rpi4/raspberry-pi-4-datasheet.pdf
[Accessed 14 March 2023].

Rozenblat, L., 2022. *COMPUTER POWER SUPPLY: PINOUT, CABLES, CONNECTORS.* [Online]
Available at: https://www.smpspowersupply.com/connectors-pinouts.html
[Accessed 26 March 2023].

RS Components, n.d. *RS online.* [Online]
Available at: https://docs.rs-online.com/d719/A700000008913624.pdf
[Accessed 4 April 2023].

RS PRO, 2023. *docs.rs-online.com.* [Online]
Available at: https://docs.rs-online.com/d719/A700000008913624.pdf

SHWETA COMPUTERS, 2023. *CV SERIES™ CV450.* [Online]
Available at: https://www.shwetacomputer.com/shop/corsair-power-supplies-cv-series-cv450-450-watt-80-plus-bronze-certified-psu/
[Accessed 2 April 2023].

SKF, n.d. *Deep groove bearing.* [Online]
Available at: https://www.skf.com/no/productinfo/productid-608
[Accessed 4 April 2023].

SKF, n.d. *Roller bearings.* [Online]
Available at: https://www.skf.com/group/products/rolling-bearings
[Accessed 16 May 2023].

Sklar, M., 2012. *Analog Inputs for Raspberry Pi Using the MCP3008.* [Online]
Available at: https://learn.adafruit.com/reading-a-analog-in-and-controlling-audio-volume-with-the-raspberry-pi
[Accessed 14 March 2023].

Smith, D., 2009. *The Fabricator.* [Online]
Available at: https://www.thefabricator.com/thefabricator/article/finishing/grinding-and-cutting-safely
[Accessed 16 May 2023].

Society Of Robots, 2005. *SENSORS - ROBOT ENCODER.* [Online]
Available at: https://www.societyofrobots.com/sensors_encoder.shtml
[Accessed 19 May 2023].

SolidWorks, n.d. *Mesh Quality Check.* [Online]
Available at:
https://help.solidworks.com/2021/english/SolidWorks/cworks/c_mesh_quality_checks.htm
[Accessed 29 April 2023].

Solomon, K., 2022. *What Would Happen If the World's Natural Resources Ran Out?.*
[Online]
Available at: https://www.rd.com/list/what-would-happen-if-worlds-natural-resources-ran-out/

Teknikbog, n.d. *Arvid Nilsson.* [Online]
Available at: https://arvidnilsson.no/content/uploads/Arvid-Nilsson-Teknikbog-NO.pdf
[Accessed 6 May 2023].

United Nations, 2023. *Goal 12 Ensure sustainable consumption and production patterns.*
[Online]
Available at: https://sdgs.un.org/goals/goal12
[Accessed 21 May 2023].

United Nations, n.d. *The 17 goals.* [Online]
Available at: https://sdgs.un.org/goals
[Accessed 21 May 2023].

Upton, E., 2022. *Supply chain update – it's good news!.* [Online]
Available at: https://www.raspberrypi.com/news/supply-chain-update-its-good-news/
[Accessed 8 May 2023].

Zawadzki, K. et al., 2022. FatigueTestingoftheSmallWindTurbineBlade. *International
Journal of Mechanical Engineering and Robotics Reserach,* 11(4), pp. 269-274.

Андрей, П., 2022. *Bolted Joint with nut.* [Online]
Available at: https://commons.wikimedia.org/wiki/File:Bolted_joint_with_nut.svg
[Accessed 6 May 2023].

8 Appendix

8.1 Instructions on setting up the Raspberry Pi with ethernet connectivity with remote desktop connection (Windows)

This section outlines how to set up a Raspberry Pi so that it can be accessed with an ethernet cable using "remote desktop connection" in Windows 10/11 based on various forum sources and foremost trial and error:

1. Make an image of Raspian to the micro SD card. Go to the webpage https://www.raspberrypi.com/software/. Click "Download for Windows" and use the wizard to make an image at the SD card. Add password in settings.

2. Connect Raspberry Pi to keyboard, mouse and monitor.

3. Make sure that raspian is connected to internet. Go to terminal in Raspian and write "sudo apt install xrdp"

4. Write in terminal "hostname -I" to get the IP.

5. Set autologin off in Raspberry Pi.

6. Log out.

7. Use "Remote desktop connection" in windows 10/11 to connect to the Raspberry Pi using the IP address from point 4 and username and password set for the user in point 1 (or when connected to the Raspberry Pi with a monitor). Alternatively, one can use the hostname instead of the IP address. The hostname is shown in the terminal as {username}@{hostname}.

8.2 Machine Software

8.2.1 Main.py

```
from gpiozero import LED
from gpiozero import PWMLED
from gpiozero import MCP3008
from time import sleep

import DCMotor
import ForceSensor
import StepperMotor
import TestMachine
import TestArmAnglePotmeter

testMachine = TestMachine.TestMachine("Test Machine")
while True:
        pass
```

8.2.2 TestMachine.py

```
from gpiozero import LED
from gpiozero import PWMLED
from gpiozero import MCP3008
from time import sleep
from gpiozero import Button

import datetime
import os
import json
import re
import threading
import time
import subprocess
import math

import DCMotor
import ForceSensor
import StepperMotor
import TestMachine
import TestArmAnglePotmeter

class TestMachine:
    def __init__(self, Name):
        print("Initializing fatigue test machine...")
        self.Name = Name
        self.status = "Not Running Test"
        self.run_pause_button_clicked = False
        self.testRunning = None

        #Various parameters.
        self.delayEjector = 0.0025

        #Buttons.
        #NB! ON-OFF button is set up in the terminal. See "OFF-ON switch for Raspberry Pi.py"
for instructions.
        self.Button_Run      = Button(26)
        self.LED_Running     = LED(24)
        self.LED_Orange      = LED(23)

        #Force sensors.
        self.ForceSensor_Right = ForceSensor.ForceSensor("Force Sensor Right", 4)
        self.ForceSensor_Left = ForceSensor.ForceSensor("Force Sensor Left", 3)
```

```
        #Volt- and ampere sensor.
        self.VoltMeter      = MCP3008(channel = 0)
        self.AmpereMeter    = MCP3008(channel = 1)

        #Stepper motors.
        self.Motor_Ejector  = StepperMotor.StepperMotor(20, 19)
        self.Motor_Magazine = StepperMotor.StepperMotor(4, 6)

        #DC Motor.
        self.DCMotor = DCMotor.MotorController();

        #Data operations.
        self.USB_Drive_Path = ""
        self.OutputFile_Path = ""
        self.tests = None
        self.LoadTests()
        self.MakeOutputFile()

        #Specs magazine lead screw.
        self.testSubjectHolder_Height = 23.0 #mm
        self.stepperMotorStepRotation = 1.8 #Degrees
        self.leadDistance = 8.0 #mm
        self.Num_steps_for_one_test_subject = math.ceil((360.0 / self.stepperMotorStepRotation
) * (self.testSubjectHolder_Height / self.leadDistance))

        #Events
        self.Button_Run.when_pressed = self.Click_Run_Test_Button

        #Make ready.
        self.InitializeTestMachine()

        #Ready signal. Shows that the machine is ready.
        self.LED_Ready = LED(25)
        self.LED_Ready.on()

        print("Finished initializing...")

    def LoadTests(self):
        #First find possible drives.
        drives = os.listdir("/media/pi")
        drives = ["/media/pi/"+drive for drive in drives]

        #Check possible drives for JSON files on top folder.
        foundJsonFiles = []
        foundTestSetups = []
        foundTestTimeModified = []

        for drive in drives:
            filesTop = os.listdir(drive)

            for file in filesTop:
                if file.endswith(".json"):
                    try:
                        fullPath = drive+"/"+file
                        fileText = open(fullPath, 'r').read()
                        jsonTest = json.loads(fileText)
                        timeModified = os.path.getmtime(fullPath)

                        #Identify JSON with correct form.
                        if "MinForce" in list(jsonTest[0].keys()):
                            foundJsonFiles.append(fullPath)
                            foundTestSetups.append(jsonTest)
                            foundTestTimeModified.append(timeModified)
                    except:
                        pass

        #Find newest test file.
        if len(foundTestSetups) == 0:
            self.LED_Orange.blink()
            self.tests = None
            self.status = "Not Found Test"

        else:
            self.tests =
foundTestSetups[foundTestTimeModified.index(min(foundTestTimeModified))]
```

```python
            print("Test imported from:
"+str(foundJsonFiles[foundTestTimeModified.index(min(foundTestTimeModified))]))
            self.status = "Not Running Test"
            self.LED_Orange.off()
            self.LED_Running.blink()

    def MakeOutputFile(self):
        if self.USB_Drive_Path == "":
            self.OutputFile_Path = self.USB_Drive_Path+"/OutPutFile
"+str(int(time.time()))+".json"

            fout = open(self.OutputFile_Path , "w")
            fout.write(";".join(["Test #", "Min. Force", "Max Force", "Cycles before failure",
"\n"]))
            fout.close()

    def Click_Run_Test_Button(self):
        if self.run_pause_button_clicked == False:
            self.run_pause_button_clicked = True

            if self.status == "Not Running Test" or self.status == "Pause":
                self.status = "Running Test"
                self.LED_Running.on()

                if self.testRunning == None:
                    #Add the code in a thread.
                    self.testRunning = threading.Thread(target = self.Run, args=())

            elif self.status == "Running Test":
                self.status = "Pause"
                self.LED_Running.blink()

            elif self.status == "Not Found Test":
                self.LoadTests()

            else:
                self.status = "Not Running Test"
                self.LED_Running.off()

            self.run_pause_button_clicked = False
            print("Machine set to status: "+ self.status)

    def InitializeTestMachine(self):
        #Add Sondre's DC Motor Test Arm code.
        pass

    def Eject(self):
        print("Ejecting...")
        self.Magazine_Move_One_TestSubject("UP")
        self.Motor_Ejector.step(60, "CCW", self.delayEjector)
        self.Motor_Ejector.step(80, "CW", self.delayEjector)
        print("Ejected...")

    def Magazine_Move_One_TestSubject(self, direction):
        if direction == "DOWN":
            self.Motor_Magazine.step(self.Num_steps_for_one_test_subject , "CW", 0.0008)
        elif direction == "UP":
            self.Motor_Magazine.step(self.Num_steps_for_one_test_subject , "CCW", 0.0008)
        else:
            raise Exception("Not valid direction! Direction input should be rather 'UP' or
'DOWN'.")

    def Magazine_Move_All_Way_Down(self):
        self.Motor_Magazine.step(6260, "CW", 0.0008)


    def Run(self):
        for test in self.tests:
            self.RunTest(test)
            self.Eject()

        self.testRunning = None

    def RunTest(self, test):
        minForce = test["MinForce"]
        maxForce = test["MaxForce"]
```

140

```
        testName = test["Name"]
        isLeftDirection = False

        failure = False
        cycles = 0
        while not failure:
            if isLeftDirection:
                failure = self.DCMotor.move_until_force(abs(minForce), "LEFT")
                self.DCMotor.move_until_force((maxForce - minForce)/ 2, "LEFT")
            else:
                failure = self.DCMotor.move_until_force(abs(maxForce), "RIGHT")
                self.DCMotor.move_until_force((maxForce - minForce)/ 2, "RIGHT")

            isLeftDirection = not isLeftDirection
            cycles += 1
        fout = open(self.OutputFile_Path , "a")
        fout.write(";".join([str(testName), str(minForce), str(maxForce), str(cycles), "\n"]))
        fout.close()
```

8.2.3 DCMotor.py

```python
from gpiozero import OutputDevice, PWMOutputDevice, RotaryEncoder
from time import sleep
from gpiozero import MCP3008
import time

from ForceSensor import ForceSensor


class MotorController:
    def __init__(self):
        self.left = ForceSensor("left", 3)
        self.right = ForceSensor("right", 4)
        self.in1 = OutputDevice(16)
        self.in2 = OutputDevice(17)
        self.pwm = PWMOutputDevice(18)
        self.encoder = RotaryEncoder(a=14, b=15, wrap=False, max_steps=1080)
        self.encoder_offset = 0
        self.min_limit_enco = -100
        self.max_limit_enco = 100
        self.max_limit_left = 20
        self.max_limit_right = 20
        self.min_limit_left=1
        self.min_limit_right=1
        self.encoder.when_rotated = self.on_rotate
        self.encoder_value = self.encoder_offset

    def brake(self):
        self.in1.off()
        self.in2.off()
        self.pwm.value = 0
        sleep(0.5)
        return False

    def forward(self, duration):
        self.in1.on()
        self.in2.off()
        self.pwm.value = 0.2
        for i in range(int(duration*10)):
            self.encoder_value = self.encoder_offset + self.encoder.steps
            right_value = self.right.GetForce()
            if encoder_value < self.max_limit_enco and right_value < self.max_limit_right:
                sleep(0.01)
            else:
                break
        self.brake()
        sleep(0.5)

    def reverse(self, duration):
        self.in1.off()
        self.in2.on()
        self.pwm.value = 0.2
```

```python
        for i in range(int(duration*10)):
            self.encoder_value = self.encoder_offset + self.encoder.steps
            left_value = self.left.GetForce()
            if encoder_value > self.min_limit_enco and left_value < self.max_limit_left:
                sleep(0.01)
            else:
                break
        self.brake()
        sleep(0.5)

    def on_rotate(self):
        p=5
      # print("Encoder value:", self.encoder_offset + self.encoder.steps)

    def return_to_apr_zero(self):
        while True:
            encoder_value = self.encoder_offset + self.encoder.steps
            if abs(encoder_value) > 20:
                if encoder_value > 0:
                    self.reverse(0.7)
                elif encoder_value < 0:
                    self.forward(0.7)
            elif abs(encoder_value)>0:
                if encoder_value > 0:
                    self.reverse(0.1)
                elif encoder_value < 0:
                    self.forward(0.1)
            else:
                break

    def save_offset(self):
        with open("encoder_offset.txt", "w") as f:
            f.write(str(self.encoder_offset + self.encoder.steps))

    def load_offset(self):
        try:
            with open("encoder_offset.txt", "r") as f:
                return int(f.read())
        except FileNotFoundError:
            return 0

    def move_until_force(self, forceTarget, direction):
        #Need further testing.
         self.encoder_offset = self.load_offset()
        while True:
            #Check if failure have occured and arm is past limits.
            if  self.encoder_value <= self.min_limit_enco or self.max_limit_enco <=
self.encoder_value:
                self.return_to_apr_zero()
                self.save_offset()

                return True

            if direction == "LEFT":
                if self.left.GetForce() < forceTarget:
                    self.reverse(1)
                else:
                    return False

            if direction == "RIGHT":
                if self.left.GetForce() < forceTarget:
                    self.reverse(1)
                else:
                    return False


    def run(self):
        self.encoder_offset = self.load_offset()
        while True:
            self.reverse(6)
            if self.left.GetForce() < self.min_limit_left:
                break
            self.forward(6)
            if self.right.GetForce() < self.min_limit_right:
                break
```

142

```
        self.return_to_apr_zero()
        self.save_offset()
        return True
```

8.2.4 ForceSensor.py

```
import gpiozero
from time import sleep
import math

class ForceSensor:
    """
    A class that represents the force sensor of the
    type FSR400 on the Test Arm of the testing machine,
    connected to a MCP3008 IC.

    Attributes
    ----------
    MCP3008_CH : int
        The channel the force sensors output is connected to.

    Name: str
        Name of

    Methods
    -------
    GetForce(MCP3008_Values = [Float])
        Returns the force applied to the sensor.
    """
    def __init__(self, Name, MCP3008_CH):
        self.Name = Name
        self.voltageSensor = gpiozero.MCP3008(channel=MCP3008_CH, differential=False,
max_voltage = 5)
        self.voltage2forceCoefficient = 19.91
        self.voltage2forceConstant = 10**-7

    def GetForce(self):
        """
        Returns Newton force applied to the sensor.

        """

        return  self.voltage2forceConstant*math.exp(self.voltage2forceCoefficient *
self.voltageSensor.value)
```

8.2.5 StepperMotor.py

```
from gpiozero import OutputDevice
import time

class StepperMotor:
    def __init__(self, dir_pin, step_pin):
        self.dir_pin = OutputDevice(dir_pin)
        self.step_pin = OutputDevice(step_pin)

    def step(self, steps, direction, delay):
        if direction == "CW":
            self.dir_pin.on()
        elif direction == "CCW":
            self.dir_pin.off()
        else:
            raise ValueError("Direction must be either 'CW' or 'CCW'")

        for i in range(steps):
            self.step_pin.on()
            time.sleep(delay)
            self.step_pin.off()
            time.sleep(delay)
```

8.2.6 TestArmAnglePotmeter.py

```
from gpiozero import MCP3008
import time

class Potentiometer:
    def __init__(self, channel, num_samples=10, delay=0.01):
        self.adc = MCP3008(channel=channel)
        self.num_samples = num_samples
        self.delay = delay

    def read(self):
        pot_values = [self.adc.value for _ in range(self.num_samples)]
        pot_value = sum(pot_values) / self.num_samples # makes a more stable signal
        degrees = pot_value * 270 # convert potentiometer value to degrees
        time.sleep(self.delay)
        return degrees

channel = 2
pot = Potentiometer(channel)
```

8.2.7 Make OFF/ON switch for Raspberry Pi in Raspbian

Procedure:

1 Connect switch to GPIO3 and GND

2 Open terminal, write the code "sudo nano /boot/config.txt"

3 This opens a text. Scroll down. At the very end enter a new code line and insert "dtoverlay=gpio-shutdown"

4 Save by pressing ctrl+O (the letter O). Press ENTER according to message. Press ctrl+X to exit the text editor

5 Reboot the Raspberry Pi, test the switch.

8.3 Google drive shared folder link to CAD files, program code, videos and drawing

Google Drive shared folder link:

https://drive.google.com/drive/folders/1JoyhSHKdlm4e1VLGYwmuIKFPKesw8H2u